2019-01-01

Low-Valent Synthons Of Titanium : Investigations On Structure-Reactivity Relationships

Rolando Aguilar
University of Texas at El Paso, jraguilarcalderon@miners.utep.edu

LOW-VALENT SYNTHONS OF TITANIUM : INVESTIGATIONS ON STRUCTURE-REACTIVITY RELATIONSHIPS

JOSUÉ ROLANDO AGUILAR CALDERÓN

Doctoral Program in Chemistry

APPROVED:

Skye Fortier, Ph.D., Chair

Luis Echegoyen, Ph.D.

Dino Villagran, Ph.D.

Srinivasa Rao Singamaneni, Ph.D.

Stephen L. Crites, Jr., Ph.D.
Dean of the Graduate School

LOW-VALENT SYNTHONS OF TITANIUM : INVESTIGATIONS ON STRUCTURE-REACTIVITY RELATIONSHIPS

by

JOSUÉ ROLANDO AGUILAR CALDERÓN, B. Sc.

DISSERTATION

Presented to the Faculty of the Graduate School of

The University of Texas at El Paso

in Partial Fulfillment

of the Requirements

for the Degree of

DOCTOR OF PHILOSOPHY

Department of Chemistry and Biochemistry

THE UNIVERSITY OF TEXAS AT EL PASO

August 2019

Abstract

Strategies for the functionalization of abundant, small molecules into products with added value provide a powerful approach to address environmental sustainability issues. Dinitrogen (N_2), and carbon oxides (CO, CO_2), are examples of the ample, yet, underutilized atmospheric feedstock of nitrogen and carbon building blocks to produce a variety of chemicals. Although, potentially valuable, small molecules are inert under most conditions, and as such, their industrial activation often requires heterogeneous catalysts operated under high pressures (200 atm) and temperatures (450-600 ºC).

To this end, great efforts in synthetic inorganic chemistry have been devoted to the generation of well-defined and highly reactive complexes capable of activating small molecules under mild conditions. An effective strategy consists of the synthesis of transition metal complexes that feature uncommon oxidation states and are held within a coordinatively unsaturated ligand environment.

Early transition metals (group III-V) are an attractive platform to explore potent low-valent chemistries given the prevalent strong electropositive character and thermodynamic preference for high oxidation states in these elements. Furthermore, low-coordination numbers at the low-valent metal center generate novel geometries and electronic structures that consequently lead to atypical reactivity patterns. Complexes that fall within these criteria have been invoked as key intermediates in small molecule activation reactions, catalytic cycles, and, preparative organic synthesis methods.

Inspired by the distinctive chemistry underpinned by low-valent early metals, we have synthesized an intramolecularly masked titanium complex supported by a strong electron-releasing 3*N*-coordinated ligand scaffold (^{ket}guan)(η^6-Im^{Dipp}N)Ti (**1.1**) (^{ket}guan = [(^{t}BuC=N)C(NDipp)$_2$]-; Im^{Dipp}N- = 1,3 bis(Dipp)imidazolin-2-iminato, Dipp = 2,6-diispropylphenyl). Additionally, titanium-based compounds have significant advantages over other transition metals given the abundance and non-toxicity of titanium.

In Chapter 1, we show that **1.1** behaves as a versatile reducing agent upon its treatment with a wide range of substrates such as pyridine, benzophenone, π-acids, fluorinated aromatics, and atom transfer reagents. Together, these reactions shed some light into the potential of reduced forms of titanium complexes for substrate functionalization. Furthermore, our group previously reported an unusual example of reversible C-H bond activation and catalytic hydrogen transfer chemistry mediated by **1.1**. Encouraged by this formal two-electron reaction, we have targeted the activation of other substrates in a similar fashion since complexes capable of mediating reversible bond cleavage-formation are sparse among early metals.

In Chapter 2, we report our findings concerning thiophene (THP) activation. Specifically, **1.1** cleaves thiophene through a C-S bond oxidative addition step to generate the corresponding thiophene ring opened complex. Interestingly, the reaction is reversible upon UV light irradiation.

In Chapter 3, some of the chemistry mediated by **1.1** is revisited using a modified supporting ligand framework. Additionally, contrasting reactivity patterns are observed despite subtle ligand modifications.

Table of Contents

List of Tables

List of Figures

List of Illustrations

Chapter 1: Small Molecule Activation

1.1 INTRODUCTION

The early transition metals, i.e. groups III-V, are typically distinguished by their high electropositive character and thermodynamic preference for d^0 valencies. Accordingly, these metals are routinely utilized as potent Lewis acid activators or catalysts in preparative organic chemistry such as in Friedel-Crafts and Diels Alder reactions.[1-2] On the industrial scale, the early metals are widely known for their utility in Ziegler-Natta catalysis for the polymerization of olefins such as ethylene.[3] However, the chemistry of low-valent early metals (LVEMs), as defined by electron counts $\geq d^2$, is accessible and plays a critical role in a number of practical chemical transformations.[4-5] LVEMs have been utilized in natural product syntheses,[5-11] can effect the coupling and cyclization of alkenes and alkynes,[7, 12-19] and are especially adept at McMurry and Pinacol reductive aldehyde and ketone coupling reactions.[8, 20-22]

To a smaller extent, the reductive prowess of LVEM's has been utilized to perform challenging chemical transformations such as the reductive cleavage of CO,[23-25] C-H bond activation via oxidative addition,[26-33] and the reduction and functionalization of N_2.[31, 33-37] In fact, low-valent titanium complexes have been shown to be sufficiently reducing to effect the catalytic activation of N_2 for nitrogen incorporation into organic compounds.[11] For instance, treatment of substoichiometric amounts of $TiCl_4$ with an excess of Li^0 and Me_3SiCl under N_2 can nitrogenate ketoalkynes to indoles in modest yields.[11] Not surprisingly, LVEMs are typically highly reactive and strong reductants that are prone to disproportionation, complicating their synthesis, handling, storage, and utility. For example, the Ti(II) compounds $TiCl_2(py)_4$ (py = C_5H_5N) and $TiCl_2(tmeda)_2$ (tmeda = $((CH_3)_2NCH_2)_2$) are effective two-electron reductants that do not persist in solution, giving Ti(III) products and intractable solids upon standing.[38-40]

To address this issue, the stabilization of LVEM complexes is usually achieved by use of π-acids, specifically CO,[41] phosphines,[42] and unsaturated hydrocarbons[43] to alleviate metal-centered charge density. Indeed, LVEMs are often sufficiently electron rich to engage the π*-orbitals of aromatic molecules which can give rise to significant charge transfer and formal reduction of the arene moiety.[44-48] As an extreme example, Diaconescu and co-workers have shown that reduction of $(NN^{fc})YI(THF)_2$ (NN^{fc} = fc(NSi^{t}BuMe$_2$)$_2$, fc = 1,1-ferrocenediyl) with 4 equiv of KC_8 in the presence of biphenyl generates the dinuclear inverted sandwich complex $[(NN^{fc})Y]_2[K(toluene)]_2(\mu\text{-}C_6H_5C_6H_5)$ featuring formally trivalent yttrium with a bridging, tetraanionic biphenylide ligand.[49]

Indeed, the propensity of LVEMs to reduce aromatic systems can lead to intramolecular reduction of peripheral arene substituents on otherwise redox innocent ligands. For instance, Powers et al. showed that the one-electron reduction of the Ti(III) complex $TiCl[N(H)Ar^{iPr6}]_2$ (Ar^{iPr6} = C_6H_3-2,6-(C_6H_2-2,4,6-^{i}Pr$_3$)$_2$) leads to the formation of Ti[(η^6-Ar^{iPr6}NH)(Ar^{iPr6}NH)] featuring a formally Ti(IV) center with a masking cyclohexadiene dianion ring from reduction of one of the terphenyl amide ligands.[44] Similarly, Stephan and coworkers have shown that magnesium reduction of CpTi[N^{t}Bu$_2$(2-C_6H_4Ph)]Cl$_2$ gives rise to the Ti(IV) complex CpTi[N^{t}Bu$_2$(2-C_6H_4-η^6-Ph)] featuring a capping interaction by a flanking, dianionic aryl substituent.[50] Further reactivity was not described in either case; however, these two reduced complexes would be anticipated to be competent reductants owing to the driving force energy provided by ring re-aromatization. Thus, we assert that accessing these masking motifs via early-metal reduction and strategic ligand design is a viable approach for obtaining isolable but highly reactive divalent synthons.

To this effect, we recently reported the synthesis of the intramolecularly arene-masked titanium complex (^{ket}guan)(η^6-Im^{Dipp}N)Ti (**1.1**) (^{ket}guan = [(^{t}BuC=N)C(NDipp)$_2$]$^-$; Im^{Dipp}N$^-$ = 1,3-bis(Dipp)imidazolin-2-iminato, Dipp = 2,6-diispropylphenyl) formed upon the two-electron reduction of (^{ket}guan)(Im^{Dipp}N)Ti^{IV}(OTf)$_2$ (**1.2**) with 2 equiv of KC_8.[51] Based upon its structural parameters, **1.1** may be considered as possessing a Ti(IV) center capped by a pendant 1,4-cyclohexadiene dianion ring. Complex **1.1** is stable as a solid under an N_2 atmosphere, but in non-polar solutions, gradually undergoes two-electron oxidation via H_2 loss to give the Ti(IV) metallacycle (Im^{Dipp}N)[(DippN)(2-^{i}PrC$_6$H$_3$-6-(η^2-CH$_3$*CCH$_2$*)N)C(NC^{t}Bu$_2$)]Ti (**1.3**).[51] This transformation seemingly signifies a highly reducing system that can mediate C-H bond activation. Curiously, though, treatment of **1** with CO affords the Ti(II) complex (Im^{Dipp}N)(^{ket}guan)Ti(CO)$_2$ (**1.4**) in low yield wherein infrared spectroscopy indicates little to modest activation of the CO units.[51]

In an effort to better understand the redox properties and reductive abilities of **1** and further expand the LVEM chemistry of titanium, we have performed a series of reactions with a wide range of substrates including small molecules. We here describe the Ti(III) and Ti(IV) products of these reactions, chemistry that unequivocally validates the characterization of **1.1** as a versatile Ti(II) synthon. In our investigation, we have found **1.1** to be an attractive platform for entry into Ti(II) chemistry as the 3*N*-coordinated ligand manifold with its isopropyl and *tert*-butyl substituents affords highly crystalline products with tell-tale NMR spectroscopic features. Additionally, the steric profile of the ligand framework generates an axially positioned pocket for directing reactivity and access to the metal.

1.2 RESULTS AND DISCUSSION

1.2.1 Redox Characteristics

While **1** is formed by treatment of (^{ket}guan)(Im^{Dipp}N)Ti(OSO$_2$CF$_3$)$_2$ (**1.5**) with 2.5 equiv of KC$_8$,[51] initially in our preliminary studies, we sought to access low valent titanium species through the reduction of the Ti(IV) dichloride precursor (^{ket}guan)(Im^{Dipp}N)TiCl$_2$ (**1.6**). Addition of sodium mercury amalgam (4 equiv) to an orange toluene slurry of **1.6** with stirring at room temperature for four days leads to the formation of a green solution from which the Ti(III) complex (^{ket}guan)(Im^{Dipp}N)TiCl (**1.7**) is isolated as a pale green solid in 89% yields (eq 1.1). Lower yields are obtained with THF as reaction solvent or magnesium turnings (10 equiv) (60%).

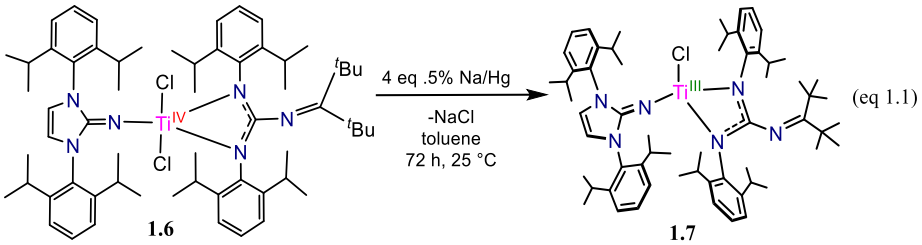

1.6 **1.7**

The ^{1}H NMR spectrum of **1.7** in C$_6$D$_6$ features broad, ill-defined resonances between 0.0 and 8.70 ppm (Figure 1.1) consistent with a paramagnetic species. Accordingly, the room temperature EPR spectrum of **1.7** in toluene features an isotropic signal with g = 1.956 attributable to a Ti(III) metal-based radical (Figure 1.2).[52]

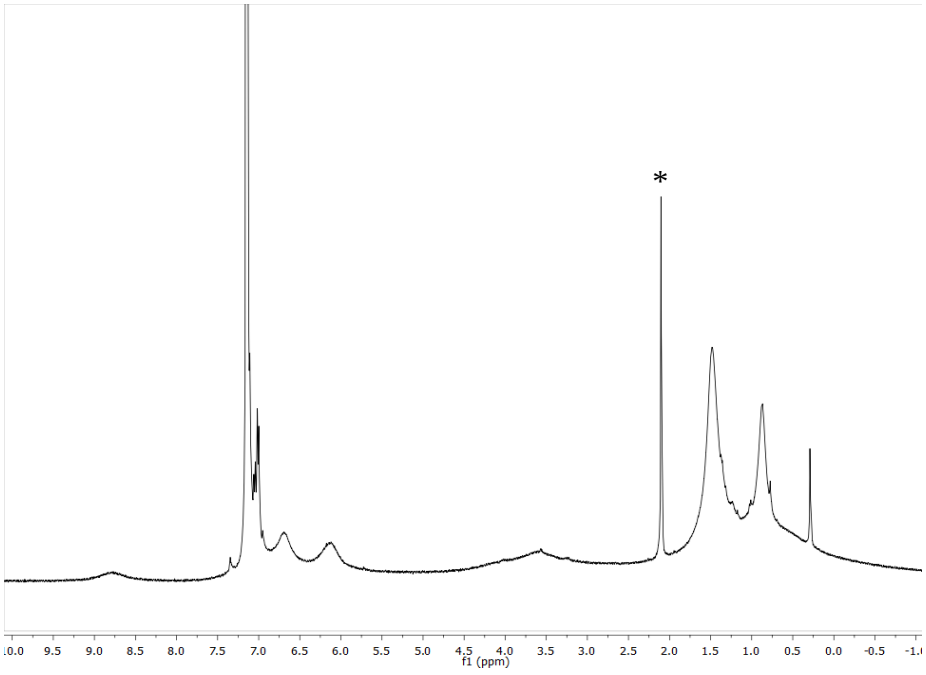

Figure 1.1: ^{1}H NMR spectrum for **1.7** in C_6D_6. Asterix (*) denotes the presence of residual toluene.

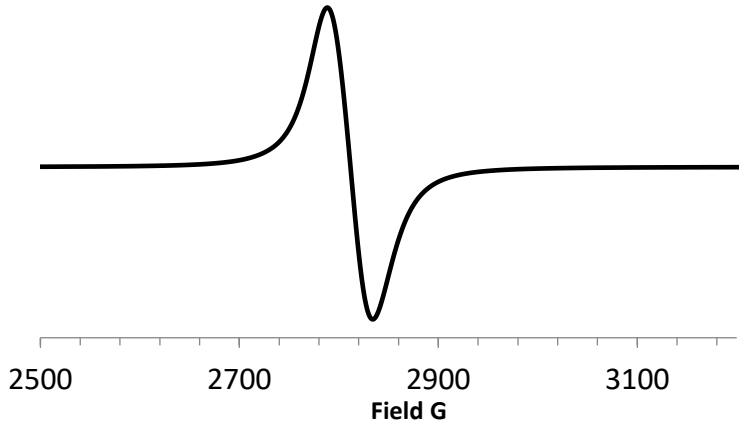

Figure 1.2: EPR spectrum for **1.7** in toluene, 298 K, 9.5 GHz.

Single crystals of **1.7** were grown from concentrated Et_2O solutions stored at –25 ºC for 2 days and crystallize in the monoclinic space group $P2_1/c$. Inspection of the solid-state molecular structure through X-ray crystallographic analysis shows a four-coordinate titanium center with tetrahedral geometry (e.g., N1-Ti1-Cl1 = 118.09(6)º; N2-Ti1-Cl1 = 120.50(5)º, and, 110.30(5)º)

as displayed in (Figure 1.3). The chloride atom resides in the apical position within a pocket formed by the peripheral Dipp groups. The Ti1-Cl1 = 2.295(1) Å bond length is identical to that found in the related 3N-coordinated Ti(III) β-diketiminate complex /[(Dipp)NC(CH_3)]$_2$CH}TiCl[N($SiMe_3$)$_2$] (Ti1-Cl1 = 2.2950(5) Å).[53] In the absence of a solid-state molecular structure for **1.6** further structural comparisons can be made to its surrogate [(Et_2N)C(NDipp)$_2$](Im'N)$TiCl_2$ (Im'N = 1,3-bis(2,6-dimethylphenyl)imidazolidin-2-iminato).[54] The guanidinate Ti-N distances of **1.7** (Ti1-N2 = 2.098(2) Å; Ti1-N3 = 2.085(2) Å) are within the range reported for [(Et_2N)C(NDipp)$_2$](Im'N)$TiCl_2$ (Ti-N = 2.097(2) Å; 2.150(4) Å). However, disparities are observed in the Ti-N_{Im} bonding parameters as the Ti1-N1 = 1.854(2) Å bond distance and Ti1-N1-C49 = 158.1(2)º bond angle of **1.7** is elongated and more acute than the corresponding Ti-N_{Im} = 1.765(3)Å and Ti-N_{Im}-C_{Im} = 170.5(3)° metrics in [(Et_2N)C(NDipp)$_2$](Im'N)$TiCl_2$. While the longer Ti-N_{Im} distance of **1.7** could be attributed to the larger ionic radius of Ti(III) (e.g., Ti(IIII) = 0.67 Å vs Ti(IV) = 0.605 Å for C.N. = 6),[55] the differences are likely a consequence of the greater steric profile of the Im^{Dipp}N- ligand of **1.7** compared to that of the Im'N- group in [(Et_2N)C(NDipp)$_2$](Im'N)$TiCl_2$.

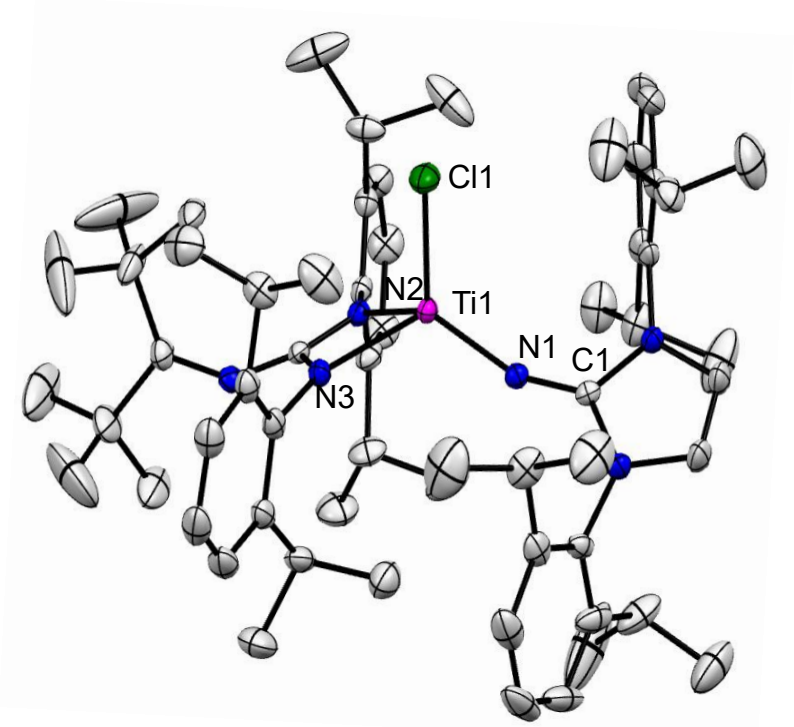

Figure 1.3: Solid-state molecular structure of **1.7** with 50% probability ellipsoids. Selected bond lengths (Å) and angles (º). Ti1-N1 = 1.854(2), Ti1-N2 = 2.085(2), Ti1-N3 = 2.082(2), N1-C1 = 1.287(3), Ti1-N1-C1 = 158.1(2), N2-Ti1-N3 = 110.3(2)

Interestingly, the inability to access low-valent titanium through the treatment of **1.6** or **1.7** with excess reducing equivalents of Na/Hg amalgam stands in stark contrast to the reduction chemistry of the Ti(IV) bisguanidinate $[Me_2NC(N^iPr)_2]_2TiCl_2$ or Ti(IV) bisamidinate $[PhC(NSiMe_3)_2]_2TiCl_2$ complexes, which are readily reduced by two electrons using excess magnesium powder or Na/Hg amalgam, respectively, to give the dinitrogen-bridged dinuclear complexes $[L_2Ti]_2(N_2)_2$.[56-57]

The disparity in reduction character seemingly indicates the 3N-ligand manifold of our $[(^{ket}guan)(Im^{Dipp}N)Ti]^{n+}$ system has superior donor abilities over the dual amidoimines of $[Me_2NC(N^iPr)_2]_2TiCl_2$ and $[PhC(NSiMe_3)_2]_2TiCl_2$, which, all other things being equal, is likely due to the excellent σ- and π-donor abilities of the ^{Dipp}ImN- ligand.[58-59] To shed further light on

this, the solution redox properties of $\mathbf{2^{Cl}}$ were investigated through cyclic voltammetry using THF solvent with $[NBu_4][PF_6]$ as the supporting electrolyte. The cyclic voltammogram (CV) of **1.6** (Figure 1.14) reveals an irreversible Ti(IV)/(III) redox wave at –2.3 V (vs $[Cp_2Fe]^{0/+}$) which is at the cusp of the Na/Hg amalgam redox potential (–2.38 V vs $[Cp_2Fe]^{0/+}$ in nonaqueous solvent).[60] Additional reduction features in the CV of **1.6** were not observed within the range of the solvent window supporting the notion that the ketimine-guanidinate/imidazolin-2-iminato ligand combination provides an especially electronic rich environment at the titanium metal center.

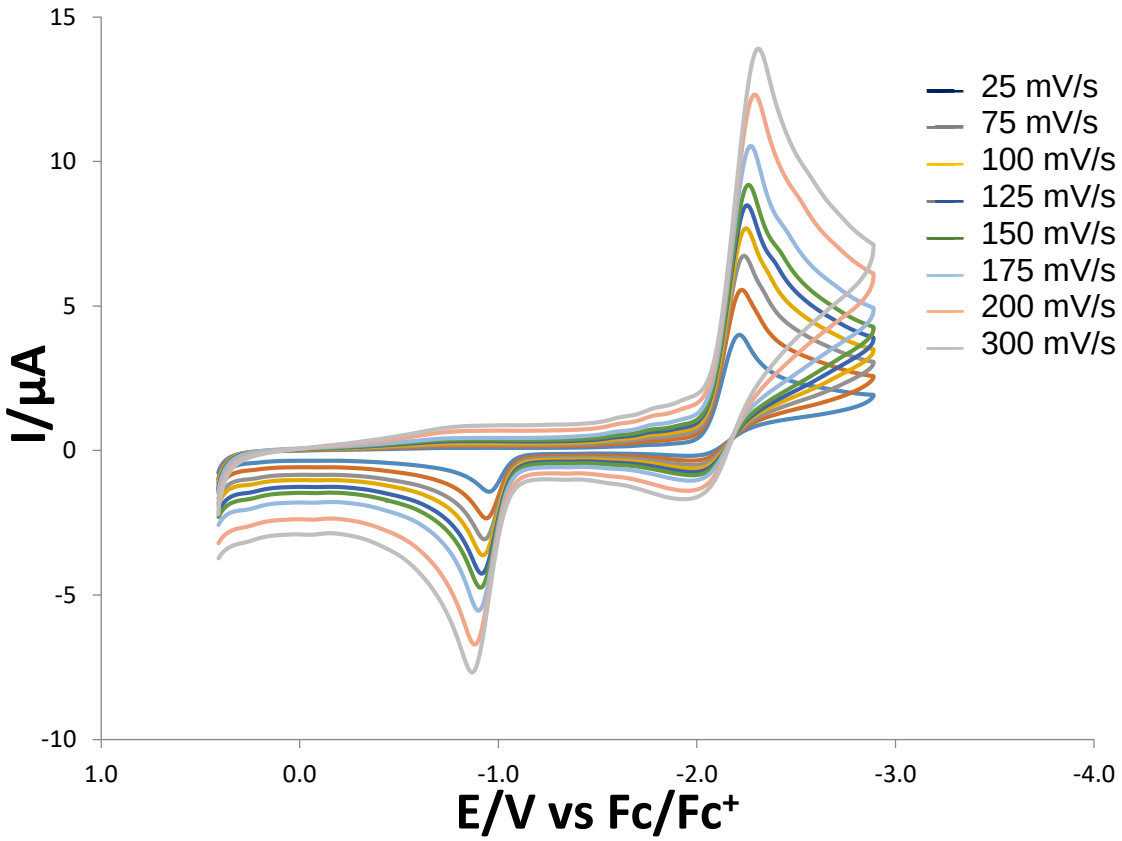

Figure 1.14: Room temperature cyclic voltammogram of **1.6** in THF (vs internally referenced Cp_2Fe/Cp_2Fe^+ $E^{1/2} = 0$ V). (0.2M $[^nBu_4N][PF_6]$ as supporting electrolyte).

In an attempt to push the reduction chemistry further, **1.6** was treated with an excess of highly reducing potassium graphite. Treatment of a stirring, THF slurry of **1.6** with 2.5 equiv of KC_8 forms a dark-brown solution overnight accompanied by formation of a black graphitic precipitate (eq 1.2). Filtering the solution and removal of the volatiles under vacuum produces a brown solid which is highly soluble in aromatic and ethereal solvents. The ^{1}H NMR spectrum of the product in C_6D_6 reveals a complicated series of sharp and broad resonances consistent with a diamagnetic product with low molecular symmetry and some fluxional solution-state behavior on the NMR time scale (Figure 1.5).

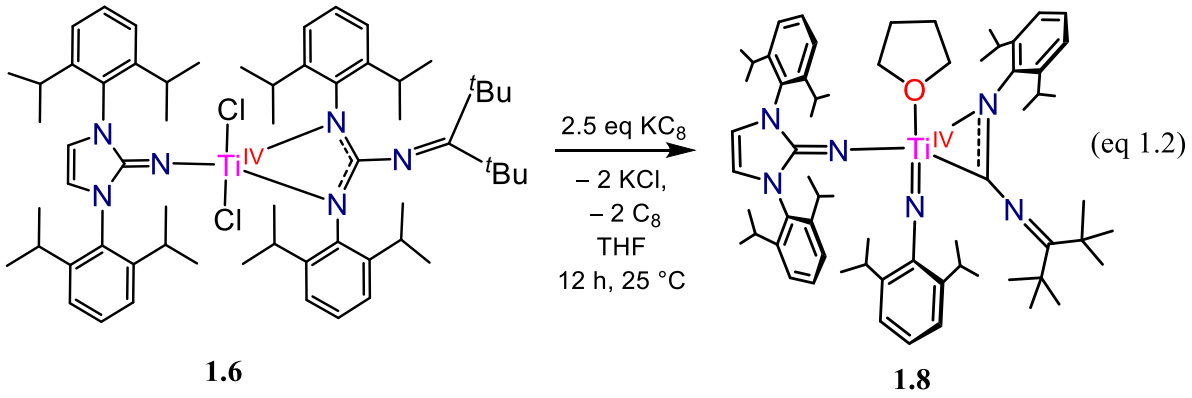

1.6 **1.8** (eq 1.2)

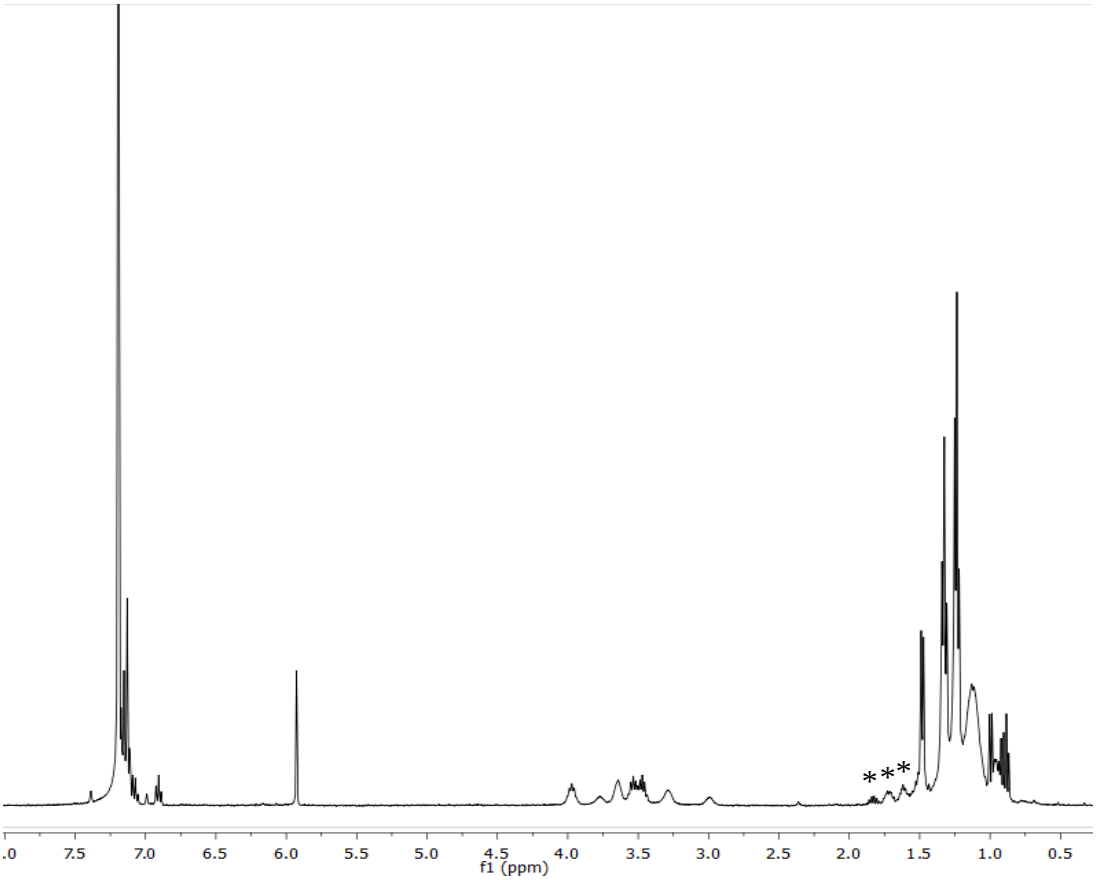

Figure 1.5: ^{1}H NMR spectrum of **4** in C_6D_6. Asterix (*) denote the presence of residual hexanes.

To elucidate the structure of the KC_8 reduction product, X-ray crystallographic analysis was performed on a crystal isolated from a THF/hexanes solution stored for 2 days at –25 ºC. The solid-state molecular structure obtained from the X-ray analysis reveals the formation of the five-coordinate Ti(IV)-imido complex ($Im^{Dipp}N$)(DippN=)[η^2-(^{t}Bu$_2$C)*NC*(NDipp)](THF)Ti (**1.8**) as shown in (Figure 1.6). Complex **4** forms from the reductive cleavage of the ketimine-guanidinate into imido and anionic iminoacyl fragments. This reduction product is surprising as guanidinates are not well-known to undergo such reductive fragmentation but is reminiscent of the reduction chemistry of early-metal β-diketiminates which can yield metal imidos.[61-62] Though, it has been shown in formamidinates that addition of external reductant, namely Zn^0 or Na/Hg, to the reaction mixture of Li[HC(NAr)$_2$] (Ar = phenyl, tolyl) with $Ta_2Cl_6(SMe_2)_3$ leads to the formation of the

imido- and iminoacyl-bridged dimer $[HC(NAr)_2]_4Ta(\mu\text{-}NAr)(\mu\text{-}\eta^2\text{-}CNAr]$.[63] Similarly, reduction of the Ti(IV) bisamidinate $[PhC(NSiMe_3)_2]_2TiCl_2$ with Na/Hg amalgam in the presence of TMEDA leads to formation of the imido and iminoacyl complexes $[PhC(NSiMe_3)_2]_2Ti(=NSiMe_3)$ and $[PhC(NSiMe_3)_2]Ti[\eta^2\text{-}Me_3SiNC(H)Ph][\eta^3\text{-}CH_2N(Me)CH_2CH_2N(Me)_2]$, respectively.[57, 64]

Inspection of the structural features of **1.8** show the Ti1-N2 = 1.750(2) Å bond length and T1-N2-C14 = 175.5(2)° bond angle is within the typical range of titanium-imido parameters (e.g., Ti-N_{imido} = 1.714(2) Å; Ti-N_{imido}-C_{imido} = 173.2(1)º for [η^2-H^{i}PrC=C(^{t}Bu)CHC(^{t}Bu)NDipp]Ti(=NDipp)(OTf)).[65] Additionally, the bond metrics of the titanium-imino acyl moiety in **4** (Ti1-C1 = 2.122(2) Å; Ti1-N3 = 2.105(2) Å; C1-N3 = 1.313(2) Å) is comparable to that known for Ti(η^2-Me*CN*Mes)[NC(^{t}Bu)$_2$] (Ti-C = 2.104(6) Å; Ti-N = 2.074(5) Å; C-N = 1.282(7) Å).[66] On the other hand, the imidazolin-2-iminato ligand displays a relatively long bond distance to the titanium (Ti1-N1 = 1.901(2) Å) despite adopting a near linear coordination mode to the metal (Ti1-N1-C27 = 169.6(2)º) when compared to $[(Et_2N)C(NDipp)_2](Im^{'}N)TiCl_2$ (Ti-N_{Im} = 1.765(3) Å; Ti-N_{Im}-C_{Im} = 170.5(3)º). The obtuse Ti-NIm angle is typically suggestive of substantial metal-nitrogen π-overlap consistent with zwitterionic, imido-type Ti=N-Im$^+$ bonding stabilized through imidazolium resonance contributions;[58-59] however, this bonding interaction is likely attenuated by the steric congestion of the titanium center in **1.8**. In line with this, the iminic N1-C27 = 1.277(2) Å bond length of **1.8** is substantially shorter than the corresponding N_{Im}-C_{Im} = 1.326(5) Å bond in $[(Et_2N)C(NDipp)_2](Im^{'}N)TiCl_2$ which does display Ti=N-Im$^+$ bonding character.

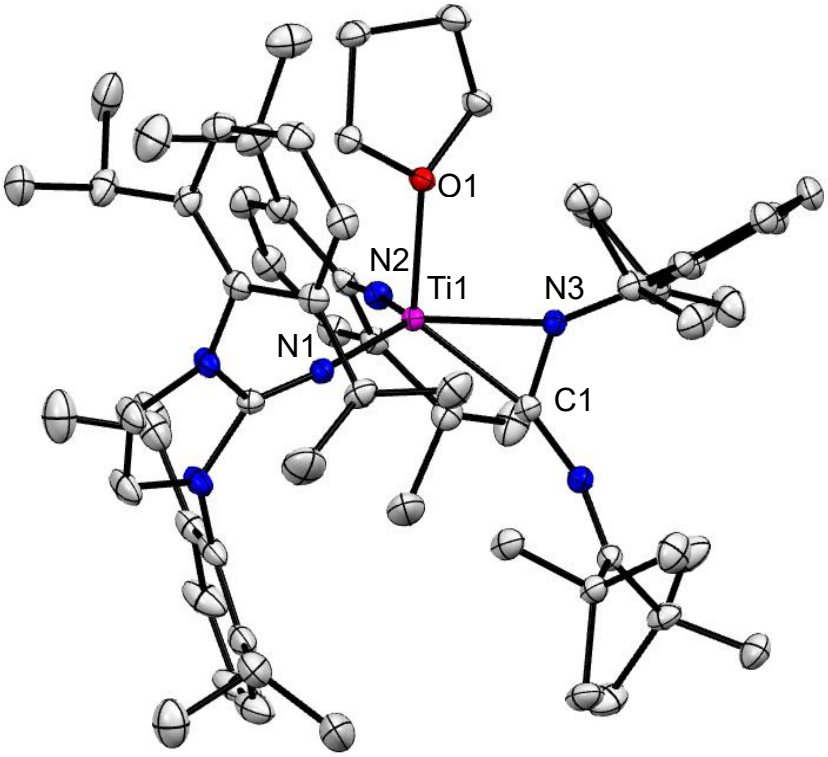

Figure 1.6: Solid-state molecular structure of **1.8** with 50% probability ellipsoids. Selected bond lengths (Å) and angles (º) Ti1-N1 = 1.900(2), Ti1-N2 = 2.085(2), Ti1-N3 = 2.082(2), N1-C1 = 1.287(3), Ti1-N1-C1 = 158.1(2), N2-Ti1-N3 = 110.3(2)

Lastly, all attempts to measure the CV data of **1.1**, to provide further insight into the redox chemistry of this system, have failed owing to the high reactivity of the complex. For instance, the CV measurements with $[NBu_4][PF_6]$ as supporting electrolyte have been hampered by the immediate reactivity of **1.1** with the $[NBu_4][PF_6]$ salt to give a complicated product mixture. Efforts to collect the CV of **1.1** in THF using anhydrous LiOTf were equally unsuccessful due to an unknown but persistent impurity in the lithium supporting electrolyte despite multiple recrystallization attempts.

1.2.2 Chemical Redox Assessment

In lieu of CV measurements, chemical probes were utilized to provide some insight into the approximate reduction potential range of **1.1**. or instance, the redox chemistry of benzophenone (Ph_2CO) encompasses two consecutive, electrochemically reversible, one-electron reduction events defined by the radical monoanion $[Ph_2CO]^{\bullet -}$ ($E_{1/2}$ = –2.3 V vs $[Cp_2Fe]^{0/+}$) followed by formation of the radical dianion $[Ph_2CO]^{2-}$ ($E_{1/2}$ = –2.9 V vs $[Cp_2Fe]^{0/+}$).[60, 67] Thus, addition of a stoichiometric amount of Ph_2CO to 1 in C_6D_6 forms a vibrant purple-red solution characteristic of the formation of a reduced form of Ph_2CO (eq 1.3).

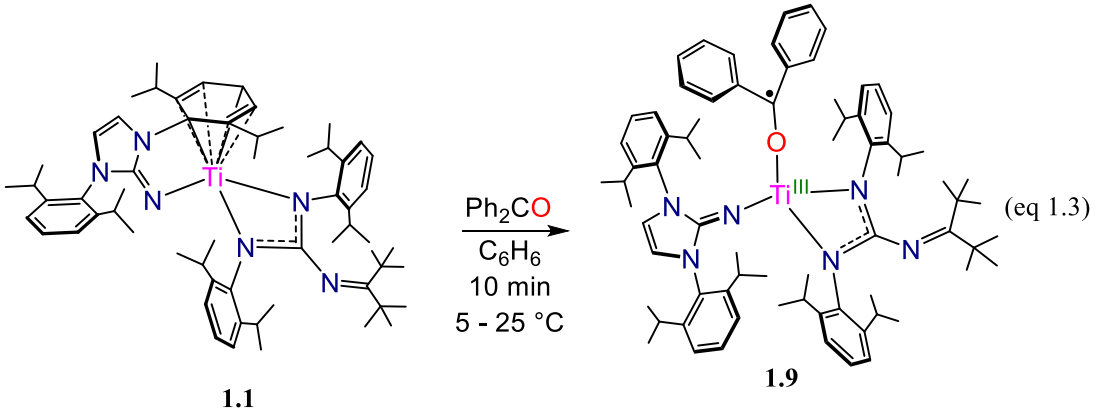

1.1 **1.9**

Analysis of this mixture via ^1H NMR spectroscopy showed complete consumption of both starting materials and appearance of broad, yet, well-defined resonances in the range of –0.30 to 7.10 ppm, suggestive of the formation of a paramagnetic species (Figure 1.6).

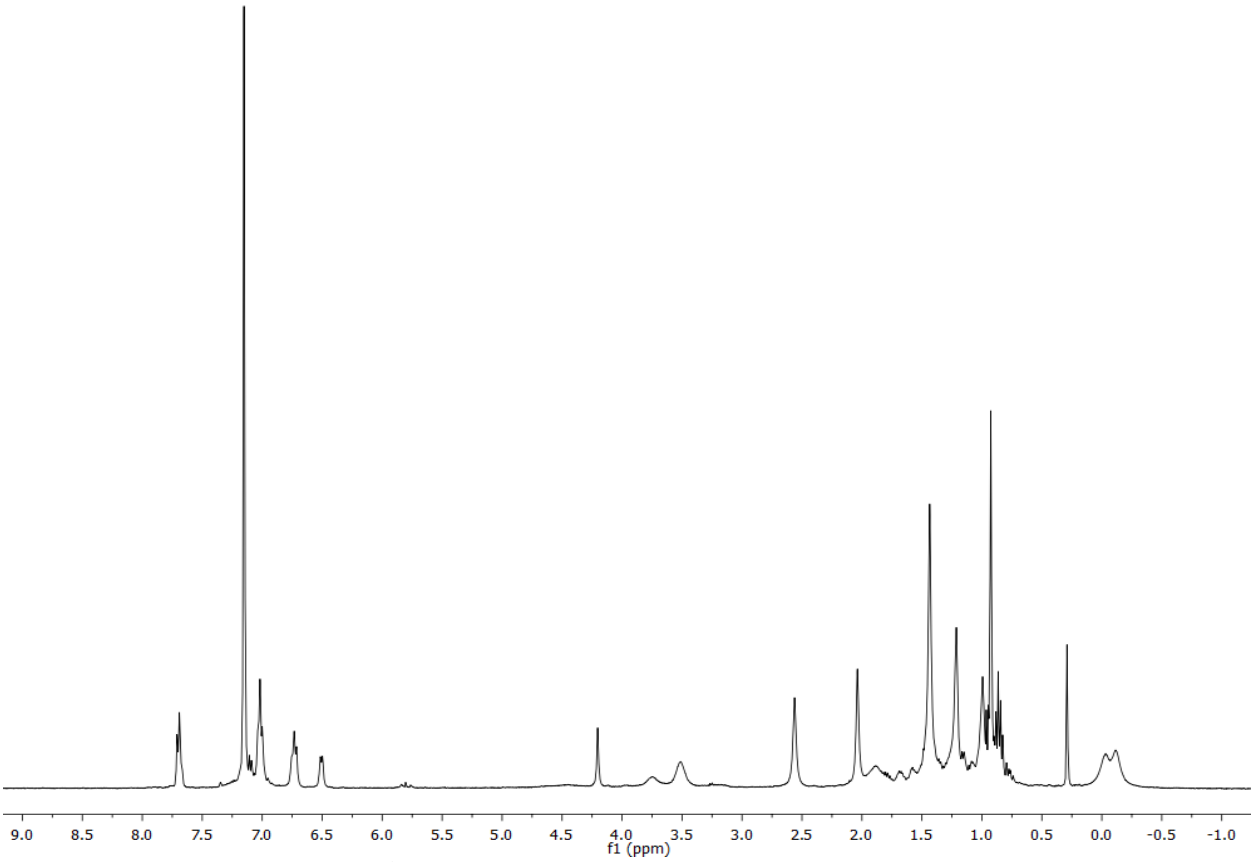

Figure 1.6: ^{1}H NMR spectrum of **1.9** in C_6D_6.

To our delight, block shaped, deep-purple crystals precipitate out of concentrated benzene solutions after ten minutes which are suitable for X-ray crystallographic analysis.

The solid-state molecular structure reveals the formation of the four-coordinate titanium complex (^{ket}Guan) (Imid^{dipp}N)Ti(η^{1}-*O*CPh$_2$) (**1.9**) where the benzophenone is observed to adopt an η^{1}-*O*CPh$_2$ form (Ti1-O1-C9 = 170.23(1)^{o}), residing in the apical position (Figure 1.5). The titanium-oxygen bond of **1.9** (T1-O1 = 1.856(2) Å) is significantly shorter than the Ti(III)-O bond found in the benzophenone adduct [Cp*$_2$Ti(OCPh$_2$)]BF$_4$ (Ti-O = 1.988(3) Å)[68] but similar to the titanium-alkoxide bonds of Ti(N^{t}Bu)[OCH(mesityl)$_2$]$_2$(py)$_2$ (Ti-O = 1.875(2) – 1.889(2) Å).[69] Moreover, the carbon-oxygen bond of the OCPh$_2$ ligand in **1.9** (C9-O1 =1.327(3) Å) is significantly longer than in free benzophenone (C-O = 1.230(0) Å)[70] and [Cp*$_2$Ti(OCPh$_2$)]BF$_4$ (C-O = 1.259(5) Å)[68] but similar to the carbon-oxygen bond in the ketyl complexes

[(($^{t\text{Bu}}$ArO)$_3$tacn)U^{IV}(OC•$^{t\text{Bu}}$Ph$_2$)] (C-O = 1.334(6) Å)[71] and Tp*$_2$U^{III}(OC•Ph$_2$) (C-O = 1.34(1) Å).[72] In addition, the sum of the bond angles about the carbonylic carbon atom in **1.9** ($\sum_{C9} \approx 360°$) is consistent with sp^2-hybridization. Overall, the bond metrics in **1.9** point towards a ketyl-type, monoanionic radical [Ph$_2$C•O]$^-$ whose charge is counterbalanced by a trivalent titanium center with the form (^{ket}guan)(Im^{Dipp}N)Ti^{III}(η^1-*O*C•Ph$_2$). In validation of this assessment, the solution EPR spectrum of **1.9** in toluene at 298 K displays two overlapping signals attributable to two different radicals (Figure 1.6).

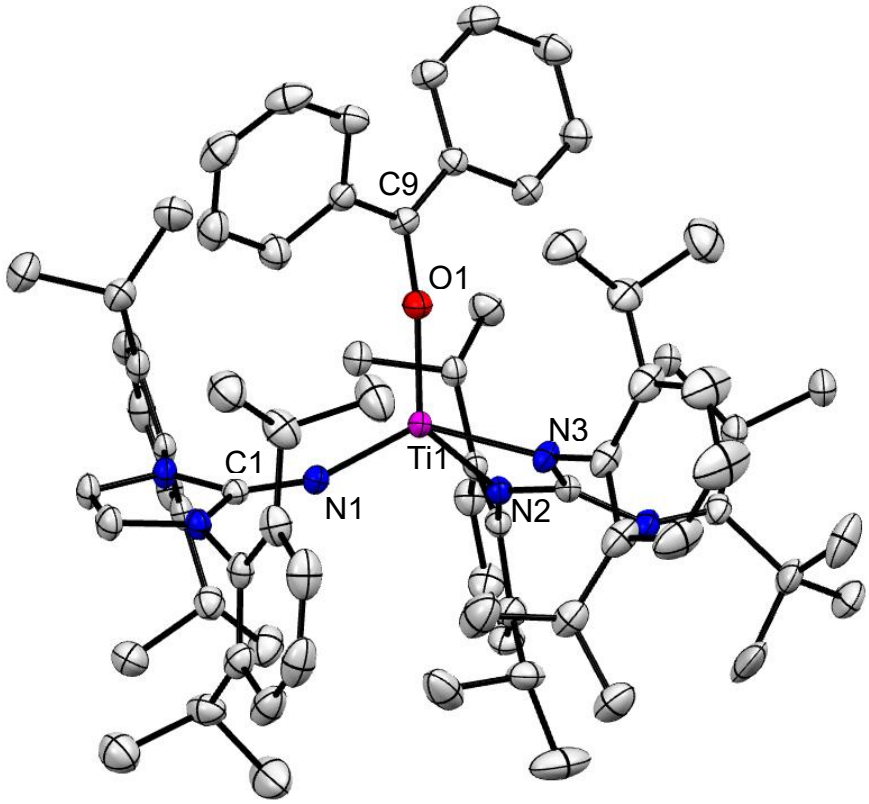

Figure 1.5: Solid-state molecular structure of **1.9** with 50% probability ellipsoids. Selected bond lengths (Å) and angles (º). Ti1-O1 = 1.856(2), O1-C9 = 1.327(3), Ti1 – N1 = 1.852(2), Ti1-N2 = 2.087(2), Ti1-N3 = 2.139(2), N1-C1 = 1.289(3), Ti1-O1-C9 = 170.1(2), Ti1-N1-C1 = 160.6(2), N2-Ti1-N3 = 110.9(2)º

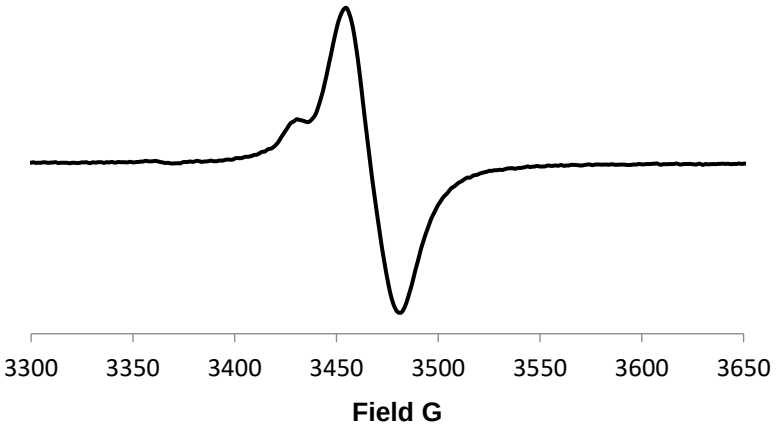

Figure 1.6: EPR spectrum of **1.9** in toluene, 298 K, 9.5 GHz.

Furthermore, the UV-vis electronic absorption spectrum of **1.9** in toluene displays an absorbance at 690 nm (ε = 678 $L \cdot mol^{-1} \cdot cm^{-1}$) which is similar to the absorption feature observed for $[Na(C_{13}H_{10}O)(HMPA)_2]_2]$ in THF (675 nm, ε = 5700 $L \cdot mol^{-1} \cdot cm^{-1}$).[73] Moreover, the UV-vis spectrum of **1.9** (Figure 1.7) qualitatively matches that known for (silox)Ti(OC•Ph_2) ((silox = $^tBu_3SiO^-$) with a band appearing at 692 (ε = 1800 $L \cdot mol^{-1} \cdot cm^{-1}$).[74]

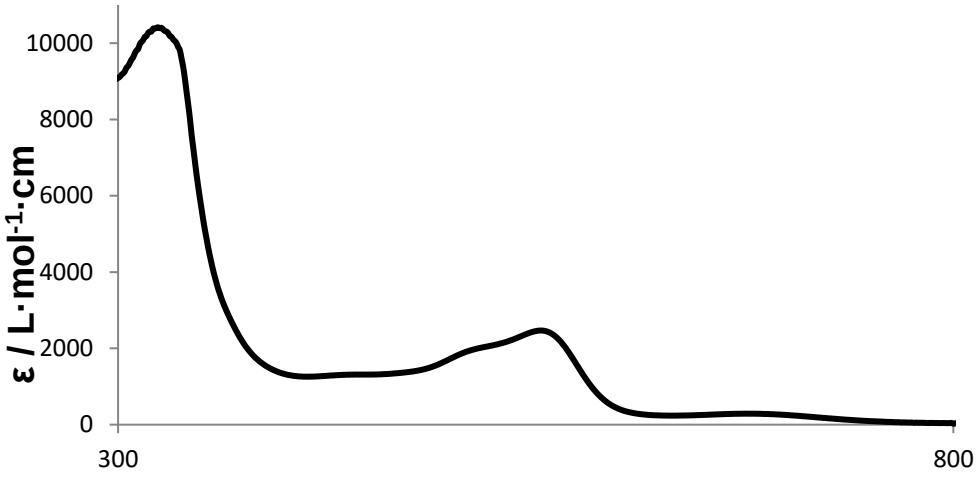

Figure 1.7: Room temperature UV/vis-NIR absorption spectra of **1.9** (toluene, 0.070 mM).

Importantly, low-valent titanium is the cornerstone reagent of McMurry and Pinacol couplings, yet the intermediates formed in these reactions, including the low-valent titanium species themselves, are not well-understood and organoradicals such as **1.9** are typically invoked as key but fleeting intermediates.[21] Although titanium-ketyl species have been previously examined in detail,[74] to the best of our knowledge, **1.9** represents the first structurally characterized ketyl complex of titanium, thus providing a potentially direct analog to the intermediates formed in these valuable coupling reactions. Notably, despite its radical character, **1.9** is remarkably stable in benzene solutions at room temperature for several weeks. We postulate that the steric profile of the 3*N*-ligand manifold of our $[(^{ket}guan)(Im^{Dipp}N)Ti]^{n+}$ system provides enhanced stability leading to the isolation of **1.9** as the kinetically trapped product. Interestingly, heating benzene solutions of **1.9** fails to produce the expected coupling products (i.e, Ph_2CCPh_2) and instead undergoes intramolecular chemistry (*vide infra*).

The one-electron reduction of benzophenone suggests that **1.1** is an appreciable reductant. Thus, as further validation of this notion, the lower boundary of the redox capabilities of **1.1** was probed using pyridine, which has a very low but chemically accessible reduction potential of ca. –3.1 V (vs $Fc^{0/+}$).[75] Accordingly, addition of excess pyridine to **1.1** in THF with stirring immediately forms a light green solution from which an insoluble product precipitates.

The ^{1}H NMR spectroscopic analysis of this material is hampered by its high insolubility in all common solvents; however, the ^{1}H NMR spectrum of a dilute sample of this compound in C_5D_5N shows the product to be paramagnetic with very broad resonances appearing from 0.80 to 1.40 ppm (Figure 1.8).

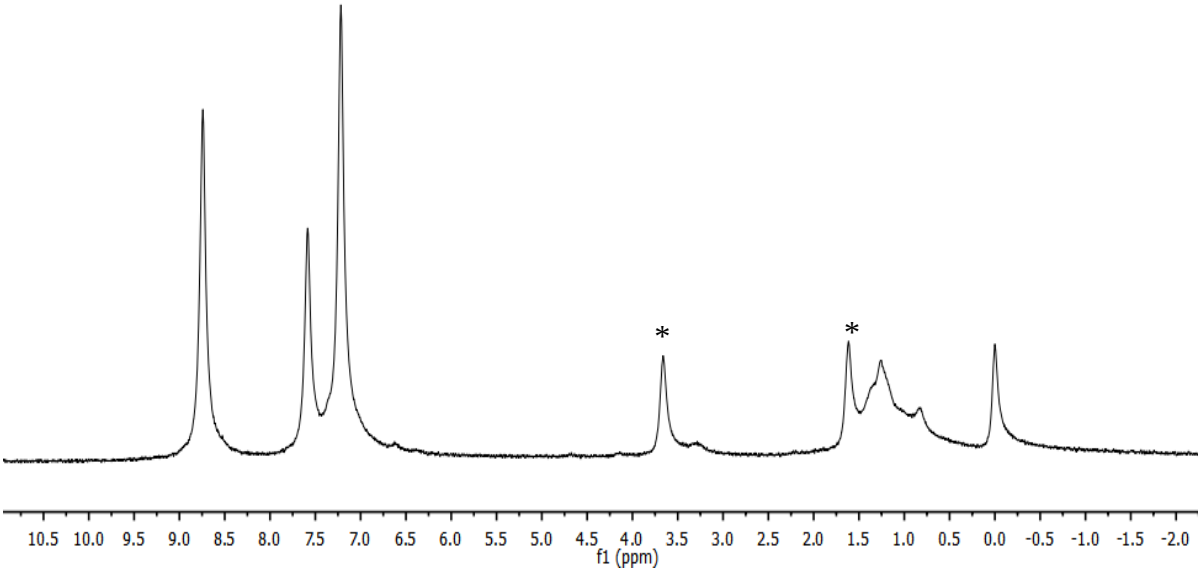

Figure 1.8: ^{1}H NMR spectrum of **1.10** in C_5D_5N. Asterix (*) denotes the presence of residual THF.

Single crystals of this compound can be grown by addition of one drop of pyridine to a THF solution of **2** followed by storage at –25 ºC for two weeks. The X-ray crystallographic analysis revealed the formation of the dinuclear complex [(^{ket}Guan)(Imid^{dipp}N)Ti]$_2$[μ-(NC_5H_5-H_5C_5N)] (**1.10**) (eq 1.4).

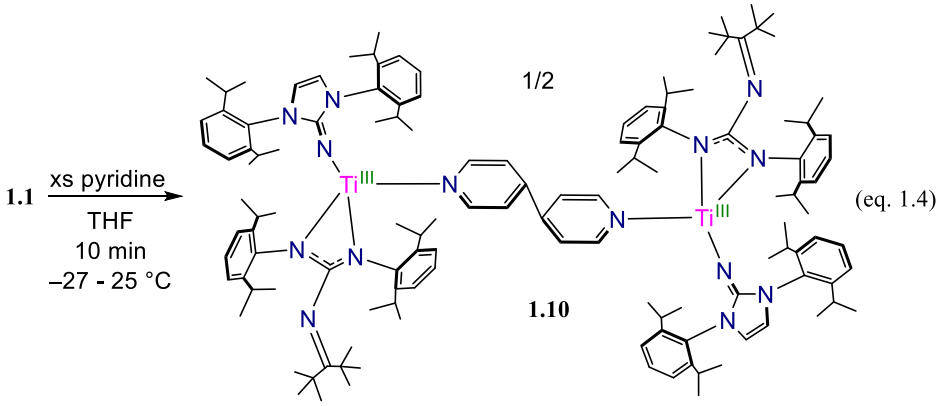

Complex **1.10** crystallizes in the monoclinic space group *C*2/*c* and contains one full [(^{ket}Guan)(Imid^{dipp}N))Ti](NC$_5$H$_5$)– monomer in the asymmetric unit, which resides on a crystallographic inversion center that provides the full dimer upon symmetry generation. The titanium centers are bridged by what initially appears as two terminally coupled pyridine ligands which adopt a stair-stepped arrangement (Figure 1.9). The inspection of the metrical parameters within the pyridine-type moieties shows localized bonding indicative of a 1,4-dihydropyridine motif (N4-C4 = 1.400(4) Å, N4-C8 = 1.104(4) Å, C4-C5 = 1.330(5) Å, C5-C6 = 1.506(5) Å, C6-C7 = 1.506(5) Å, and C7-C8 = 1.327(5) Å), C6-C6' = 1.565(0), consistent with the loss of aromatization.

This coupling and ring dearomatization is reminiscent of the chemistry observed between the titanium complex Ti(ODipp)$_2$(η^2-^{t}BuNCCH$_2$Ph)(CH$_2$Ph) and excess pyridine which yields [Ti(ODipp)$_2$(py)$_2$]$_2$[μ-(NC$_5$H$_5$-H$_5$C$_5$N)][76] as well as the reduction of pyridine by [(Dipp)NC(CH$_3$)]$_2$CH}Fe^{I}(C$_6$H$_6$) to give [/[(Dipp)NC(CH$_3$)]$_2$CH}Fe^{II}]$_2$[μ-(NC$_5$H$_5$-H$_5$C$_5$N)].[75] Thus, **1.10** an be described as the Ti(III) product of the reductive C-C coupling of pyridine.

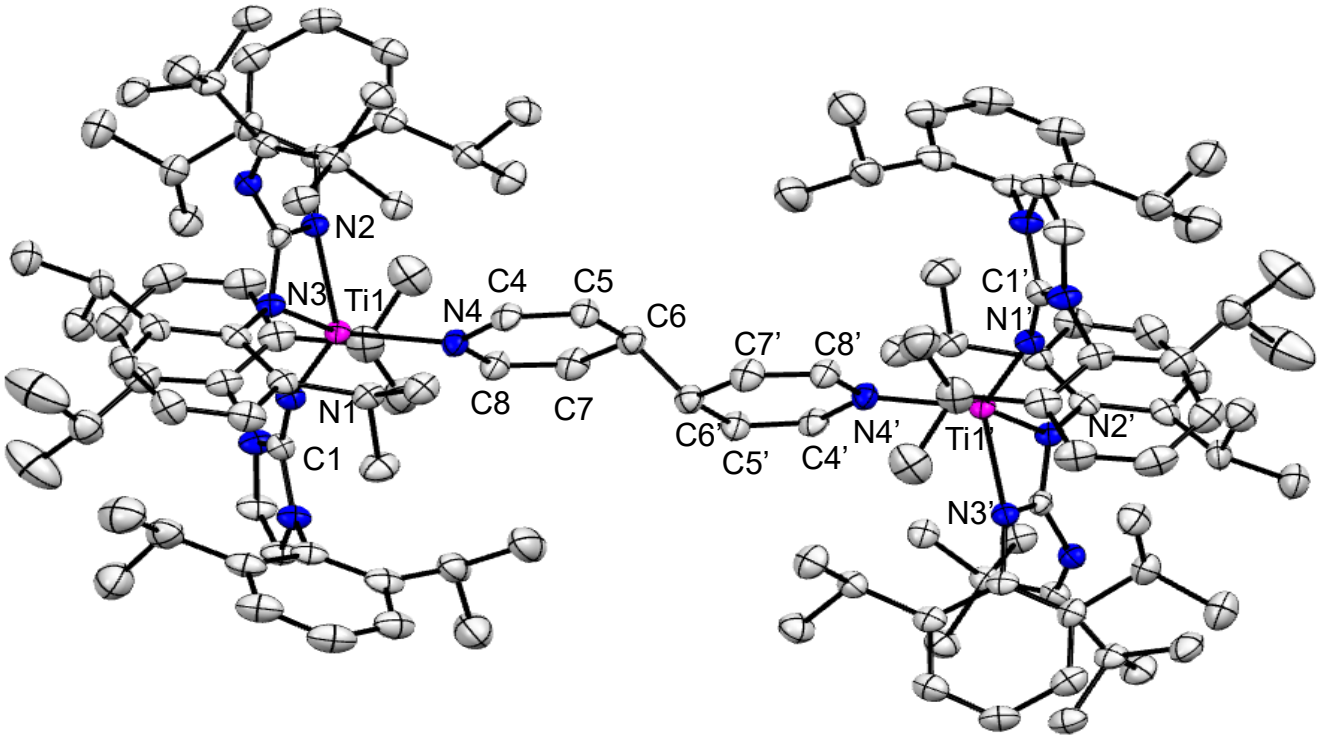

Figure 1.9: Solid-state molecular structure of **1.10** with 50% probability ellipsoids. Selected bond lengths (Å) and angles (º). N4-C4 = 1.400(4), N4-C8 = 1.104(4), C4-C5 = 1.330(5), C5-C6 = 1.506(5), C6-C7 = 1.506(5), and C7-C8 = 1.327(5), C6-C6' = 1.565(0). Ti1-N4 = 2.202(3), Ti1 – N1 = 1.861(3), Ti1-N2 = 2.107(3), Ti1-N3 = 2.123(3), N1-C1 = 1.284(4), Ti1-N1-C1 = 162.1(3)º, N2-Ti1-N3 = 111.4(3)º

As such, the solution EPR spectrum of **1.9** in toluene at 298 K shows a highly isotropic signal at g = 1.957 (Figure 1.10) similar to that observed for **1.7**, signifying a Ti(III) metal-based radical.[52]

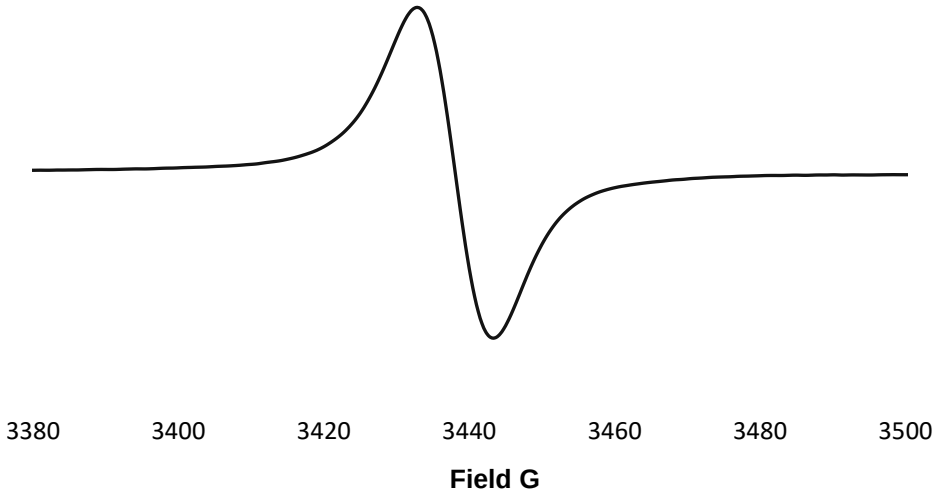

Figure 1.10: EPR spectrum for **1.10** in toluene, 298 K, 9.5 GHz.

Taken together, the reduction of benzophenone and pyridine by **1** provides an approximate range for the redox potential of **1.1** between ca. –2.3 to –3.1 V (vs $Fc^{0/+}$). In comparison to the Ti(II)/(III) redox couple of Tp_2Ti (Tp = hydrotris(pyrazol-1-yl)borate) ($E_{1/2}$ = –1.84 V vs $Fc^{0/+}$),[77] the potential of **1.1** is considerably lower. Of course, these chemical assays are only rough approximations of the Ti(II) redox character of **1** as they do not take into account other thermodynamic parameters which can contribute to the observed electron-transfer reactivity. Nonetheless, these tests with benzophenone and pyridine do illustrate that **1.1** is an operative and potent reductant which effectively behaves as a Ti(II) synthon.

1.2.3 π-Acid Reactivity

As noted above, the addition of excess CO to a solution of **1.1** in benzene leads to the formation of the diamagnetic Ti(II) dicarbonyl complex **1.4**.[51] In our exploration of the redox behavior and Ti(II) synthon character of **1.1**, its reactivity with other π-acids was examined.

Isocyanides have been shown capable of stabilizing Ti(II) complexes,[78-81] and as C≡N-R is isoelectronic and isolobal to CO, this reagent class seemed an appropriate choice for the attempted isolation of a Ti(II) product. Treatment of a brown, thawing benzene solution of **1.1** with 2 equiv of C≡NCy (Cy = cyclohexyl) results in a modest darkening of the solution within a few minutes. Removal of the volatiles affords a dark-brown material that upon dissolution in Et_2O and storage at −25 °C for two days produces a crop of small, yellow crystals. This contrasts the dark red color of **1.4**, and the ^{1}H NMR spectrum of the product in C_6D_6 reveals the formation of a paramagnetic compound with very broad, non-descriptive resonances appearing from 0.0 to 8.5 ppm (Figure 1.11).

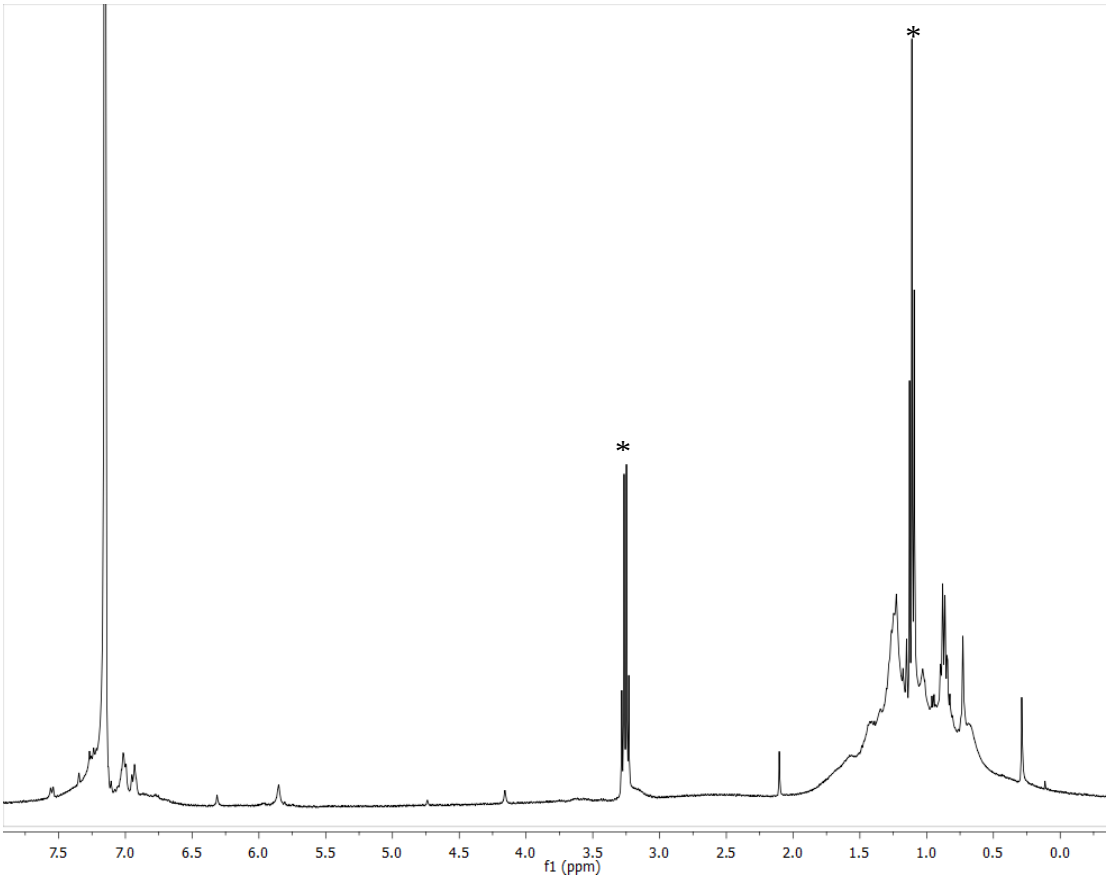

Figure 1.11: ^{1}H NMR spectrum of **1.11** in C_6D_6. Asterix (*) denotes the presence of residual Et_2O.

The synchrotron radiation X-ray crystallographic analysis of the yellow crystals revealed the formation of the Ti(III)-cyanide complex ($Im^{Dipp}N$)(^{ket}guan)Ti(CN)(CNCy) (**1.10**) (Figure 1.12) (eq 1.5) which crystallizes in the P-1 space group

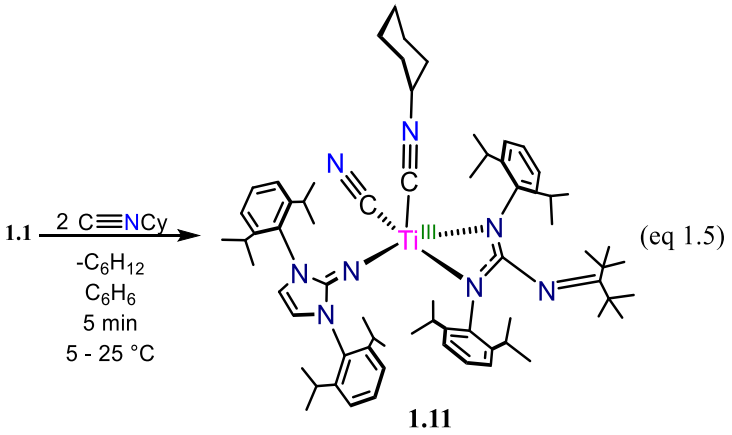

1.11

In the solid-state, **1.11** exhibits severe positional disorder whereby two full molecules are superimposed in slightly offset orientations pivoted at the titanium center, precluding in-depth metrical analysis of the structural parameters. Despite the significant molecular disorder, the titanium center and cyanide moiety are ordered, providing some structural information.

Interestingly, **1.11** is a relatively rare example of a terminally-bound titanium-cyanide complex as only a handful of structurally characterized compounds of this type have been reported.[82-87] The titanium-cyanide bond length of **1.11** (Ti1-C2 = 2.218(6) Å) is similar to that of the Ti(III)-cyanides $[NEt_4]_3[Ti(CN)_6]$ (Ti-C = 2.20 Å (avg.))[83] and $[NEt_4][TpTi(CN)_3]$ (Ti-C = 2.18 Å (avg.))[84] but exhibits a cyanide C-N bond length (C1-N7 = 1.155(5) Å) within the range found for those complexes (1.139(3) – 1.166(4) Å).

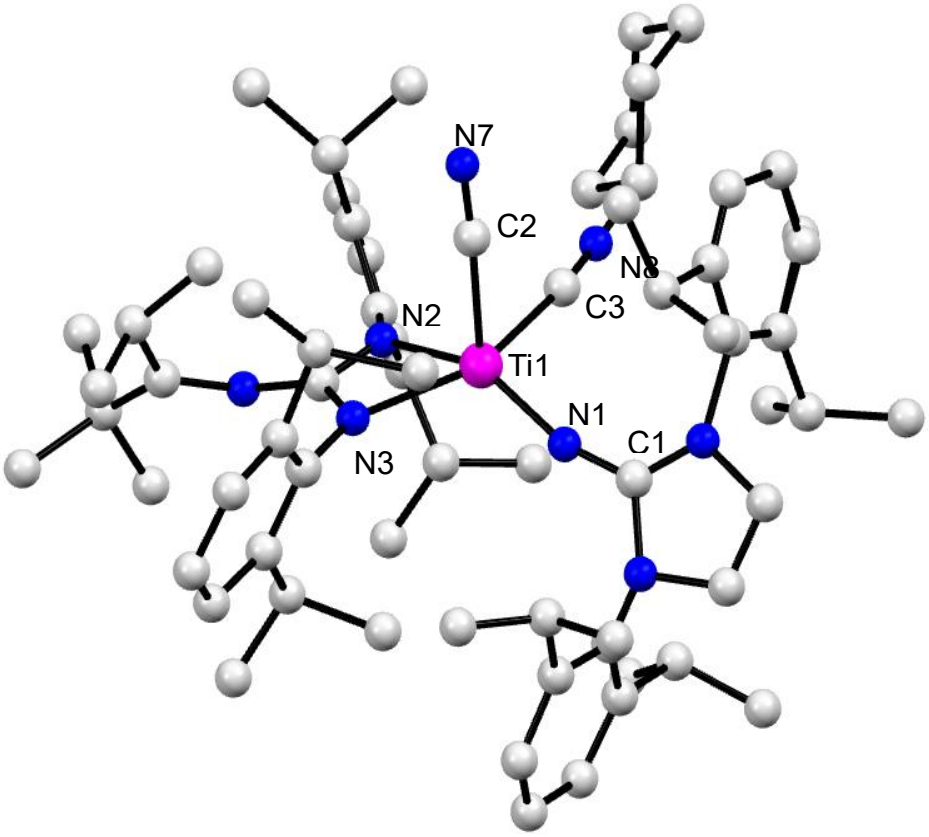

Figure 1.13: Ball and stick solid-state molecular structure of **1.11**.

The infrared spectrum of **1.11** (KBr pellet) displays a ν_{CN} = 2071 cm^{-1} (Figure 1.14) that is in the range of the hexacyanotitanates $[NEt_4]_3[Ti(CN)_6]$ (ν_{CN} = 2017 cm^{-1}) and $K_3[Ti(CN)_6]$ (ν_{CN} = 2088 cm^{-1}),[83] but lower than that found for $[NEt_4][TpTi(CN)_3]$ (ν_{CN} = 2116 and 2103 cm^{-1}),[84] while the cyano stretching frequency of its coordinated CNCy ligand (ν_{CN} = 2278 cm^{-1}) is higher than that reported for the Ti(III) metallocene $Cp^*_2Ti(CNXy)(CCSiMe_3)$ (Xy = xylyl) (ν_{CN} = 2115 cm^{-1})[80] and to that found for $CpTi(CNXy)I_2$ (ν_{CN} = 2156 cm^{-1}).[78]

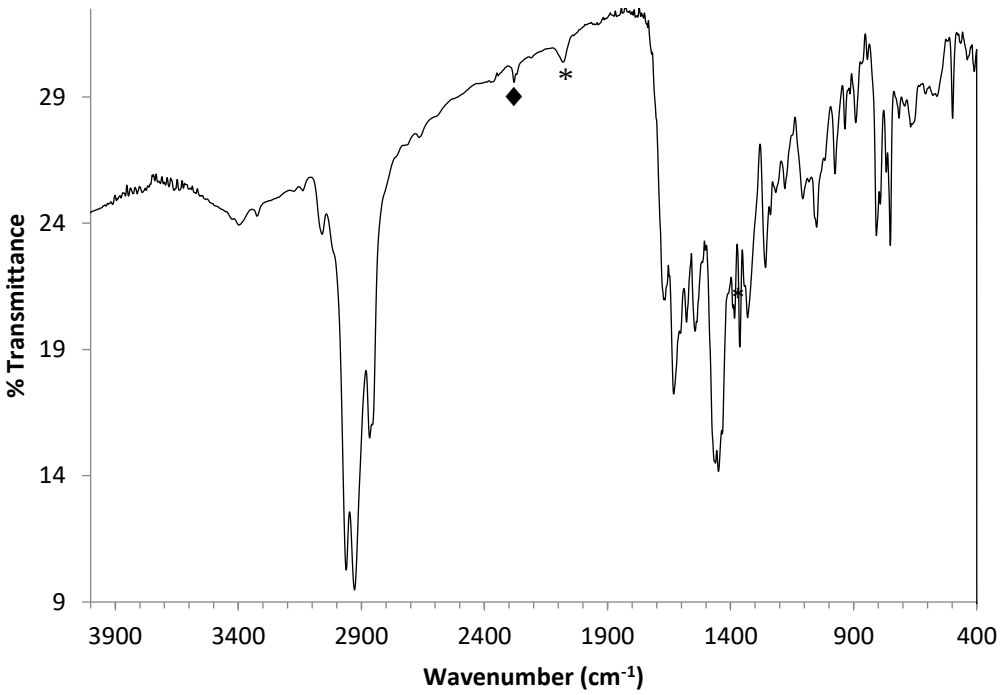

Figure 1.14: IR spectrum (KBr pellet) of **1.11**. Peaks marked with asterisks (*) denotes the CN stretch (2071 cm^{-1}), and with rhombus (♦) the *CN*-Cy stretch (2278 cm^{-1}).

Finally, the EPR spectrum of **1.11** as a solid and in toluene at 298 K exhibit complicated anisotropic signals (Figures 1.15-1.16) in agreement with a low-symmetric ligand environment.

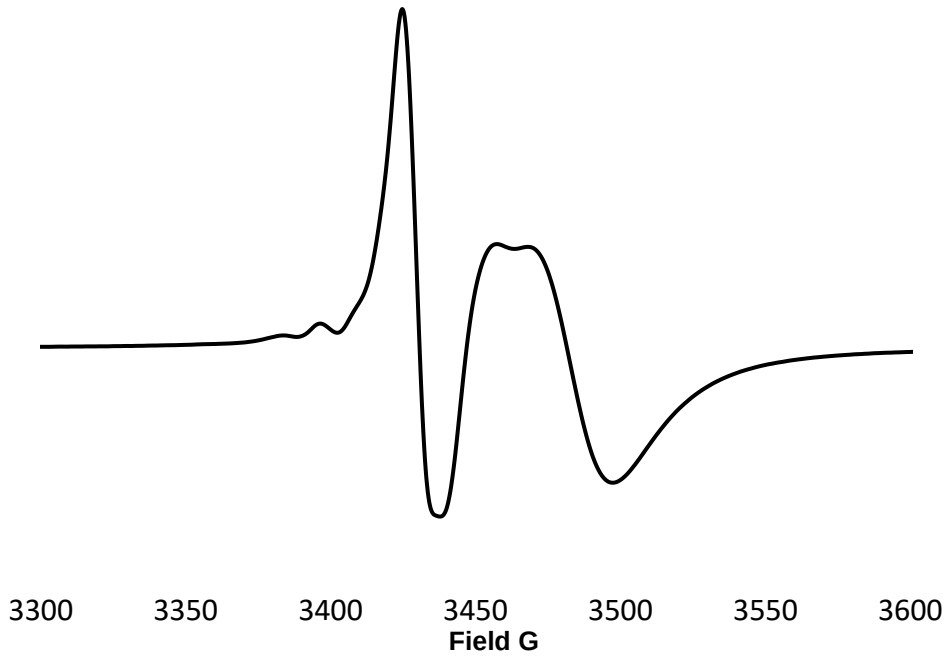

Figure 1.15: EPR spectrum for **1.11** in toluene, 298 K, 9.5 GHz.

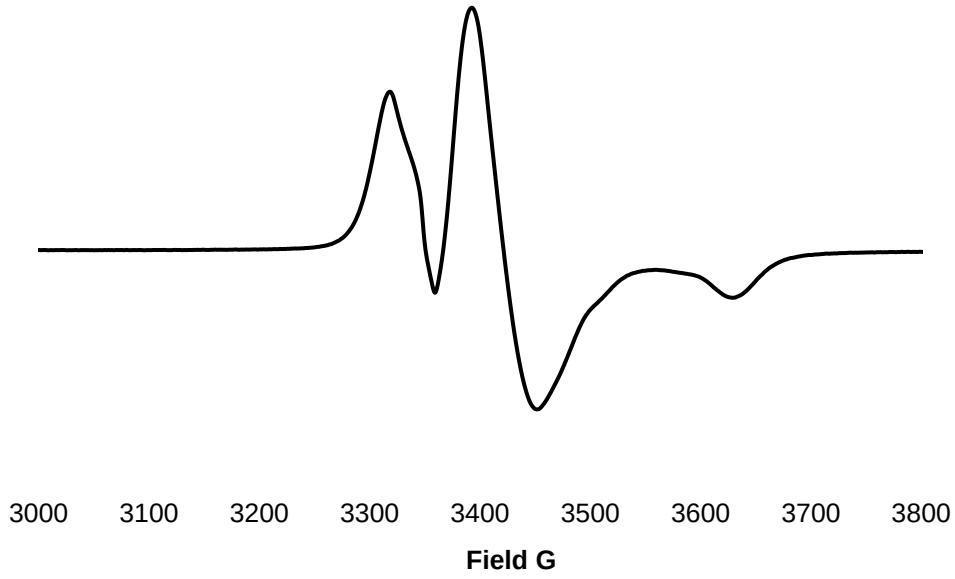

Figure 1.16: Solid-State EPR spectrum for **1.11**, 298 K, 9.5 GHz.

The fate of the isocyanide cyclohexyl fragment in the formation of **1.11** was monitored by ^{1}H NMR spectroscopy, giving a complicated product mixture. Nonetheless, the unexpected formation of **1.11** from the CN-Cy bond scission is not without precedent in the literature. For instance, addition of 3 equiv of C≡N^{t}Bu to Cp*$_2$Ti[(CH$_2$)$_2$CH^{i}Pr] affords the half-sandwich enediamidate Cp*Ti[(N^{t}BuC)$_2$(CH$_2$)$_2$CH(^{i}Pr)](CN) bearing a cyanide ligand.[82] Additionally, treatment of vandocene (Cp*$_2$V) with cyclohexyl cyanide leads to the formation of an intermediate V(II) species that subsequently undergoes free radical isocyanide dealkylation to generate the V(III) complex Cp*$_2$(CN)(CNCy) concomitant with the formation of cyclohexane.[88] This suggests that **1**, akin to Cp*$_2$V, in its reaction with C≡NCy is acting as a reductant, which consequently leads to the observed bond scission through free-radical activation.

The formation of **1.11** prompted us to examine the reactivity of **1.1** with nitriles to test for similar behavior. As such, addition of a slight excess of N≡C^{t}Bu to a thawing benzene solution of **1.1** leads to the formation of a homogeneous yellow solution after five minutes. Removal of the volatiles and recrystallization from concentrated Et$_2$O solutions yields yellow crystals after storage for two days at –25 ºC.

The solid-state molecular structure as revealed by X-ray crystallographic determination is displayed in Figure 1.17 and shows the formation of the cyclometalated Ti(IV)-ketimide complex (Im^{Dipp}N)[(DippN)(2-^{i}PrC$_6$H$_3$-6-(η^2-CH$_3$CH*CH$_2$*)N)C(NC^{t}Bu$_2$)]Ti[NC(H)^{t}Bu] (**1.12**) (eq 1.6). Complex **1.12**·Et$_2$O crystallizes in the triclinic space group P-1 with two full molecules in the asymmetric unit accompanied by a molecule of Et$_2$O. One of the titanium molecules exhibits non-metallated/cyclometalled disorder at two of its Dipp groups, thus only the metrical parameters of the ordered molecule are presented.

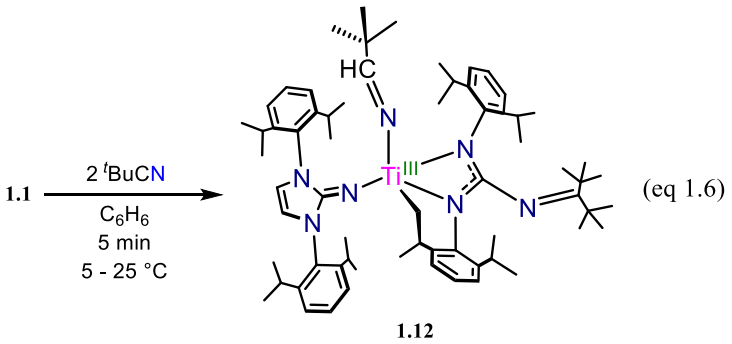

1.12 (eq 1.6)

The Ti-ketimide bond length of **1.12** (Ti1-N7 = 1.914(3) Å) is unremarkable and falls within the established range of titanium-ketimide bonds such as those found in $TiCl(NC^tBu_2)_3$ (Ti-N = 1.82(1) - 1.836(8) Å)[89] and /[(Dipp)NC(CH_3)]$_2$CH}Ti(NCPh_2)/N[P($CH_2{}^t$Bu)$C_6H_2{}^t$Bu$_3$]} (Ti-N = 1.918(3) Å).[90] Furthermore, as compared to other titanium-ketimide complexes which commonly exhibit more linear coordination modes of the ketimide ligand (cf. $TiCl(NC^tBu_2)_3$: Ti-N-C = 170.8(7) – 175.6(7)°), the Ti1-N7-C2 = 155.8(3)º bond angle in **1.12** is rather bent, a likely consequence of the steric congestion about the titanium center. In line with this, the coordination of the ^{Dipp}ImN-group in **1.12** is also bent (Ti1-N3-C32 = 166.9(2)º), yet slightly more linear than that of the

corresponding angle in **1.7** (Ti1-N1-C49 = 158.1(2)°), though the Ti-N_{Im} bond length of Ti1-N3 = 1.842(2) Å in **1.12** is equivalent to the Ti1-N1 = 1.854(2) Å bond of **1.11** within the 3σ-criterion.

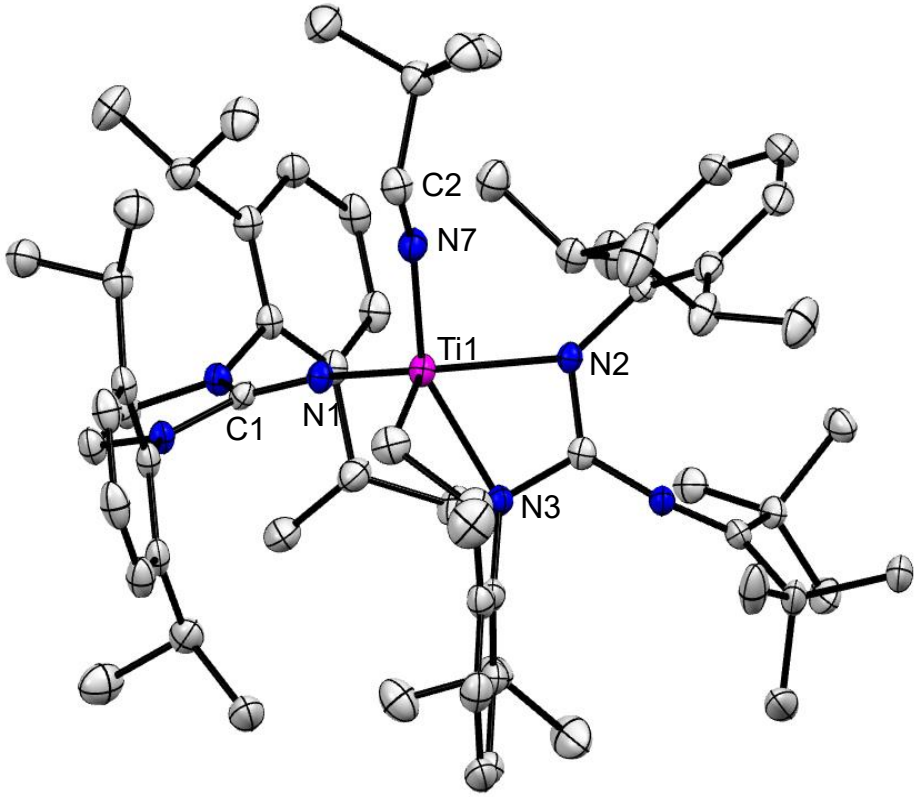

Figure 1.17: Solid-state molecular structure of **1.12** with 50% probability ellipsoids. Selected bond lengths (Å) and angles (º). Ti1-N7 = 1.914(3) Å, Ti1-N1 = 1.842(2) Å, Ti1-N7-C2 = 155.8(3)º, Ti1-N1-C1 = 166.9(2)

The formation of **1.12** suggests the initial reduction of a coordinated nitrile ligand to generate a Ti(III) species with radical character on the nitrile, which subsequently undergoes H-atom abstraction from a pendant isopropyl methyl group. Consequently, this would form a radical isopropyl fragment that then undergoes oxidative bond coupling with the titanium center, rendering the observed Ti(IV) metallacycle **1.12**. This obviously deviates from the synthesis of **1.11** which undergoes isocyanide CN-R bond scission. If the proposed radical mechanism in the formation of

1.12 is the operative pathway, then it conceivable that similar chemistry could be elicited with the Ti(III) organoradical ketyl complex **1.9**.

To test this, heating a benzene solution of **1.9** at 50 ºC for 12 h bleaches the purple solution to give a pale-yellow color and formation of a new diamagnetic product. The ^{1}H NMR spectrum of the new product is complicated (Figure 1.18), suggestive of C_1 symmetry in solution, with spectral features reminiscent of the metallacycle **1.3**.

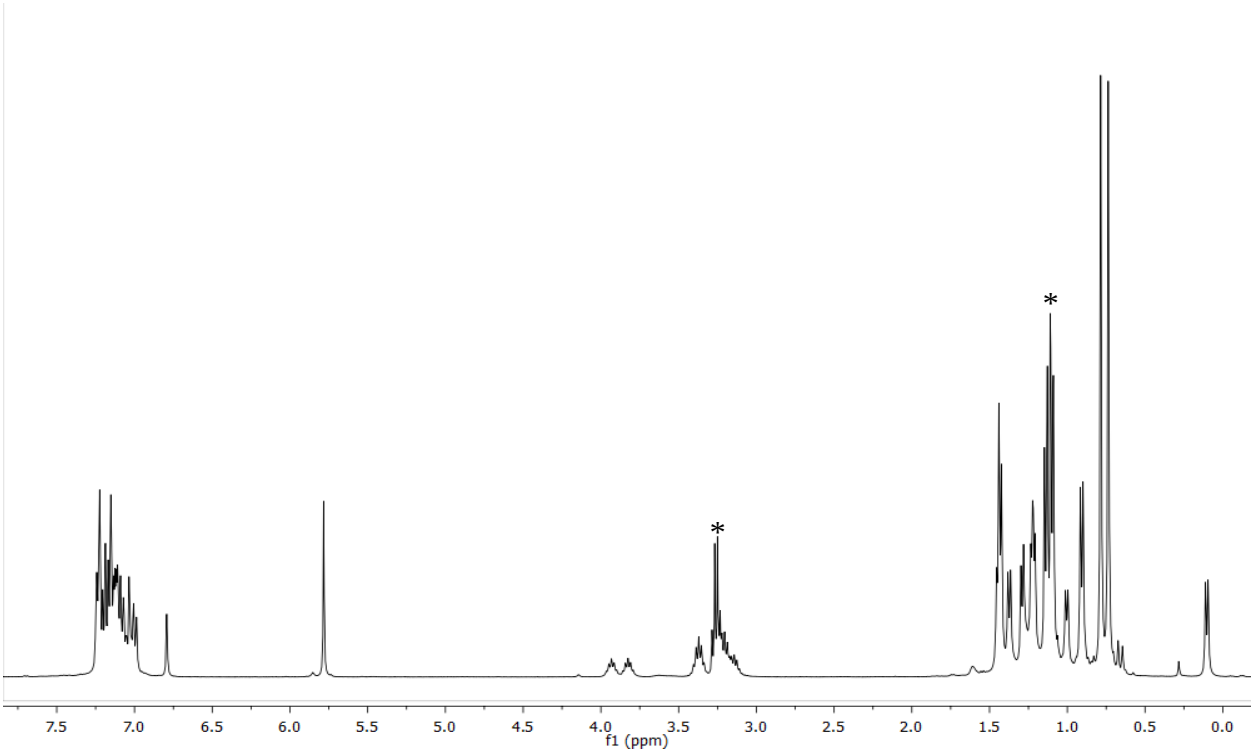

Figure 1.18: ^{1}H NMR spectrum of **1.13** in C_6D_6. Asterix (*) denotes the presence of co-crystallized Et_2O.

Indeed, X-ray crystallographic analysis of single crystals grown from Et_2O at –25 °C shows the formation of the Ti(IV)-alkoxide metallacycle (Im^{Dipp}N)[(DippN)(2-^{i}PrC$_6$H$_3$-6-(η^2-CH$_3$CH*CH$_2$*)N)C(NC^{t}Bu$_2$)]Ti (**1.13**) shown in (Figure 1.19) (eq 1.7).

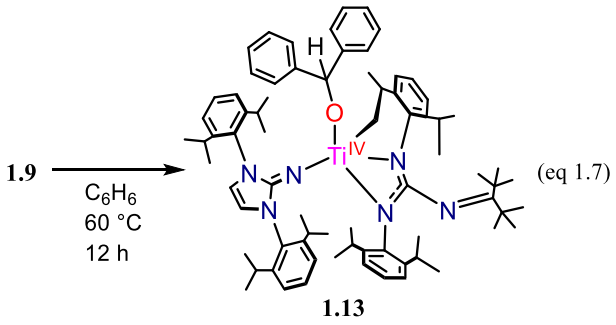

(eq 1.7)

1.13

Complex **1.13**·2Et_2O crystallizes in the P-1 space group with two full molecules in the asymmetric unit. The structural parameters of the two molecules are nearly identical, and the metrical details of only one is discussed for clarity. By far, the most salient feature of **1.13**·2Et_2O is the structural changes that are observed at the reduced benzophenone moiety. The Ti1-O1 = 1.825(9) Å bond length in **1.12**·2Et_2O is slightly shorter than that found in **1.9** (T1-O1 = 1.856(2) Å) while the O1-C1 = 1.416(2) Å bond is significantly elongated in comparison to the corresponding bond in **1.9** (O1-C1 = 1.327(3) Å). Furthermore, the sum of the bond angles around the C1 atom in **1.13**·2Et_2O ($\sum_{C1} \approx 334.5°$) indicate sp^3-hybridation. In total, these structural features are consistent with full reduction of the benzophenone group to a diphenylmethyl alkoxide ligand. In line with this, the parameters of the alkoxide ligand in **1.13**·2Et_2O are comparable to those found for the bis(mesityl)methyl alkoxide groups in the Ti(IV) complex Ti(N^{t}Bu)[OCH(mesityl)$_2$]$_2$(py)$_2$ (Ti-O = 1.875(2) Å; O-C = 1.402(4) Å).[69]

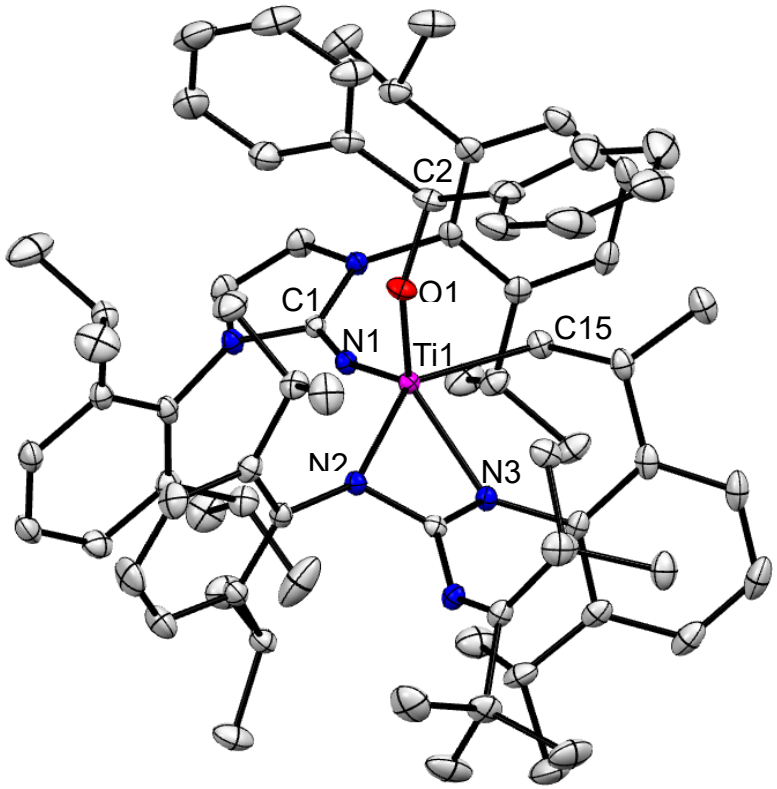

Figure 1.19: Solid-state molecular structure of **1.13** with 50% probability ellipsoids. Selected bond lengths (Å) and angles (º). Ti1-O1 = 1.825(9), Ti1-C15 = 2.121(9), O1-C2 = 1.416(2), Ti1 – N1 = 1.846(9), Ti1-N2 = 2.191(9), Ti1-N3 = 2.117(9), N1-C1 = 1.288(2), Ti1-O1-C9 = 141.6(9), Ti1-N1-C1 = 162.8(9º, N2-Ti1-N3 = 117.1(9)º.

The formation of **1.13** is somewhat surprising as the molecule neither eliminates tetraphenylethylene, as the expected McMurry Coupling product, nor is radical coupling between the benzophenone ketyls observed as in the complexes $Ti(OC•Ph_2)(silox)_3$ and $U(OC•Ph_2)[N(SiMe_3)_2]_3$, which both undergo C-C radical bond coupling to give the dinuclear compounds $(L)_3M[OC(Ph)(C_6H_4)C(Ph)_2O]M(L)_3$ (M = U, L = $N(SiMe)_3$; M = Ti, L = silox).[74, 91] However, the Ti(III) ketyl complexes $Ti(OC•MeR)(silox)_3$ (R = H, Me) do undergo an H-atom abstraction event to give the Ti(IV) alkoxides $Ti(OCHMeR)(silox)_3$.[74]

Altogether, the formation of metallacycles **1.12** and **1.13** indicate a convergent reactivity profile between the addition of pivalonitrile and benzophenone to **1.1**, implicating a Ti(III)-organoradical species as key intermediate generated through the one-electron reduction of the substrate by a highly reducing Ti(II) type synthon. The reactivity of **1.1** towards π-acids such as CO, isocyanide, and nitriles is apparently not straightforward and gives rise to a number of Ti(II)/Ti(III)/Ti(IV) complexes which demonstrates that the redox chemistry of LVEMs is rich and highly varied.

Finally, in an attempt to displace the intramolecular Ti-arene capping interaction of **1.1**, with the compound was dissolved in *o*-difluorobenzene ($C_6H_4F_2$). We reasoned that the increased π-acidity of the partially fluorinated benzene molecule would potentially favor intermolecular arene capture and reduction to give a complex of the type "(^{ket}guan)(Im^{Dipp}N)Ti($C_6H_4F_2$)," though it has been shown in the literature that LVEMs are highly capable of reductively cleaving C-F bonds to give new fluoride products.[92]

Dissolving **1.1** in neat $C_6H_4F_2$ gradually gives way to a yellow color over a 12 h period (eq 8). Removal of the volatiles and extraction into Et_2O, followed by concentration and storage at –25 ºC, yields a crop of yellow crystals after two days. The ^{1}H NMR spectral analysis showed the formation of a diamagnetic product with resonances appearing from 1.30 to 7.50 ppm with a spectral profile consistent with C_1 symmetry in solution (Figure 1.20).

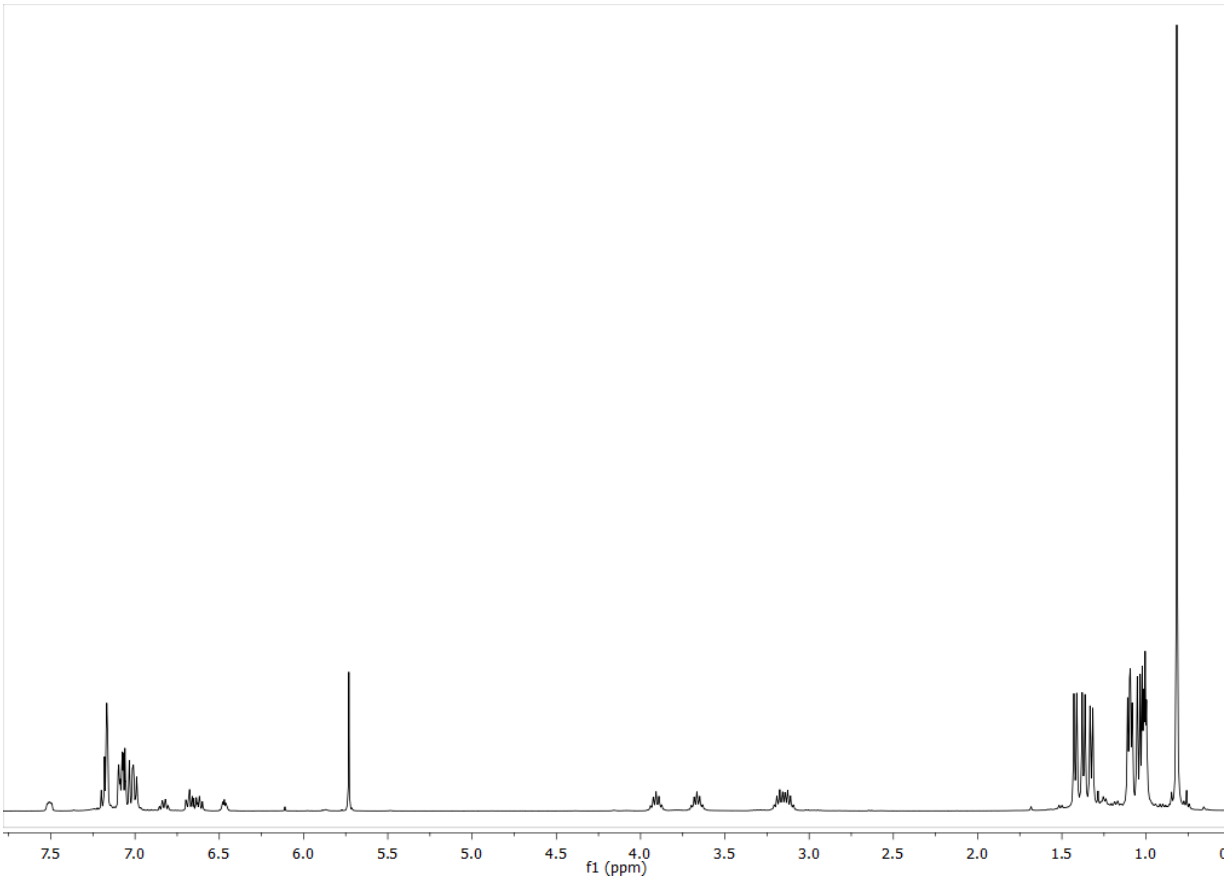

Figure 1.20: ^{1}H NMR spectrum of **1.14** in C_6D_6.

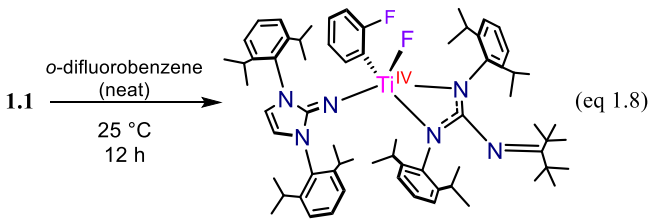

(eq 1.8)

1.14

Elucidation of the solid-state molecular structure by X-ray crystallographic analysis revealed the formation of the Ti(IV) organometallic fluoride complex (^{ket}guan)(Im^{Dipp}N)Ti(F)(C_6H_4F) (**1.14**) (eq 1.8) (Figure 1.22). Crystals of **1.14** were analyzed using synchrotron radiation, yet, the crystals diffracted weakly and only provided sufficient data for atom connectivity, precluding any metrical

analyses. Nonetheless, the solid-state molecular structure of **1.14** conforms to the C_1 solution-phase symmetry observed by NMR analyses.

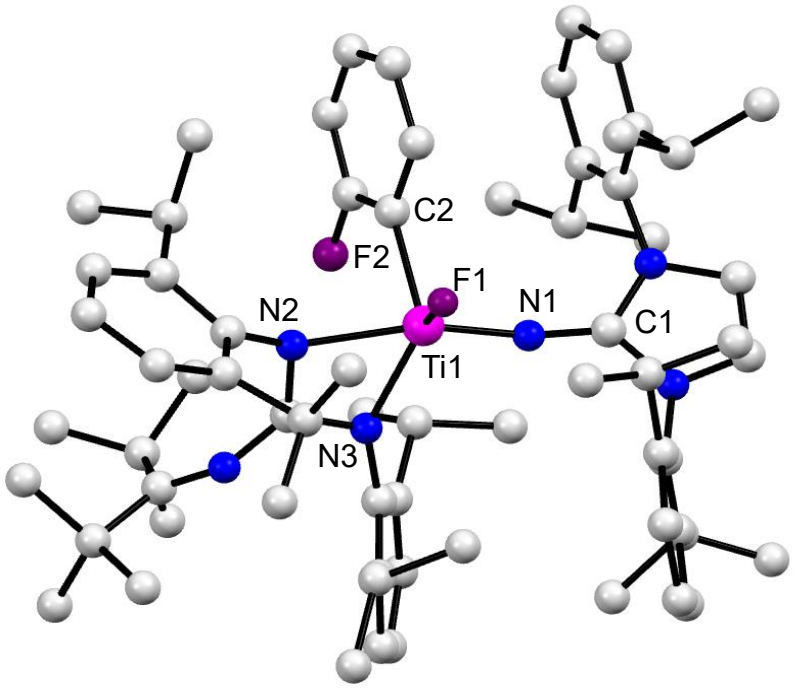

Figure 1.21: Ball and stick model of **1.14** to show atom connectivity.

As noted, the formation of **1.14** is not unexpected and follows the reactivity observed for the low valent Nb(III) complex [(Dipp)NC(CH$_3$)]$_2$CH}Nb(N^{t}Bu), which reacts with fluorinated arenes (Ar-F) to give Nb(V) products of the type /[(Dipp)NC(CH$_3$)]$_2$CH}Nb(N^{t}Bu)(F)(Ar).[92] In the case of the Nb(III) complex, the reaction with fluoroarenes generates a complex mixture of unidentified intermediates when followed by NMR spectroscopy; however, DFT analysis of the Nb(III) reaction indicates initial formation of a capped fluorarene species of the type /[(Dipp)NC(CH$_3$)]$_2$CH}Nb(N^{t}Bu)(η^6-Ar-F) which then undergoes a bimetallic activation step. Given the steric profile of **1.1**, the formation of **1.14** is unlikely to proceed via a bimetallic mechanism, and future studies will be needed to elucidate the C-F cleavage pathway of our system.

Regardless, the formation of **1.14** is further testament of the strong reductive capabilities of **1** and demonstrates a proclivity for two-electron chemistry.

1.2.4 Two-electron Reactivity and Small Molecule Activation

The reactivity of LVEMs (or their synthon equivalents) with chalcogenides or pnictogen group transfer reagents to give terminally-bound, metal-ligand multiply bonded complexes of the type M=E (E = chalocogen, N-R) is well documented in the literature.[56, 64, 93-102] For instance, addition of S_8 to the Zr(II) metallocene $Cp^*_2Zr(CO)_2$ in the presence of pyridine produces the Zr(IV) sulfide complex $Cp^*_2Zr(S)(py)$,[95-96] while addition of N_2O to the Ti(II) synthon $Cp^*_2Ti(H_2CCH_2)$ in a mixture of THF and pyridine affords the Ti(IV) oxo $Cp^*_2Ti(O)(py)$.[93] In both of these examples, pyridine coordination is needed to prevent chalcogenide bridging. Moreover, similar reactivity towards chalcogenides is observed in the titanium complexes /$[PhC(NSiMe_3)_2]_2Ti\}_2(N_2)$ and Tp_2Ti.[64, 97] Alternatively, titanium imidos can be synthesized through a host of reactions including the treatment of Ti(II) sources with hydrazine or organoazide reagents.[56, 99, 103]

Leveraging the two-electron redox chemistry of **1.1**, a series of chalcogenide and imido complexes were targeted in order to assess the efficacy of our $[(^{ket}guan)(Im^{Dipp}N)Ti]^{n+}$ platform to access and stabilize metal-ligand multiple bonds. Treatment of benzene or Et_2O solutions of **1.1** with N_2O, $1/8^{th}$ eq of S_8, or excess elemental selenium leads to the formation of the respective Ti(IV) chalcogenides $(^{ket}guan)(Im^{Dipp}N)Ti(E)$ (E = O (**1.15**), S (**1.16**), Se (**1.17**)) (Scheme 1) as dark red to dark orange solids. The reaction between **1** and N_2O to give **1.15** is clean; however, use of elemental sulfur or selenium leads to several side products in the reactions of **1.17** and **1.18**. These side products can be eliminated or greatly diminished by the use of 1 equiv of $SPPh_3$ or $SePPh_3$ to give the sulfido and selenido complexes in improved yields of 61 and 71%, respectively. It must be noted that the use of $S{=}PPh_3$ as transfer reagent generates PPh_3 which we have found

difficult to completely remove from samples of **1.17** due to comparable solubility properties. Additionally, treatment of **1** with excess propylene sulfide leads to the formation of the Ti(IV) disulfide (^{ket}guan)(Im^{Dipp}NTi(η^2-S_2) **(1.18)** (Scheme 1). (N.B. Compound **1.16** can by synthesized from the comproportination reaction of **1.1** and **1.18** or from the addition of elemental mercury to **1.18**) The reaction between **1** and tellurium or Te=PPh_3 seems to generate a new compound consistent with a formulation of (^{ket}guan)(Im^{Dipp}N)Ti(Te), but the reaction is slow, very low yielding, and complicated by the competitive formation of **1.3** from the prolonged stirring of **1.1**.

Similarly, the addition of one equiv of Me_3SiN_3 or 1-azidoadamantane (AdN_3) to stirring C_6H_6 solutions of **1.1** result in a rapid color change of the solution from dark brown to red, accompanied by the evolution of N_2, to give the Ti(IV) imido compounds (^{ket}guan)(Im^{Dipp}N)Ti(NR) (R = Me_3Si (**1.19**), Ad (**1.20**)) (Scheme 2) in 88-81% yields.

Single crystals of **1.15**·Et_2O, 1.16·Et_2O, **1.17**·Et_2O, 1.18·Et_2O, **1.19**·Et_2O, and **1.20**·Et_2O (Figure 1.13-1.18) can be readily grown out of concentrated Et_2O solutions that have been stored at –25 °C for at least several days. Despite their similarities, the molecules crystallize across a number of crystallographic systems in the P-1, $P2_1/c$, $P2_1/c$, Pc, $P2_1$, and $P2_1$ space groups, respectively. The compounds are structurally analogous and show the chalcogenide atom or imido ligand sitting in the apical position within a pocket formed by the peripheral Dipp groups.

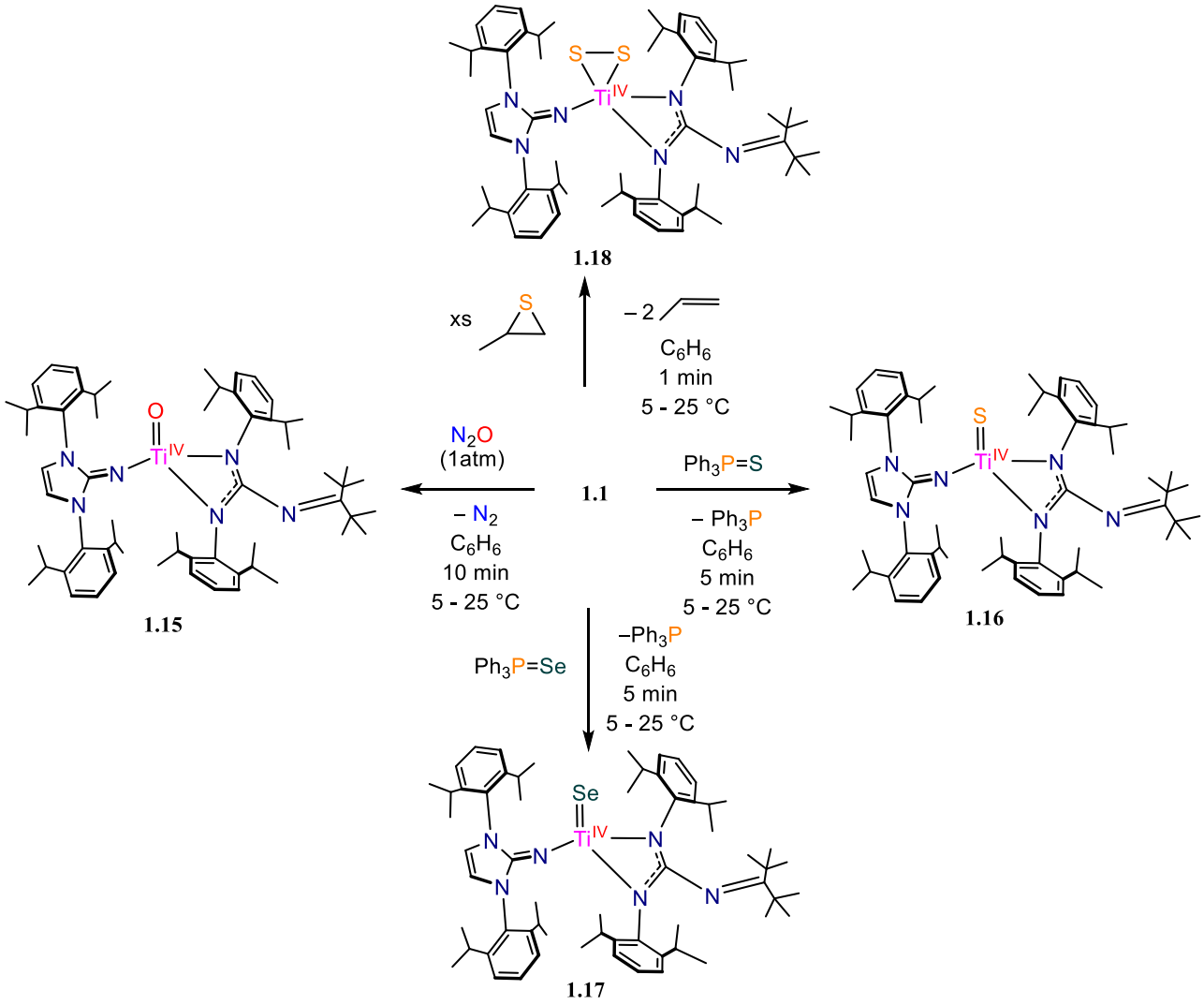

Scheme 1.1: Atom transfer reactions.

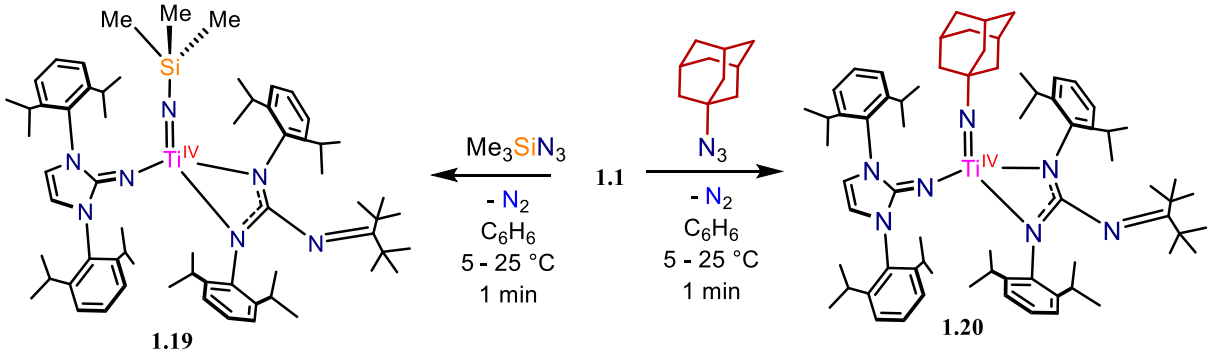

Scheme 1.2: Synthesis of titanium imido's via azide reduction.

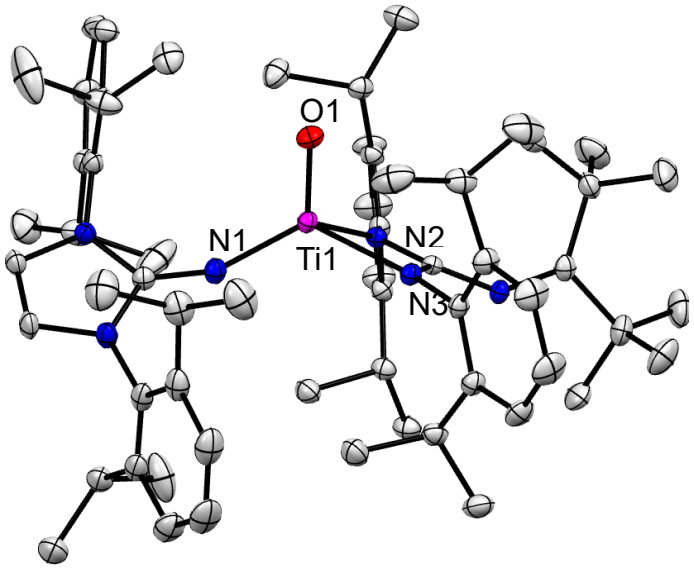

Figure 1.22: Solid-state molecular structure of **1.15** with 50% probability ellipsoids. Selected bond lengths (Å) and angles (º). Ti1-O1 = 1.642(1), Ti1 – N1 = 1.873(1), Ti1-N2 = 2.094(9), Ti1-N3 = 2.104(9) Å, N1-C1 = 1.290(9), Ti1-N1-C1 = 157.9(1)º, N2-Ti1-N3 = 112.4(9)º

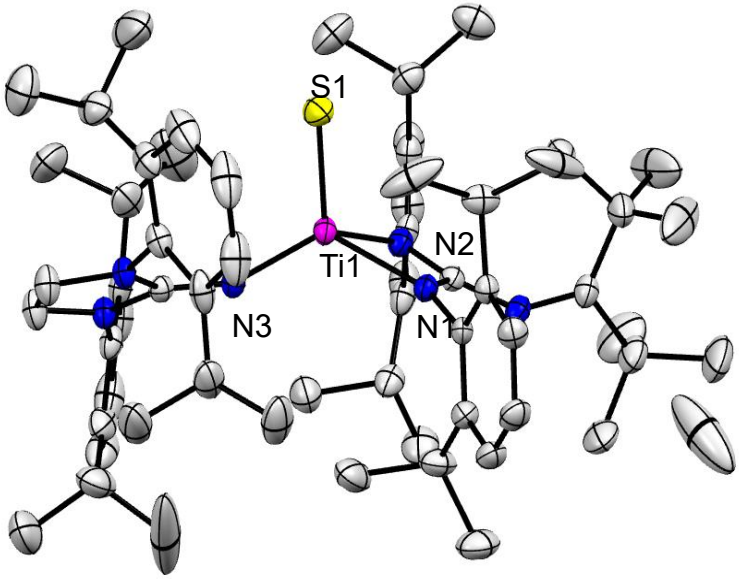

Figure 1.23: Solid-state molecular structure of **1.16** with 50% probability ellipsoids. Selected bond lengths (Å) and angles (º). Ti1-S1 = 2.132(1), Ti1 – N1 = 1.840(2), Ti1-N2

= 2.080(2) Å, Ti1-N3 = 2.067(2), N1-C1 = 1.298(3), Ti1-N1-C1 = 153.1(2), N2-Ti1-N3 = 112.2(2)

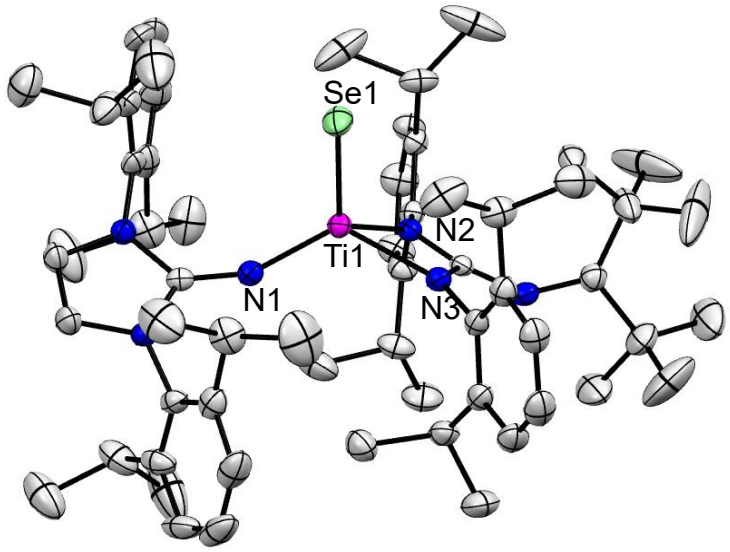

Figure 1.24: Solid-state molecular structure of **1.17** with 50% probability ellipsoids. Selected bond lengths (Å) and angles (º). Ti1-Se1 = 2.295(7), Ti1 – N1 = 1.840(2), Ti1-N2 = 2.080(2) Å, Ti1-N3 = 2.067(2), N1-C1 = 1.298(3), Ti1-N1-C1 = 153.1(2)º, N2-Ti1-N3 = 112.2(2)

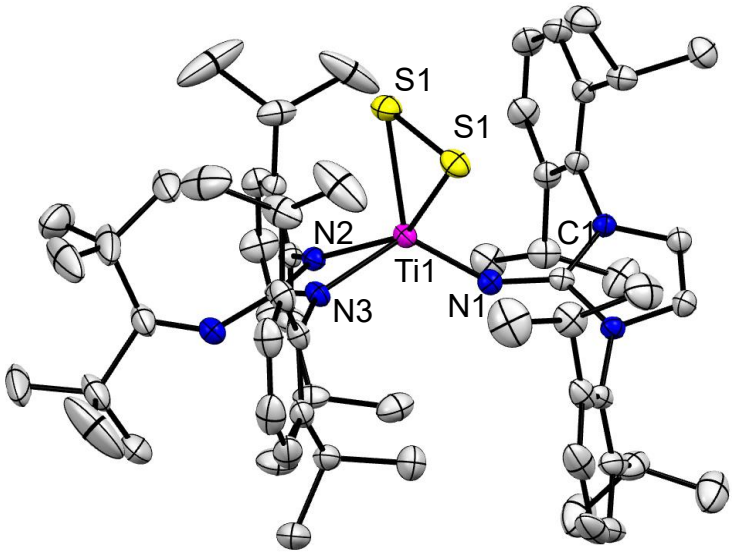

Figure 1.25: Solid-state molecular structure of **1.18** with 50% probability ellipsoids. Selected bond lengths (Å) and angles (º). Ti1-S1 = 2.312(6), Ti1-S1 = 2.334(2), Ti1 – N1 = 1.832(9), Ti1-N2 = 2.152(9) Å, Ti1-N3 = 2.063(9), N1-C1 = 1.298(2), Ti1-N1-C1 = 141.6(9), N2-Ti1-N3 = 111.6(9), Ti1-S1-S2 = 62.9(2)

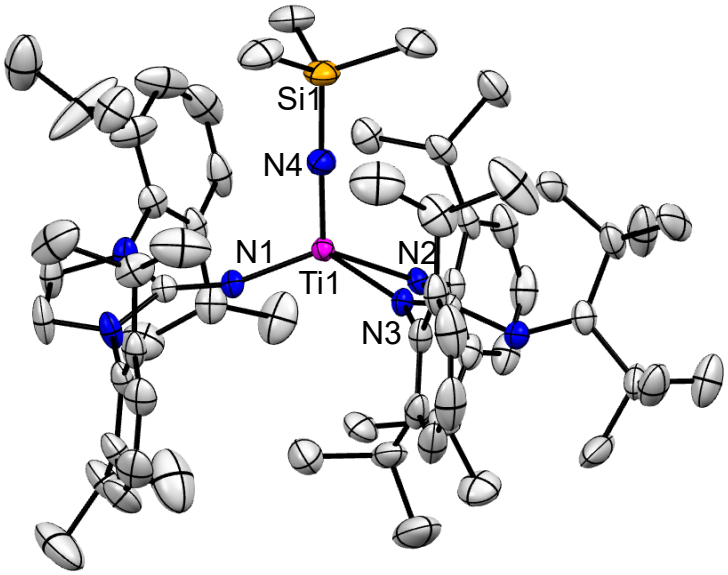

Figure 1.26: Solid-state molecular structure of **1.19** with 50% probability ellipsoids. Selected bond lengths (Å) and angles (º). Ti1 – N1 = 1.879(3), Ti1-N2 = 2.118(4) Å, Ti1-N3 = 2.101(4), N1-C1 = 1.280(5), Ti1 – N4 = 1.718(4), N4 – Si1 = 1.719(4) Ti1-N1-C1 = 162.5(3), N2-Ti1-N3 = 112.8(4), Ti1-N4-Si1 = 176.1(4).

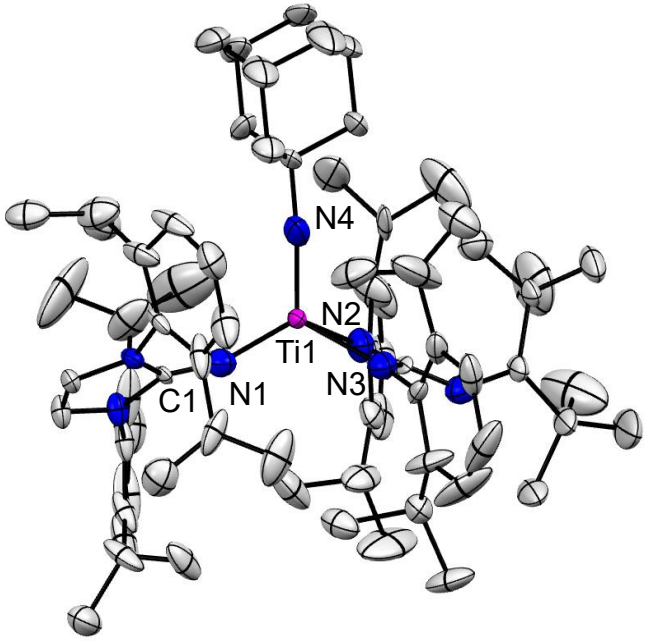

Figure 1.27: Solid-state molecular structure of **1.20** with 50% probability ellipsoids to show atom connectivity.

Table 1.1: Select solid-state metrical parameters.

Compound	Ti=E (Å)	Ti-N_{Im} (Å)	Ti-N_{Im}-C_{Im} (°)
1.15·Et_2O	1.642(1)	1.873(1)	157.9(2)
1.16·Et_2O	2.132(1)	1.840(2)	153.1(2)
1.17·Et_2O	2.296(1)	1.839(3)	154.0(2)
1.18·Et_2O	–	1.83 (avg.)	146.7 (avg)
1.19·Et_2O	1.721(4)	1.880(4)	162.7(3)
1.20·Et_2O	1.75(1)	1.898(9)	162.7(6)

Titanium oxo and imido complexes are well known and the Ti=O bond in **1.15**·Et_2O (Ti1-O1 = 1.642(1) Å) and the Ti=NR bonds in **1.19**·Et_2O (Ti1-N7 = 1.721(4) Å) and **1.20**·Et_2O (Ti1-N7 = 1.75(1) Å) are well within the normal bond length ranges (cf. $Cp^*_2Ti(O)(py)$: Ti-O = 1.665(3) Å; (η^5-$C_5H_4SiMe_3)_2Ti(NSiMe_3)$: Ti-N = 1.722(4) Å).[93, 101] On the other hand, **1.16**·Et_2O and **17**·Et_2O

join the ranks of only a handful of heavier Ti=E (E = S;[100, 104-108] Se[77, 97]) chalcogenide complexes that have been reported; yet, the titanium-chalcogenide bonds in **1.16**·Et_2O (Ti1-S1 = 2.132(1) Å) and **1.17**·Et_2O (Ti1-Se1 = 2.296(1) Å) are comparable to known Ti=E bond distances (cf. $[PhC(NSiMe_3)_2]_2$Ti(S)(py): Ti-S =2.139(1) Å; (κ^3-Tp)(κ_2-Tp)Ti(Se): Ti-Se = 2.254(1) Å).[97, 100] Moreover, titanium-disulfides are relatively rare though well-studied,[56, 64, 94, 97, 108-111] and the Ti-S bonds in **1.18**·Et_2O (Ti-S = 2.32 Å (avg)) are close to those found for (TpTP)Ti(S_2) (TpTp = tetraphenyl porphyrin) (Ti-S = 2.30 Å (avg)).[109]

The ^{1}H NMR spectra of **1.15** – **1.17** (Figures 1.29-1.31) and **1.19-1.20** (Figures 1.33-1.34) in C_6D_6 are qualitatively identical and show a resonance pattern consistent with C_s symmetry in solution where the Ti-NIm bond does not appear rotationally restricted on the NMR timescale, leading to one isopropyl methine and one olefinic proton signal attributable to the imidazolin-2-iminato group in a 4:2 ratio, respectively. Interestingly, the resonance peak of the methine protons of the ^{Ket}guan- ligand in closest proximity to the 'E'-group are a spectral hallmark of these compounds. These protons are highly deshielded, appearing from 4.69 ppm in **1.15**·Et_2O to 5.97 ppm in **1.17**·Et_2O, though there seems to be no obvious correlation between the relative electronegativity of the chalocenide or imido groups and the chemical shift values of the methine protons.

A similar spectral feature has been observed in the the Ti(IV) imido $[HC(NDipp)_2]_2$Ti(Ntolyl) which displays two distinct methine resonances in its ^{1}H NMR spectrum with one set appearing more deshielded at 4.58 ppm,[112] which is near the corresponding peak value of 4.73 ppm found for **1.19** and **1.20**. This dishielding effect appears to be a solution-phase phenomenon as the distance of the Ti=E--H bonds of the calculated proton positions in the solid-state structures of **1.15**·Et_2O – **1.20**·Et_2O are unexceptional (e.g. Se1-H48 = 2.98 Å in **1.17**·Et_2O).

Interestingly, the ^{Ket}guan- ligand environment of **1.18** is highly dynamic and is not observed in NMR time scale at room temperature (Figure 1.32).

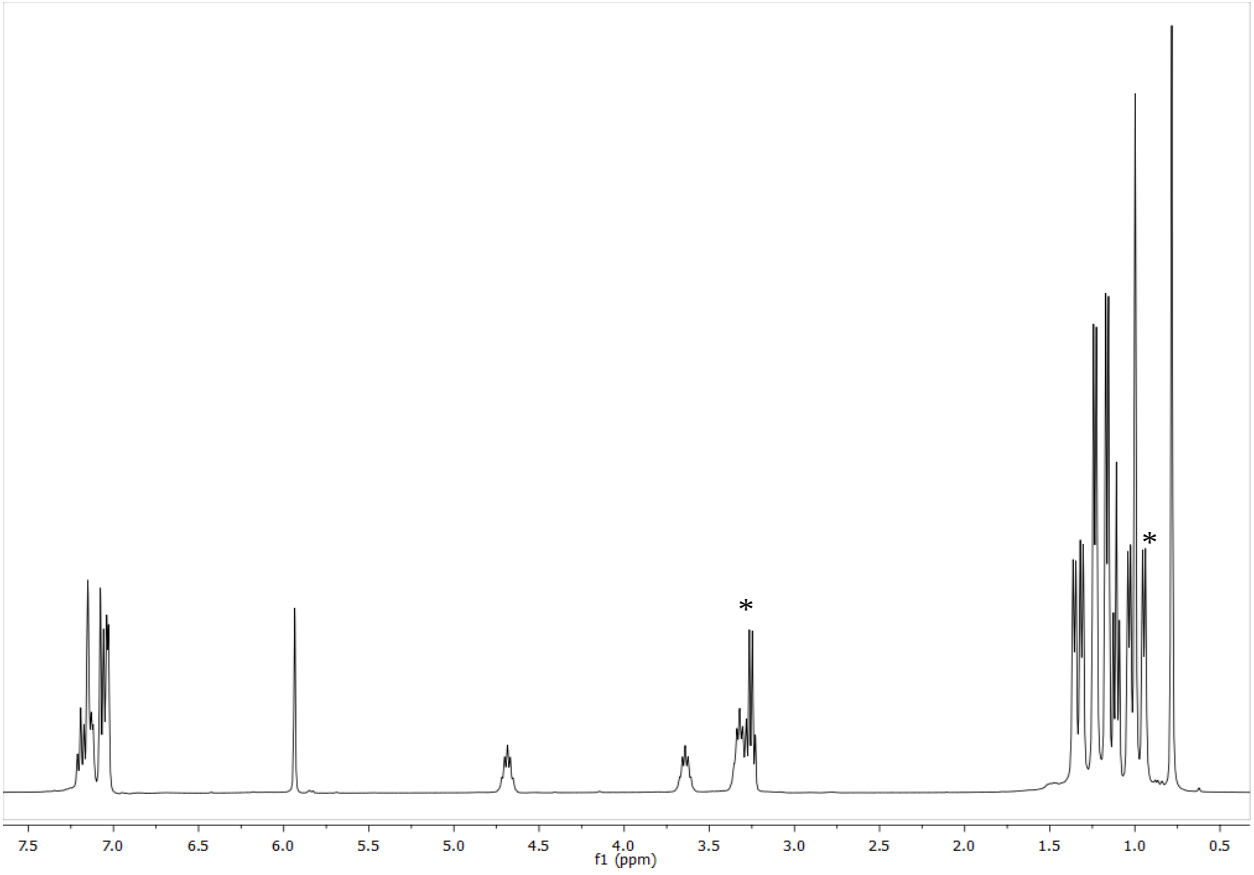

Figure 1.28: ^{1}H NMR spectrum of **1.15** in C_6D_6. Asterisks (*) denote presence of residual co-crystallized Et_2O.

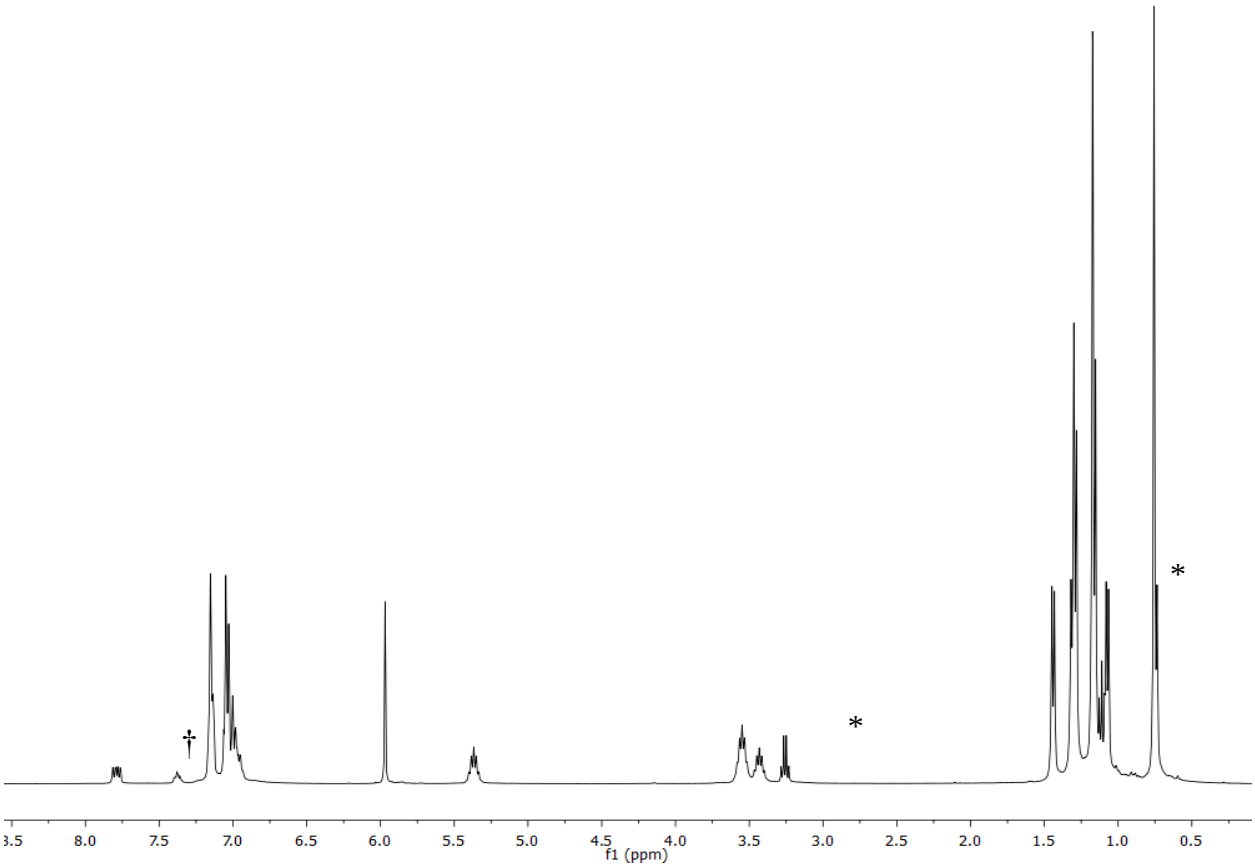

Figure 1.29: ^{1}H NMR spectrum of **1.16** in C_6D_6. Asterisks (*) denote presence of residual co-crystallized Et_2O. Dagger denotes the presence of residual PPh_3

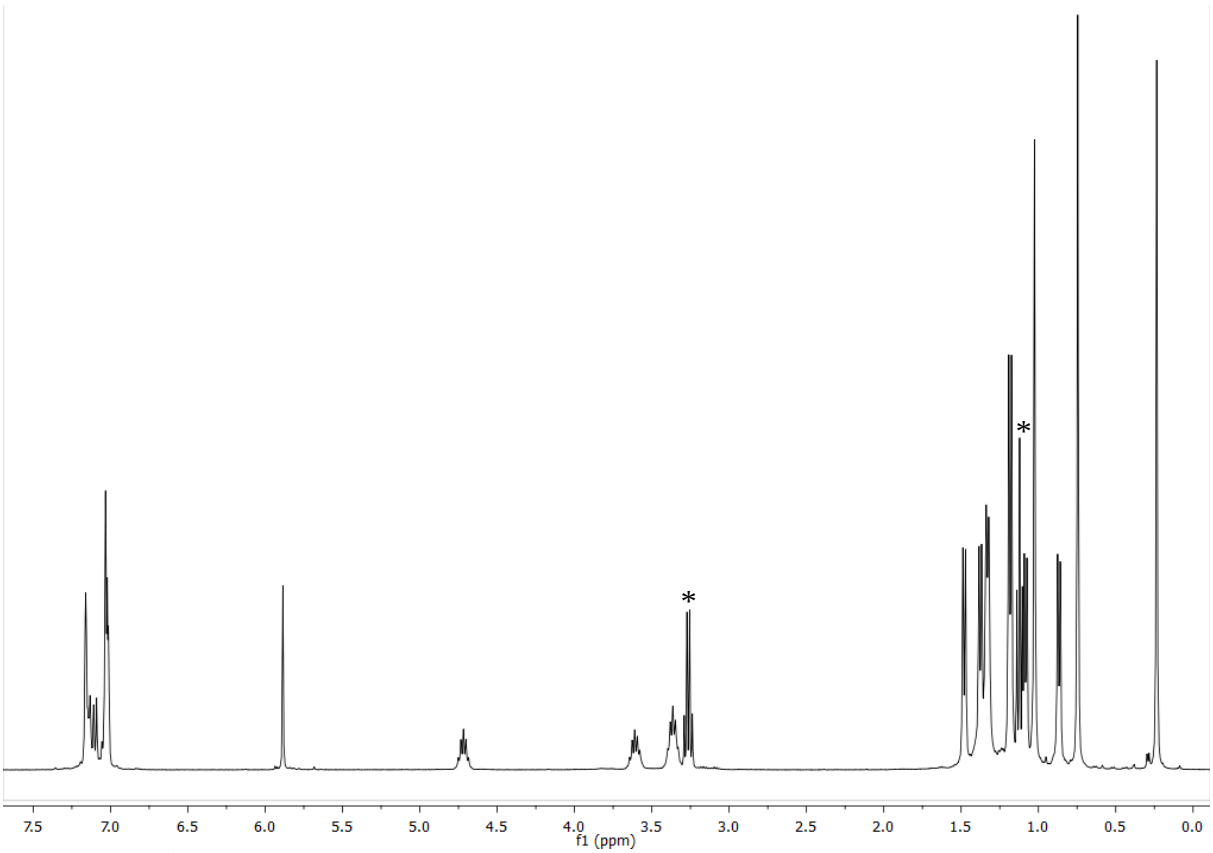

Figure 1.30: ^{1}H NMR spectrum of **1.17** in C_6D_6. Asterisks (*) denote presence of co-crystallized Et_2O.

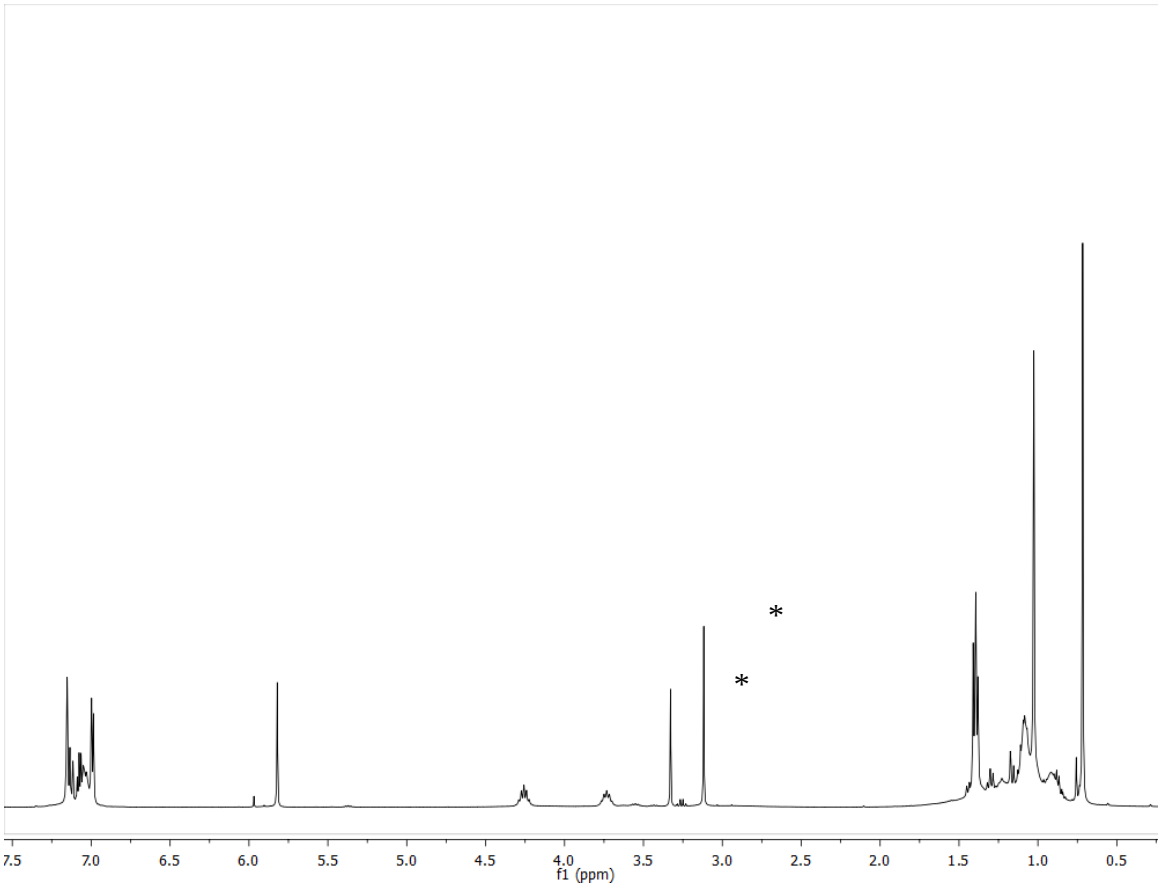

Figure 1.31: ^{1}H NMR spectrum of **1.18** in C_6D_6. Asterisks denote presence of residual co-crystallized DME.

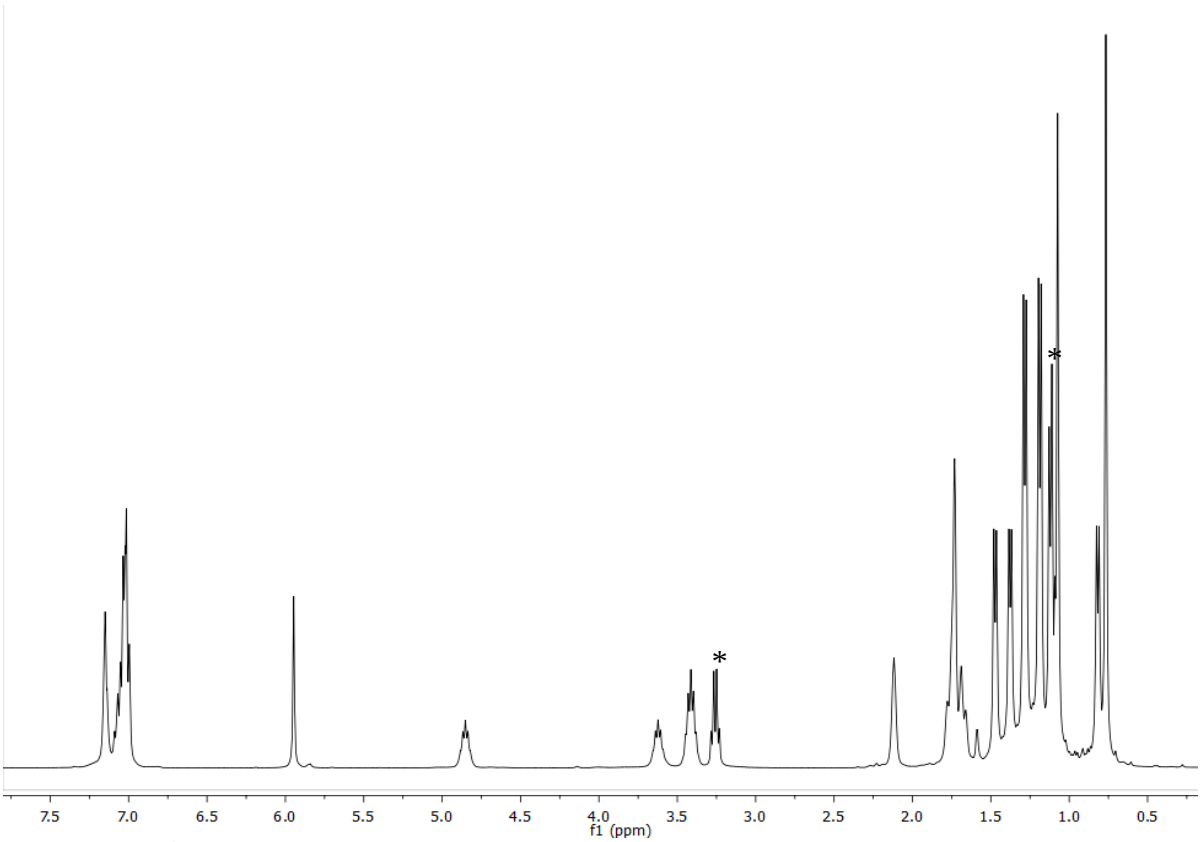

Figure 1.32: ^{1}H NMR spectrum of **1.19** in C_6D_6. Asterisks denote presence of residual co-crystallized Et_2O.

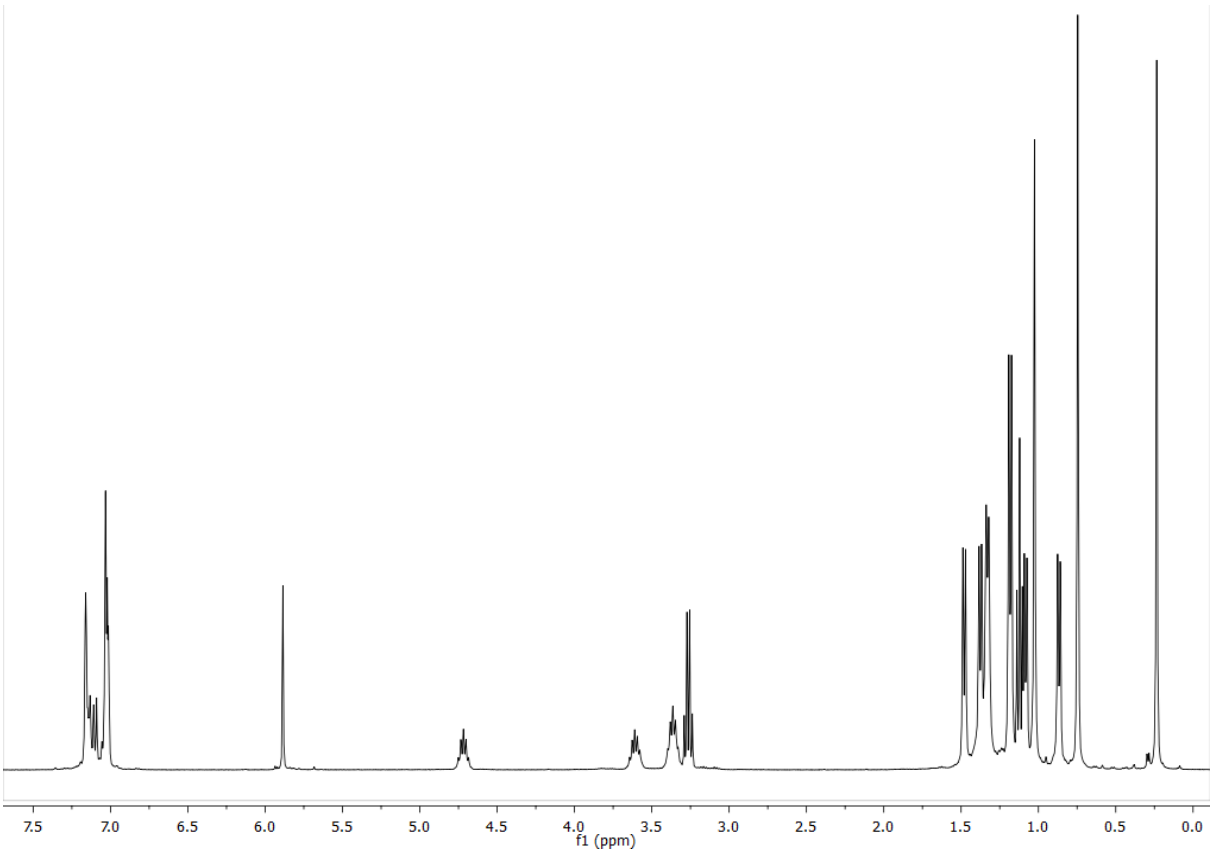

Figure 1.33: ^{1}H NMR spectrum of **1.20** in C_6D_6. Asterisks denote presence of residual co-crystallized Et_2O.

1.3 CONCLUSIONS

We recently reported the synthesis of the intramolecularly arene-masked titanium complex (^{ket}guan)(η^6-Im^{Dipp}N)Ti (**1.1**) which is best formulated as a Ti(IV) compound coordinated to a redox non-innocent 1,4-cyclohexadiene dianion formed by reduction of a peripheral imidazolin-2-iminato Dipp group.[51] In this canonical form, the metal center can be formally described as high-valent, d^0 titanium. Nonetheless, we haven previously shown that **1.1** behaves as a potent two-electron reductant that can reductively activate C-H bonds. This reactivity suggests that **1.1** may be best treated as a Ti(II) synthon. Accordingly, we have performed an exhaustive examination of the redox chemistry of **1.1**. Through its reactivity with substrates such as

benzophenone or pyridine, to give the Ti(III) complexes (^{ket}guan)(Im^{Dipp}N)Ti(η^1-*O*CPh$_2$) (**1.9**) and [(^{ket}guan)(Im^{Dipp}N)Ti]$_2$[μ-(NC$_5$H$_5$-H$_5$C$_5$N)] (**1.10**), the one-electron reduction of these substrates approximately bookends the "Ti(II)/(III)" redox potential of **1.1** between –2.3 to –3.1 V (vs Fc$^{0/+}$). In line with this, Na/Hg amalgam is insufficient to reduce (^{ket}guan)(Im^{Dipp}N)TiCl$_2$ (**1.6**) to **1.1** but instead gives (^{ket}guan)(Im^{Dipp}N)TiCl (**1.7**). Notably, treatment of **1.1** with π-acids leads to a host of products from the bona fide Ti(II) dicarbonyl (^{ket}guan)(Im^{Dipp}N)Ti(CO)$_2$ (**1.4**)[51] to the Ti(III) and Ti(IV) complexes (^{ket}guan)(Im^{Dipp}N)Ti(CN)(CNCy) (**1.11**) and (Im^{Dipp}N)[(DippN)(2-^{i}PrC$_6$H$_3$-6-(η^2-CH$_3$CH*CH$_2$*)N)C(NC^{t}Bu$_2$)]Ti[NC(H)^{t}Bu] (**1.12**), with the latter two products forming as a consequence of the one-electron reduction of the π-acid. The propensity of **1** to effect two-electron chemistry was surveyed through its reactivity with chalcogens and organoazides to generate the Ti(IV) complexes (^{ket}guan)(Im^{Dipp}N)Ti (E) (E = O (**1.14**), S (**1.15**), Se (**1.16**), S$_2$ (**.17**), Me$_3$SiN (**1.18**), AdN (**1.19**)). The synthesis of **1.14** – **1.19** further corroborates the Ti(II) character of **1.1** and unequivocally shows that the [(^{ket}guan)(Im^{Dipp}N)Ti]$^{n+}$ manifold can readily accommodate titanium metal-ligand multiple bonds. In summary, the redox chemistry of **1.1** in its capacity as a Ti(II) synthon clearly shows the chemical variety of low-valent early metals (LVEMs) and their ability to reductively activate a host of substrates. We are continuing to study the chemistry of **1.1** and its less sterically encumbering analogs for the unique activation of other small molecules.

1.4 EXPERIMENTAL SECTION

1.4.1 General Considerations

All air and moisture-sensitive operations were performed in a M. Braun dry box under an atmosphere of purified nitrogen or using high vacuum standard Schlenk techniques. Benzene, Et$_2$O, hexanes, pentane, toluene and THF were dried using a Pure Process Technology Solvent Purification System and subsequently stored under a dinitrogen atmosphere over activated 4 Å

molecular sieves. All deuterated solvents were purchased from Cambridge Isotope Laboratories Inc. The deuterated solvents, 1,2-Diflourobenzene and pivalonitrile were degassed by three freeze-pump-thaw cycles and were dried over activated 4 Å molecular sieves for 24 h prior to use. The Celite and the 4 Å molecular sieves were heated to 150 ºC for at least 24 h and then cooled under vacuum. Lithium Triflate was purchased from Alfa Aesar. All other reagents were purchased from commercial sources and used as received. NMR spectra were recorded on a Bruker AVANCE III 400 MHz spectrometer. Resonance assignments in the ^{13}C NMR spectra were based upon $^{1}H - ^{13}C$ HSQC 2D correlation spectra. ^{1}H NMR and ^{13}C NMR spectra are referenced to the residual ^{1}H solvent peaks as internal standards or the characteristic ^{13}C resonances of the solvent. ^{19}F spectra were referenced to external α,α,α-trifluorotoluene (-63.72 ppm relative to $CFCl_3$ at 0 ppm). The X-band (~ 9.5 GHz) EPR spectrum was obtained using a BrukerEMXplus spectrometer with an ER073 magnet at room temperature. IR data were collected using a Thermo Scientific Nicolet iS5 spectrometer. UV-vis/NIR spectra were recorded on a Zhengzhou Nanbei instrument spectrophotometer. Single crystal X-ray studies for reported structures **1.7**, **1.8**, **1.9**, **1.10**, **1.13**, **1.14**, **1.19**, and **1.20** were carried out using a Bruker 3-axis platform diffractometer equipped with an APEX I CCD detector using a graphite monochromator with a Mo Kα X-ray source (λ = 0.71073 Å) at 100(2) K under a flow of nitrogen gas during data collection. Alternatively, data for structures **1.11**, **1.12**, **1.14**, **1.17** and **1.18** were collected at ChemMatCARS located at the Advanced Photon Source (APS), Argonne National Laboratory (ANL), using synchrotron radiation (λ = 0.41328 Å) in conjunction with a Bruker D8 three-circle platform goniometer equipped with Dectris PILATUS 100 detector under a nitrogen cryo-steam at 100(2) K. Crystals were mounted on a glass fiber or on a Mitigen Kapton loop using NVH crystallographic immersion oil.. Data was collected using φ and ω scan collection strategies. Data collection and cell parameter

determination were conducted using the SMART program. Integration of the data and final cell parameter refinements were performed using SAINT software with data absorption correction implemented through SADABS. Structure solutions and structure refinements were completed using direct methods determinations in SHELXTL or Olex2 crystallographic packages. All hydrogen atom positions were idealized and treated as riding on the parent atom. A summary of relevant crystallographic data is presented in Table 1.2.

1.4.2 Synthesis of (Ketguan)(ImDippN)TiCl (1.7).

A 20 mL scintillation vial was loaded with metallic sodium (0.009 g, 0.390 mmol), elemental mercury (0.179 g), toluene (5 mL) and **1.6** (0.100 g, 0.098 mmol) forming an orange slurry which was vigorously stirred. During 4 d. a gradual color change to green was observed, accompanied by precipitation of a fine gray solid. The mixture was filtered through a Celite column (2 cm × 0.5 cm) supported on glass wool to give a dark green filtrate plus a gray plug. The Celite column was washed with 5 ml of toluene. All volatiles were removed via reduced pressure until a pale green solid was obtained. The material was crystallized using a solution of Et_2O (2 mL) followed by storage at –25 ºC, giving amber crystals after two days. The supernatant was decanted and crystals dried under reduced pressure to afford a pale green solid. Yield: (0.087 g, 0.087 mmol, 89%). ^{1}H NMR (25 ºC, 400 MHz, C_6D_6): 0.3 (bs), 0.88 (bs), 1.46 (bs), 2.11 (bs), 6.14 (bs), 6.69 (bs), 8.82 (bs). UV-vis/NIR (toluene, 0.210 mM, 25 ºC, L•mol-1 •cm-1): 320 (ε = 1000).

Synthesis of (Im^{Dipp}N)(DippN=)[η^2-(^{t}Bu$_2$C)*NC*(NDipp)](THF)Ti (1.8).

A 20 mL scintillation vial was loaded with **1.6** (0.200 g, 0.194 mmol), KC_8 (0.078 g, 0.582 mmol) and THF (10 mL), forming a dark-brown slurry which was vigorously stirred**.** After 12 h a black precipitate formed. All volatiles were removed via reduced pressure until a very dark solid was obtained. This was triturated in 10 ml of hexanes and filtered through a Celite column (2 cm

× 0.5 cm) supported on glass wool to give a light cherry filtrate plus a black plug (C_8). All volatiles were removed via reduced pressure until a pale orange solid obtained. The material was crystallized using a solution THF (2 mL) layered hexanes (2 mL) followed by storage at –25 ºC, giving light orange crystals after seven days Yield: (0.125 g, 0.121 mmol, 62%). ^{1}H NMR (25 ºC, 400 MHz, C_6D_6): 0.85 (m, 4H, J_{HH} = 7 Hz), 0.92 (d, 2H, J_{HH} = 7 Hz), 0.95 (d, 3H, J_{HH} = 7 Hz), 1.09 (bs, 18H, *Me*$_3$C), 1.20 (m, 22H, *Me*$_2$CH) 1.29 (m, 16H, *Me*$_2$CH), 1.46 (d, 6H, J_{HH} = 7 Hz, *Me*$_2$CH,), 2.94 (bs, 1H), 3.23 (bs, 2H), 3.42 (sept, 2H, J_{HH} = 7 Hz, Me$_2$C*H*), 3.49 (sept, 2H, J_{HH} = 7 Hz, Me$_2$C*H*), 3.62 (bs, 2H), 3.71 (bs, 1H), 3.94 sept, 2H, J_{HH} = 7 Hz, Me$_2$C*H*), 5.90 (s, 2H, ImidN*H*), 6.86-7.16 (12H, aryl protons). UV-vis/NIR (toluene, 0.013 mM, 25 ºC, L•mol-1 •cm-1): 340 (ε = 44250).

Synthesis of (^{Ket}guan)(Im^{Dipp}N)Ti(η^{1}-*O*CPh$_2$) (1.9).

A 20 mL scintillation vial was loaded with **1.1** (0.100 g, 0.104 mmol) and toluene (3 mL), forming a dark-brown solution. The solution was chilled at –25 ºC and benzophenone (0.019 g, 0.104 mmol) was added in one portion accompanied and an instantaneous chance to vibrant purple color was observed. The vial was let stand at 25 ºC for 24 h and purple crystals were deposited. Supernatant was decanted, crystals were washed with 5 ml of cold (–25 ºC) hexanes (5 ml) and dried under reduced pressure to afford a bright purple solid. Yield: (0.097 mg, 0.085 mmol, 81%). ^{1}H NMR (25 ºC, 400 MHz, C_6D_6): –1.09 (bs, 9H), –0.02 (bs, 9H), 0.87 (m, 6H, J_{HH} = 6 Hz), 0.93 (bs, 9H), 1.00 (bs, 6H), 1.22 (bs, 12H), 1.44 (bs, 16H), 1.89 (bs, 6H) 2.04 (bs, 6H), 2.57 (bs, 6H), 3.51 (bs, 4H), 3.75 (bs, 2H), 4.21 (bs, 2H), 6.51 (d, 2H, J_{HH} = 7 Hz), 6.74 (m, 6H, J_{HH} = 8 Hz), 7.03 (m, 6H, J_{HH} = 7 Hz), 7.13 (m, 4H, J_{HH} = 7 Hz), 7.70 (m, 4H, J_{HH} = 8 Hz).). UV-vis/NIR (toluene, 0.070 mM, 25 ºC, L•mol-1 •cm-1): 326 (ε = 10400), 442 (ε = 1312), 512 (ε = 1960), 355 (ε = 2460), 688 (ε = 780), 1113 (ε = 86), 1211 (ε = 54). IR (KBr Pellet, cm^{1-}): 415 (w), 569 (w),

606 (w), 627 (w), 639 (w), 703 (m), 753 (w), 793 (w), 807 (w), 842 (w), 901 (w), 922 (w), 940 (w), 905 (w), 921 (w), 940 (w), 975 (w), 1016 (w), 1051 (w), 1106 (w), 1179 (w), 1215 (w), 1273 (m), 1328 (m), 1364 (m), 1407 (m), 1546 (s), 1578 (m), 1597 (m), 1664 (m), 1678 (m), 2345 (w), 2364 (w), 2870 (m), 2930 (s), 2963 (s), 3058 (w), 3411 (w).

Synthesis of (^{Ket}guan)(Im^{Dipp}N)Ti]$_2$[μ-(NC$_5$H$_5$-H$_5$C$_5$N)] (1.10)

A 20 mL scintillation vial was loaded with **1.1** (0.100 g, 0.104 mmol) and pre-chilled (–25 ºC) THF (3 mL), forming a dark-brown solution. To this solution, pyridine (0.026 g, 0.025 mL, 0.312 mmol) was added via a micropipette resulting in an instantaneous color change to deep-purple. The deep-purple color gradually turned into dark-brown within 5 min of stirring and the formation of a green precipitate was observed. The supernatant was decanted, and the green precipitate was washed with 5 ml of hexanes and dried under dynamic vacuum to afford a green-forest solid. Yield: (0.055 g, 0.053 mmol, 53%). ^{1}H NMR (25 ºC, 400 MHz, C_5H_5N): 1.3 (bs) UV-vis/NIR (toluene, 0.070 mM, 25 ºC, L•mol-1 •cm-1): 355 (ε = 25470), 380 (ε = 25040), 540 (ε = 648), 590 (ε = 555), 715 (ε = 1598), 880 (ε = 880), 915(ε = 833), 715 (ε = 1598), 880 (ε = 880), 915(ε = 833).

Synthesis of (^{ket}guan)(Im^{Dipp}N)Ti(CN)(CNCy) (1.11).

A 20 mL scintillation vial was loaded with **1.1** (0.100 g, 0.104 mmol) and benzene (5 mL), forming a dark brown solution. Solution was frozen at 5 ºC. To this thawing solution, cyclohexyl isocyanide (0.028 g, 0.028 mL, 0.220 mmol) was added via a micropipette accompanied. A a gradual chance to a darker brown color was observed upon thawing. After 5 min, all volatiles were removed via reduced pressure until a very dark brown solid was obtained. The material was crystallized using a solution of Et_2O (2 mL) followed by storage at –25 ºC, giving yellow crystals after two days. Yield: (0.051 g, second crop: 0.024 mg, 0.069 mmol, 66%). UV-vis/NIR (toluene,

0.094 mM, 25 ºC, L•mol-1 •cm-1): 310 (ε = 26600), 340 (ε = 22000), 371 (ε = 14000), 385 (ε = 9660). IR (KBr Pellet, cm^{1-}): 498 (w), 572 (w), 670 (w), 715 (w), 752 (w), 767 (w), 808 (w), 892 (w), 935 (w), 1049 (w), 1108 (w), 1052 (w), 1106 (w), 1179 (w), 1218 (w), 1237 (w), 1257 (m), 1329 (m), 1364 (m), 1386 (m), 1448 (s), 1460 (s), 1547 (m), 1578 (m), 1630 (s), 1671 (m), 2865 (s), 2926 (s), 2963 (s), 3060 (w), 3148 (w), 3182 (w), 3326, 3396 (w). 2078. CN = 2170 cm^{1}. This value is lower to those found for Ti(II)-CN^{t}-Bu complexes such as that of $[Cp_2Ti(CO)(CN^{t}\text{-}Bu)]$, (2170 cm^{1}) and [*ansa*-$Me_2Si(Cht)(Cp)Ti(CN^{t}\text{-}Bu)$] (Cht = cycloheptatrienyl), (2153 cm^{1}) $[Ti(Cp^{*})_2(CO)_2]$ (1946 cm^{-1}).

Synthesis of (Im^{Dipp}N)[(DippN)(2-^{i}PrC$_6$H$_3$-6-(η^2-CH$_3$CH*C*H_2)N)C(NC^{t}Bu$_2$)]Ti[NC(H)^{t}Bu] (1.12).

A 20 mL scintillation vial was loaded with **1** (0.100 g, 0.104 mmol) and benzene (5 mL), forming a dark brown solution. Solution was frozen at –25 ºC. To this thawing solution, pivalonitrile (0.018 g, 0.025 mL, 0.220 mmol) was added via a micropipette accompanied by a gradual chance to yellow color. After 5 min of stirring, all volatiles were removed via reduced pressure until a yellow solid was obtained. The material was crystallized using a solution of Et_2O (2 mL) followed by storage at –25 ºC, giving yellow crystals after two days. Yield: (0.057 g, second crop: 0.014 g, 066 mg, 66%). IR (KBr Pellet, cm^{1-}): 507 (w), 543 (w), 610 (w), 674 (w), 714 (w), 752 (m), 794 (m), 899 (m) 921 (m), 923 (m), 972 (m), 1050 (m), 1109 (w), 1180 (w), 1211 (m), 1325 (s), 1364 (s), 1390 (s), 1432 (s), 1465 (s), 1558 (s), 1597(s), 1676 (m), 2048 (s), 2133 (m), 2868 (s), 2966 (s), 3063 (w).

Synthesis of ($Im^{Dipp}N$)[(DippN)(2-$^{i}PrC_6H_3$-6-(η^1-CH_3CHCH_2)N)C(NC$^{t}Bu_2$)]Ti($OCPh_2H$) (1.13).

A 50 mL round bottom Cajon flask was loaded with **6** (0.120 g, 0.106 mmol) and toluene (10 mL), forming a vibrant-purple solution. The solution was heated at 60 ºC for 12 h and bleaching to yellow color was observed. All volatiles were removed under reduced pressure leaving a pale-yellow solid. The material was crystallized using an Et_2O solution (2 mL) stored at –25 ºC for three days to give yellow blocks. Yield: (0.087 g, second crop: 0.026 g, 0.100 mmol, 96%). ^{1}H NMR (25 ºC, 400 MHz, C_6D_6): 0.09 (d, 3H, J_{HH} = 7 Hz, *Me*$_2$CH), 0.65 (d, 1H, J_{HH} = 11 Hz, Ti-C*H*), 0.74 (s, 9H, *Me*$_3$C), 0.79 (s, 9H, *Me*$_3$C), 0.90 (d, 6H, J_{HH} = 7 Hz, *Me*$_2$CH), 1.00 (d, 3H, J_{HH} = 6 Hz, *Me*$_2$CH), 1.09 (d, 6H, J_{HH} = 7 Hz, *Me*$_2$CH), 1.14 (d, 7H, *Me*$_2$CH overlapping with Ti-C*H*), 1.23 (m, 6H, two overlapping *Me*$_2$CH), 1.29 (d, 3H, J_{HH} = 7 Hz, *Me*$_2$CH), 1.37 (d, 3H, J_{HH} = 7 Hz, *Me*$_2$CH), 1.44 (m, 9H, two overlapping *Me*$_2$CH), 3.14 - 3.20 (m, 6H, three overlapping Me$_2$C*H*), 3.37 (sept, 2H, J_{HH} = 7 Hz, Me$_2$C*H*), 3.83 (sept, 1H, J_{HH} = 7 Hz, Me$_2$C*H*), 3.94 (sept, 1H, J_{HH} = 7 Hz, Me$_2$C*H*), 5.79 (s, 2H, Imid*H*), 6.80 (s, 1H, Ti-OC*H*Ph$_2$), 6.99-7.25 (aryl). ^{13}C ^{113} NMR (25 ℃, 101 MHz, C_6D_6): 22.36 (*Me*$_2$CH), 23.00 (*Me*$_2$CH), 23.07 (*Me*$_2$CH), 23.32 (*Me*$_2$CH), 23.63 (*Me*$_2$CH), 24.86, 25.07 (*Me*$_2$CH), 25.17, 25.83 (*Me*$_2$CH), 26.18, 26.56 (*Me*$_2$CH), 27.64, 27.80, 28.63 (Me$_2$C*H*), 28.86 (Me$_2$C*H*), 29.06 (Me$_2$C*H*), 29.50 (Me$_3$*C*), 29.87 (Me$_3$*C*), 35.25, 43.46, 43.98, 79.50 (Ti-*C*H$_2$), 87.57 (Ti-O*C*HPh$_2$), 115.42 (Imid *C*=*C*), 121.99, 122.40, 123.33, 123.52, 123.60, 124.20, 124.64, 124.91, 126.22, 126.71, 127.65, 127.95, 128.06, 129.49, 129.73, 140.18, 142.93, 143.19,144.17, 145.27, 145.47, 146.00, 146.36, 146.42, 147.32, 148.24, 15.62. 162.18 (^{t}Bu$_2$*C*=N), 177.20 (*C*N$_3$). UV-vis/NIR (toluene, 0.110 mM, 25 ºC, L•mol-1 •cm-1): 341 (ε = 16010). IR (KBr Pellet, cm^{1-}): 415 (w), 569 (w), 606 (w), 627 (w), 639 (w), 703 (m), 753 (w), 793 (w), 807 (w), 842 (w), 901 (w), 922 (w), 940 (w), 905 (w), 921 (w), 940 (w), 975 (w), 1016 (w),

1051 (w), 1106 (w), 1179 (w), 1215 (w), 1273 (m), 1328 (m), 1364 (m), 1407 (m), 1546 (s), 1578 (m), 1597 (m), 1664 (m), 1678 (m), 2345 (w), 2364 (w), 2870 (m), 2930 (s), 2963 (s), 3058 (w), 3411 (w).

Synthesis of (^{Ket}guan)(Im^{Dipp}N)Ti(F)(C_6H_4F) (1.14).

A 20 mL scintillation vial was loaded with **1** (0.100 g, 0.104 mmol) and 1 2-difluorobenzene (3 mL), forming a dark brown solution. The solution was stirred for 12 h and a change to yellow color was observed. All volatiles were removed via reduced pressure until a pale-yellow solid was obtained. The material was crystallized using a solution of Et_2O (1 mL) followed by storage at –25 ºC, giving yellow crystals after two days. Yield: (0.069 g, second crop: 0.020 g, 0.083 mmol, 80%). ^{1}H NMR (25 ºC, 400 MHz, C_6D_6): 0.81 (s, 9H, *Me*$_3$C), 1.00 (m, 12H, *Me*$_2$CH), 1.03 (d, 6H, *Me*$_2$CH, J_{HH} = 7 Hz), 1.09 (m, 12H, *Me*$_2$CH), 1.31 (d, 6H, J_{HH} = 7 Hz, *Me*$_2$CH), 1.35 (d, 6H, J_{HH} = 7 Hz, *Me*$_2$CH), 1.40 (d, 6H, J_{HH} = 7 Hz, *Me*$_2$CH), 3.14 (m, 8H, Me$_2$C*H*), 3.66 (sept, 2H, J_{HH} = 7 Hz, Me$_2$C*H*), 3.90 (sept, 4H, J_{HH} = 7 Hz, Me$_2$C*H*), 5.72 (s, 2H, Imid*H*), 7.20-7.02 (12H, *aryl*). ^{13}C ^{113} NMR (25 ℃, 101 MHz, C_6D_6): 22.67 (*Me*$_2$CH), 23.21(*Me*$_2$CH), 23.48 (*Me*$_2$CH), 25.93 (*Me*$_2$CH), 25.98, 27.10, 27.26 (*Me*$_2$CH), 28.30 (Me$_2$*C*H), 28.75 (Me$_2$*C*H), 28.81, 28.91 (Me$_2$*C*H), 30.10 (*Me*$_3$C), 43.66, 113.58, 113.88, 116.64 (Imid *C*=*C*) , 117.47, 122.51, 123.3, 123.47, 124.30, 124.78, 128.06, 130.27, 134.53, 138.05, 138.24, 142.77, 143.7, 145.06, 145.19, 147.19, 147.27, 163.34, 165.64, 167.10, 171.80, 172.07, 172.62 (^{t}Bu$_2$*C*=N), 179.95 (*C*N$_3$). UV-vis/NIR (toluene, 1.93 mM, 25 ºC, L•mol-1 •cm-1): 271 (ε = 37100), 345 (ε = 16300), 371 (ε = 14000), 380 (ε = 15900).

Synthesis of (^{ket}guan)(Im^{Dipp}N)Ti=O. (1.15).

A 50 mL round bottom Cajon flask was loaded with **1** (0.200 g, 0.208 mmol) and benzene (10 mL), forming a dark brown solution. The solution was subjected to three freeze-pump-thaw

cycles and the headspace was backfilled with 1 atm of N_2O turning the solution to yellow color. After 10 min solution turned orange color. All volatiles were removed under reduced pressure until a shiny yellow solid was obtained. The material was crystallized using an Et_2O solution (2 mL) stored at –25 ºC for four days to give yellow blocks. Yield: (0.138 g, second crop: 0.051 g, 0.116 mmol, 79%). ^{1}H NMR (25 ºC, 400 MHz, C_6D_6): 0.79 (s, 9H, *Me*$_3$C), 0.97 (d, 6H, J_{HH} = 7 Hz, *Me*$_2$CH), 1.01 (s, 9H, *Me*$_3$C), 1.06 (d, 6H, J_{HH} = 7 Hz, *Me*$_2$CH), 1.18 (d, 12H, J_{HH} = 4 Hz, *Me*$_2$CH), 1.26 (d, 12H, J_{HH} = 7 Hz, *Me*$_2$CH), 1.34 (d, 6H, J_{HH} = 7 Hz, *Me*$_2$CH), 1.34 (d, 6H, J_{HH} = 7 Hz, *Me*$_2$CH), 3.35 (sept, 4H, J_{HH} = 6 Hz, Me$_2$C*H*), 3.66 (sept, 2H, J_{HH} = 7 Hz, Me$_2$C*H*), 5.94 (s, 2H, Imid*H*), 7.20-7.02 (12H, *aryl*). ^{13}C {^{1}H} NMR (25 ºC, 101 MHz, C_6D_6): 22.02 (*Me*$_2$CH), 22.16 (*Me*$_2$CH), 23.64 (*Me*$_2$CH), 24.78 (*Me*$_2$CH), 25.48 (*Me*$_2$CH), 28.12, 29.12 (Me$_3$*C*), 29.34, 30.82 (Me$_3$*C*), 43.9, 115.46 (Imid *C*=*C*), 122.27, 123.75, 124.12 (^{t}Bu$_2$*C*=N), 125.27 (*C*N$_3$). UV-vis/NIR (toluene, 1.050 mM, 25 ºC, L•mol-1 •cm-1): 335 (ε = 2807547), 415 (ε = 660754).

Synthesis of (^{Ket}guan) (Im^{Dipp}N) Ti=S (1.16).

A 20 mL scintillation vial was loaded with **1** (0.100 g, 0.104 mmol) and benzene (5 mL), forming a dark brown solution. The solution was frozen at 5 ºC. To this thawing solution, propylene sulfide (0.008 g, 0.009 mL, 0.114 mmol) was added in one portion via a micropipette. The addition was accompanied by an instantaneous chance to purple color and strong bubbling (CH_2=CH_2CH_3). After 5 min, all volatiles were removed via reduced pressure until a dark purple solid was obtained. The material was crystallized using a solution of Et_2O (1 mL) followed by storage at –25 ºC, giving dark purple crystals after two days. Crystals were dried under reduced pressure. Yield: (0.043 g, second crop: 0.020 g, 0.064 mmol 61 %. ^{1}H NMR (25 ºC, 400 MHz, C_6D_6): 0.74 (d, 6H, J_{HH} = 7 Hz, *Me*$_2$CH), 0.76 (s, 9H, *Me*$_3$C), 1.09 (d, 6H, J_{HH} = 7 Hz, *Me*$_2$CH), 1.16 (d, 12H, J_{HH} = 7 Hz, *Me*$_2$CH) 1.18 (s, 9H, *Me*$_3$C), 1.18 (d, 12H, J_{HH} = 7 Hz, *Me*$_2$CH), 1.29 (m, 18H, two overlapping

Me$_2$CH), 1.46 (d, 6H, J_{HH} = 7 Hz, *Me*$_2$CH), 3.45 (sept, 4H, J_{HH} = 7 Hz, Me$_2$C*H*), 3.55 (sept, 2H, J_{HH} = 7 Hz, Me$_2$C*H*), 5.39 (sept, 2H, J_{HH} = 7 Hz, Me$_2$C*H*), 5.97 (s, 2H, ImidN*H*), 6.99-7.16 (12H, *aryl*). $^{13}C\{^1H\}$ NMR (25 ºC, 101 MHz, C_6D_6): 22.11 (*Me*$_2$CH), 23.86 (*Me*$_2$CH), 25.20 (*Me*$_3$C), 25.53 (*Me*$_2$CH), 28.1 (*Me*$_2$CH), 28.39 , 29.04 (*Me*$_2$CH), 29.11 (*Me*$_2$CH), 29.17, 30.81 (*Me*$_3$C), 43.83, 44.1,116.31 (Imid *C*=*C*), 122.23 (aryl), 124.44 (aryl), 124.49 (aryl), 125.71, 129.94 (aryl), 134.81 141.08¸ 143.47, 146.24, 147.3, 148.33, 161.31 (^{t}Bu$_2$*C*=N), 184.47 (*C*N$_3$). UV-vis/NIR (toluene, 0.089 mM, 25 ºC, L•mol-1 •cm-1): 350 (ε = 30626), 360 (ε = 31891), 545 (ε = 31891). IR (KBr Pellet, cm^{1-}): 499 (m), 520 (m), 537 (w), 554 (w), 600 (w), 686 (m), 718 (w), 750 (s), 793 (s), 807 (m), 922 (m), 935 (m), 973 (m), 1015 (w), 1108 (m), 1178 (m), 1213 (s), 1264 (s), 1321 (s), 1364 (s), 1385 (s), 1431 (s), 1460 (s), 1519 (s), 1578 (s), 1600 (s), 1620 (s), 1679 (s), 2867 (s), 2927 (s), 2964 (s), 3060 (w), 3148 (w), 3182 (w), 3326, 3396 (w).

Synthesis of (^{Ket}guan)(Im^{Dipp}N)Ti=Se (1.17).

A 20 mL scintillation vial was loaded with **1** (0.100 g, 0.104 mmol) and benzene (5 mL), forming a dark brown solution. The solution was frozen at 5 ºC. To this thawing solution, triphenylphosphine selenide (0.036 g, 0.104 mmol) was added in one portion via a micropipette. The addition was accompanied by gradual color chance to green over 12 h. All volatiles were removed via reduced pressure until a green solid was obtained. The material was extracted in Et_2O (2 mL) followed by storage at –25 ºC, giving green crystals after two days. Crystals were dried under reduced pressure to afford a green solid. Yield: (0.073 g, 0.074 mmol 71 %). ^{1}H NMR (25 ºC, 400 MHz, C_6D_6): 0.66 (d, 6H, J_{HH} = 7 Hz, *Me*$_2$CH), 0.76 (s, 9H, *Me*$_3$C) 1.09 (d, 6H, J_{HH} = 7 Hz, *Me*$_2$CH), 1.17 (d, 12H, J_{HH} = 7 Hz, *Me*$_2$CH) 1.26 (s, 9H, *Me*$_3$C), 1.32 (m, 18H, two overlapping *Me*$_2$CH), 1.50 (d, 6H, J_{HH} = 7 Hz, *Me*$_2$CH), 3.35 (sept, 2H, J_{HH} = 7 Hz, Me$_2$C*H*), 3.64 (sept, 4H, J_{HH} = 7 Hz, Me$_2$C*H*), 5.55 (sept, 2H, J_{HH} = 7 Hz, Me$_2$C*H*), 6.00 (s, 2H, ImidN*H*), 6.99-7.16 (12H,

aryl). $^{13}C\{^{1}H\}$ NMR (25 ºC, 101 MHz, C_6D_6): 22.11 (*Me*$_2$CH), 23.86 (*Me*$_2$CH), 25.20 (*Me*$_3$C), 25.53 (*Me*$_2$CH), 28.1 (*Me*$_2$CH), 28.39, 29.04 (*Me*$_2$CH), 29.11 (*Me*$_2$CH), 29.17, 30.81 (*Me*$_3$C), 43.83, 44.1,116.31 (Imid *C*=*C*), 122.23 (aryl), 124.44 (aryl), 124.49 (aryl), 125.71, 129.94 (aryl), 134.81 141.08¸ 143.47, 146.24, 147.3, 148.33, 161.31 (^{t}Bu$_2$*C*=N), 184.47 (*C*N$_3$). $^{13}C\{^{1}H\}$ NMR (25 ºC, 101 MHz, C_6D_6): 22.07 (*Me*$_2$CH), 23.30 (*Me*$_2$CH), 24.06 (*Me*$_2$CH), 25.27 (*Me*$_2$CH), 25.48 (*Me*$_2$CH), 26.98 (Me$_2$*C*H), 28.39 (Me$_2$*C*H), 28.64 (Me$_2$*C*H), 29.25 (*Me*$_3$C), 30.77 (*Me*$_3$C), 43.86 (Me$_3$*C*), 44.17 (Me$_3$*C*), 30.88 (adamantyl), 116.02 (Imid *C*=*C*), 122.26, (aryl), 124.57 (aryl), 125.77 (aryl), 128.59 (aryl), 128.80 (aryl), 128.87 (aryl), 130.02 (aryl), 141.26, 143.41, 146.23, 147.20, 147.75, 161.74 (^{t}Bu$_2$*C*=N) 181.47 (*C*N$_3$). UV-vis/NIR (toluene, 1.020 mM, 25 ºC, L•mol-1 •cm-1): 415 (ε = 24400. IR (KBr Pellet, cm^{1-}): 499 (m), 520 (m), 537 (w), 554 (w), 600 (w), 686 (m), 718 (w), 750 (s), 793 (s), 807 (m), 922 (m), 935 (m), 973 (m), 1015 (w), 1108 (m), 1178 (m), 1213 (s), 1264 (s), 1321 (s), 1364 (s), 1385 (s), 1431 (s), 1460 (s), 1519 (s), 1578 (s), 1600 (s), 1620 (s), 1679 (s), 2867 (s), 2927 (s), 2964 (s), 3060 (w), 3148 (w), 3182 (w), 3326, 3396 (w).

Synthesis of (^{Ket}guan)(Im^{Dipp}N)Ti(η^2-S$_2$) (1.18).

A 20 mL scintillation vial was loaded with **1** (0.100 g, 0.104 mmol) and benzene (5 mL), forming a dark brown solution. The solution was frozen at 5 ºC. To this thawing solution, propylene sulfide (0.120 g, 0.128 mL, 1.700 mmol) was added in one portion accompanied by a gradual chance to deep purple color and strong bubbling (CH_2=CH_2CH_3). After 10 min, all volatiles were removed via reduced pressure until a dark purple solid was obtained. The material was crystallized using a solution of Et_2O (3 mL) followed by storage at –25 ºC, giving dark-purple crystals after three days. Crystals were dried under reduced pressure to afford a purple solid. Yield: (0.042 g, second crop: 0.049 g, 0.089 mmol, 86%). Mono and disulfide always co-crystallize ^{1}H NMR (25 ºC, 400 MHz, C_6D_6): 0.74 (d, 6H, J_{HH} = 7 Hz, *Me*$_2$CH), 0.76 (s, 9H, *Me*$_3$C), 1.09 (d, 6H, J_{HH} = 7

Hz, *Me*$_2$CH), 1.16 (d, 12H, J_{HH} = 7 Hz, *Me*$_2$CH) 1.18 (s, 9H, *Me*$_3$C), 1.18 (d, 12H, J_{HH} = 7 Hz, *Me*$_2$CH), 1.29 (m, 18H, two overlapping *Me*$_2$CH), 1.46 (d, 6H, J_{HH} = 7 Hz, *Me*$_2$CH), 3.45 (sept, 4H, J_{HH} = 7 Hz, Me$_2$C*H*), 3.55 (sept, 2H, J_{HH} = 7 Hz, Me$_2$C*H*), 5.39 (sept, 2H, J_{HH} = 7 Hz, Me$_2$C*H*), 5.97 (s, 2H, ImidN*H*), 6.99-7.16 (12H, *aryl*). UV-vis/NIR (toluene, 0.012 mM, 25 ºC, L•mol-1 •cm-1): 335 (ε = 12132), 393 (ε = 9564), 516 (ε = 2575).

Synthesis of (^{Ket}guan)(Im^{Dipp}N)Ti(NSiMe$_3$) (1.19).

A 20 mL scintillation vial was loaded with **1** (0.100 g, 0.104 mmol) and benzene (5 mL), forming a dark brown solution. The solution was frozen at 5 ºC. To this thawing solution, trimethylsilyl azide (0.138 g, 0.181 mL, 0.120 mmol) was added in one portion via a micropipette. Upon thawing, a gradual change to red color and strong bubbling (N_2) were observed. After 5 min, all volatiles were removed via reduced pressure until bright orange solid was obtained. The material was crystallized using a solution of Et_2O (1 mL) followed by storage at –25 ºC, giving dark red crystals after two days. Crystals were dried under reduced pressure to afford an orange solid. Yield: (0.076 g, second crop: 0.020 mg, 0.092 mmol, 88%). ^{1}H NMR (25 ºC, 400 MHz, C_6D_6): δ 0.23 (s, 9H, *Me*$_3$Si), 0.75 (s, 9H, *Me*$_3$C), 0.87 (m, 6H, J_{HH} = 7 Hz), 1.03 (s, 9H, *Me*$_3$C), 1.07 (d, 6H, J_{HH} = 7 Hz, *Me*$_2$CH), 1.19 (d, 12H, J_{HH} = 7 Hz, *Me*$_2$CH), 1.32 (d, 6H, J_{HH} = 7 Hz, *Me*$_2$CH), 1.38 (d, 6H, J_{HH} = 7 Hz, *Me*$_2$CH,), 1.50 (d, 6H, J_{HH} = 7 Hz, *Me*$_2$CH), 3.38 (sept, 4H, J_{HH} = 7 Hz, Me$_2$C*H*), 3.62 (sept, 2H, J_{HH} = 7 Hz, Me$_2$C*H*), 4.73 (sept, 2H, J_{HH} = 7 Hz, Me$_2$C*H*), 5.90 (s, 2H, ImidN*H*), 7.02-7.20 (12H, aryl protons). ^{13}C{^{1}H} NMR (25 ºC, 101 MHz, C_6D_6): 4.72 (*Me*$_3$Si), 21.97 (*Me*$_2$CH), 22.94 (*Me*$_2$CH), 23.96 (*Me*$_2$CH), 24.84 (*Me*$_2$CH), 25.74 (*Me*$_2$CH), 27.46 (Me$_2$*C*H), 28.98 (Me$_2$*C*H), 29.419, 29.26 (*Me*$_3$C), 29.26 (Me$_2$*C*H), 30.84 (*Me*$_3$C), 43.56, 44.43, 115.35 (Imid *C*=*C*), 122.33 (aryl), 123.98, 124.82 (aryl), 125.18 (aryl), 128.59, 129.19 (aryl), 135.54, 141.8, 144.13, 145.49, 146.95, 161.81 (^{t}Bu$_2$*C*=N), 182.57 (*C*N$_3$). UV-vis/NIR (toluene,

0.135 mM, 25 ºC, L•mol-1 •cm-1): 365 (ε = 5222), 484 (ε = 644). **IR (KBr Pellet, cm^{1-})**: 674(w), 751 (m), 794 (m), 802 (w), 839 (m), 891 (w), 913 (w), 936 (m), 972 (m), 1011 (w), 1078 (m), 1092 (m), 1047 (w), 1182 (w), 1246 (m), 1326 (m), 1364 (s), 1362 (s), 1385 (s), 1432 (s), 1462 (s), 1558 (s), 1598 (s), 1675 (s), 2867 (s), 2927 (s), 3059 (w), 3137 (w), 3386 (w).

Synthesis of [(^{Ket}guan) (Im^{Dipp}N) Ti(NAd)] (1.20).

A 20 mL scintillation vial was loaded with **1** (0.100 g, 0.104 mmol) and benzene (15 mL), forming a dark brown solution. Solution was frozen at 5 ºC. To this thawing solution 1-azidoadamantane (0.016 g, 0.090 mmol) was added in one portion accompanied by an instantaneous chance to red color and strong bubbling (N_2). After 5 min, all volatiles were removed via reduced pressure until a dark red solid was obtained. The material was crystallized using a solution of Et_2O (2 mL) followed by storage at –25 ºC, giving dark red crystals after four days. Yield: (0.062 g, second crop: 0.031 g, 0.084 mmol 81%). ^{1}H NMR (25 ºC, 400 MHz, C_6D_6): 0.78 (s, 9H, *Me*$_3$C), 0.84 (d, 6H, J_{HH} = 7 Hz, *Me*$_2$CH), 1.08 (s, 9H, *Me*$_3$C), 1.13 (d, 6H, J_{HH} = 6 Hz, *Me*$_2$CH), 1.19 (d, 12H, J_{HH} = 7 Hz, *Me*$_2$CH), 1.32 (d, 6H, J_{HH} = 7 Hz, *Me*$_2$CH), 1.38 (d, 6H, J_{HH} = 7 Hz, *Me*$_2$CH,), 1.50 (d, 6H, J_{HH} = 7 Hz, *Me*$_2$CH), 1.74 (b, 12H, adamantyl), 2.13 (s, 3H, adamantyl) 3.38 (sept, 4H, J_{HH} = 7 Hz, Me$_2$C*H*), 3.62 (sept, 2H, J_{HH} = 7 Hz, Me$_2$C*H*), 4.73 (sept, 2H, J_{HH} = 7 Hz, Me$_2$C*H*), 5.90 (s, 2H, ImidN*H*), 7.20-7.02 (12H, *aryl*). ^{13}C{^{1}H} NMR (25 ºC, 101 MHz, C_6D_6): 21.98 (*Me*$_2$CH), 23.53 (*Me*$_2$CH), 24.05 (*Me*$_2$CH), 25.10 (*Me*$_2$CH), 25.77 (*Me*$_2$CH), 26.98 (Me$_2$*C*H), 29.04 (Me$_2$*C*H), 29.16 (Me$_2$*C*H), 29.31 (*Me*$_3$C), 29.41(*Me*$_3$C), 30.77 (*Me*$_3$C), 30.07, 30.88 (adamantyl), 35.96, 37.33 (adamantyl), 41.62, 43.53, 44.59, 45.36 (adamantyl), 71.31, 115.02 (Imid *C*=*C*), 122.33, 124.16 (aryl), 124.77 (aryl), 128.93 (aryl), 135.97, 142.55, 144.43, 144.53, 145.01, 147.08, 161.74 (^{t}Bu$_2$*C*=N), 185.50 (*C*N$_3$). UV-vis/NIR (toluene, 0.194 mM, 25 ºC, L•mol-1 •cm-1): 323 (ε = 9284), 382 (ε = 3298), 526 (ε = 301). **IR (KBr Pellet, cm^{1-}**

): 415 (w), 432 (w), 473 (w), 507 (w), 556 (w), 573 (w), 609 (w), 675 (w), 751 (m), 793 (w), 893 (m), 945 (m), 973 (m), 1050 (m), 1113 (m), 1178 (w), 1218 (m), 1262 (m), 1330 (m), 1364 (s), 1386 (s), 1434 (s), 1456 (s), 1559 (s), 1598 (s), 2677 (s), 2087 (m), 2870 (s), 2908 (s), 2962 (s), 3060 (m).

Table 1.1: X-ray crystallographic data for **1.17** – **1.19**.

	(**1.7**•Et_2O)	(**1.8**•THF**)**	(**1.9**•C_6H_6)
empirical formula	$C_{65}H_{98}ClN_6OTi$	$C_{69}H_{104}N_6O_2Ti$	$C_{80}H_{104}N_6OTi$
crystal habit, color	Amber Blocks	Yellow Plates	Purple Blocks
crystal size (mm)	0.2 × 0.2 × 0.1	0.5 × 0.2 × 0.1	0.4 × 0.3 × 0.01
crystal system	Monoclinic	Monoclinic	Triclinic
space group	P 2_1/c	P 2_1	P-1
Volume (Å^3)	6023.8(4)	3261.0(6)	3750(5)
a	25.2027(10	13.8080(14)	13.275(9)
b	12.3586(5)	12.6418(12)	14.356(10)
c	19.4175(8)	19.7261(19)	22.544(16)
α	90	90	99.65(2)
β	95.1220(10)	108.732(2)	116.510(10)
γ	90	90	93.079(15)
Z	6	2	1
F_w (g/mol)	1038.73	1046.54	1062.0
density (calcd) (Mg/m^3)	1.145	1.066	0.892
abs coeff (mm^{-1})	0.230	0.193	0.149
F_{000}	2240.0	1042.0	1062.0
total no. of reflns	66458	42709	40649
unique reflns	13801	19317	16935
final *R* indices [$I > 2\sigma(I)$]	R1 = 0.0583, wR2 = 0.1593	R1 = 0.0500, wR2 = 0.1081	R1 = 0.0617, wR2 = 0.1524
largest diff peak and hole (e/ Å^3)	0.8 and -0.6	0.44 and -0.33	1.77 and -0.39
GOF	1.023	1.028	1.020

	(**1.10**•$THF_{1.5}$)	(**1.11**•Et_2O)	(**1.12**•Et_2O)
empirical formula	$C_{138}H_{196}N_{14}O_{1.5}Ti_2$	$C_{73}H_{86}N_8OTi$	$C_{73}H_{107}N_7OTi$
crystal habit, color	Green Blocks	Yellow Plates	Yellow Plates
crystal size (mm)	0.5 × 0.2 × 0.01	0.4 × 0.3 × 0.01	0.2 × 0.1 × 0.1
crystal system	Monoclinic	Monoclinic	Triclinic
space group	C 2/c	P $2_{1/n}$	P-1
Volume (Å^3)	16445.5(12)	7230(42)	6498.5(6)
a	29.6747(12)	13.97(5)	14.3541(7)
b	22.6641(9)	37.65(12)	20.7125(10)
c	27.1216(11)	14.45(5)	22.544(16)
α	90	90	66.2490(10)
β	115.6330(10)	108.04(7)	73.8020(10)
γ	90	90	87.7130(10)
Z	12	4	4
F_w (g/mol)	965.63	1139.44	1071.09
density (calcd) (Mg/m^3)	1.170	1.047	1.095
abs coeff (mm^{-1})	0.202	0.163	0.178
F_{000}	5776.0	2440.0	2312.0
total no. of reflns	74574	146377	145792
unique reflns	14729	12303	22532
final *R* indices [$I > 2\sigma(I)$]	R1 = 0.0652, wR2 = 0.1653	R1 = 0.0748, wR2 = 0.02118	R1 = 0.0743, wR2 = 0.1953
largest diff peak and hole (e/ Å^3)	0.55 and -0.41	0.84 and -0.44	1.34 and -0.80
GOF	1.020	1.060	1.071

	(**1.13**•Et_2O)	(**1.14**)	(**1.15**•Et_2O),
empirical formula	$C_{78}H_{108}N_6O_2Ti$	$C_{67}H_{92}N_6F_2Ti$	$C_{65}H_{98}N_6O_2Ti$
crystal habit, color	Yellow Squares	Yellow Blocks	Yellow Plates
crystal size (mm)	0.5 × 0.5 × 0.1	0.5 × 0.5 × 0.1	0.5 × 0.5 × 0.1
crystal system	Monoclinic	Monoclinic	Triclinic
space group	C 2/c	P 2_1	P-1
Volume (Å^3)	16445.5(12)	3261.0(6)	3131.1(2)
a	29.6747(12)	13.8080(14)	12.1771(5)
b	22.6641(9)	12.6418(12)	15.5708(6)
c	27.1216(11)	19.7261(19)	17.4020(7)
α	90	90	98.7190(10)
β	115.6330(10)	108.732(2)	95.1300(10)
γ	90	90	104.3920(10)
Z	12	2	4
F_w (g/mol)	965.63	1046.54	969
density (calcd) (Mg/m^3)	1.170	1.066	1.104
abs coeff (mm^{-1})	0.202	0.193	0.182
F_{000}	5776.0	1042.0	1123.0
total no. of reflns	74574	42709	39139
unique reflns	14729	19317	17129
final *R* indices [$I > 2\sigma(I)$]	R1 = 0.0652, wR2 = 0.1653	R1 = 0.0500, wR2 = 0.1081	R1 = 0.0598, wR2 = 0.1499
largest diff peak and hole (e/ Å^3)	0.55 and -0.41	0.44 and -0.33	0.73 and -0.41
GOF	1.020	1.028	1.025

	(**1.16**•Et_2O)	(**1.17**•Et_2O)	(**1.18**•Et_2O)
empirical formula	$C_{65}H_{98}N_6OSTi$	$C_{65}H_{98}N_6OSeTi$	$C_{65}H_{98}N_6OS_2Ti$
crystal habit, color	Purple Plates	Green Plates	Purples Needles
crystal size (mm)	0.4 × 0.3 × 0.05	0.5 × 0.5 × 0.1	0.4 × 0.3 × 0.05
crystal system	Monoclinic	Monoclinic	Monoclinic
space group	P 2_1/c	P 2_1/c	P 2_1/c
Volume (Å^3)	6003.7(5)	6010.2(6)	6040.7(4)
a	25.1577(13)	25.2819(16)	25.3940(10)
b	12.3661(6)	12.3368(7)	12.2674(4)
c	19.3644(10)	19.3582(12)	19.5579(8)
α	90	90	90
β	94.7400(10)	95.4830(10)	97.4890(10)
γ	90	90	90
Z	4	4	4
F_w (g/mol)	2213.0	1188.71	973.00
density (calcd) (Mg/m^3)	1.134	1.314	1.070
abs coeff (mm^{-1})	0.222	1.296	0.251
F_{000}	2213.0	2332.0	2016.0
total no. of reflns	70558	127577	209332
unique reflns	16989	10719	18756
final *R* indices [$I > 2\sigma(I)$]	R1 = 0.0645, wR2 = 0.1648	R1 = 0.0607, wR2 = 0.1551	R1 = 0.0620, wR2 = 0.1564
largest diff peak and hole (e/ Å^3)	1.48 and -0.62	0.66 and -0.70	0.92 and -0.76
GOF	0.997	1.032	1.098

	(**1.19**•Et_2O)	(**1.20**•Et_2O)
empirical formula	$C_{68}H_{107}N_7OSiTi$	$C_{75}H_{113}N_7OTi$
crystal habit, color	Orange Plates	Orange Blocks
crystal size (mm)	0.3 × 0.2 × 0.5	0.6 × 0.7 × 0.5
crystal system	Monoclinic	Monoclinic
space group	P 2_1	P 2_1/c
Volume (Å^3)	3351.9(4)	6010.2(6)
a	12.8027(10)	25.2819(16)
b	11.9488(9)	12.3368(7)
c	22.0457(17)	19.3582(12)
α	90	90
β	96.3260(10)	95.4830(10)
γ	90	90
Z	4	4
F_w (g/mol)	557.04	1188.71
density (calcd) (Mg/m^3)	1.104	1.314
abs coeff (mm^{-1})	0.267	1.296
F_{000}	1109.0	2332.0
total no. of reflns	29808	127577
unique reflns	12866	10719
final *R* indices [$I > 2\sigma(I)$]	R1 = 0.0591, wR2 = 0.1439	R1 = 0.0607, wR2 = 0.1551
largest diff peak and hole (e/ Å^3)	0.66 and -0.37	0.66 and -0.70
GOF	0.968	1.032

Chapter 2: Thiophene Activation

2.1 INTRODUCTION

Reversible oxidative addition (OA) and reductive elimination (RE) reactions are the cornerstones of many catalytic transformations.[35, 114] Cycling between OA and RE is a dual-redox exchange at which noble metal-based catalysts (NMBC's) are exceptionally efficient in virtue of their thermodynamic preference for two-electron chemistries.[115] However, the sustainability and toxicity drawbacks inherent to NMBC's have propelled a quest for more viable alternatives.[116-118] In line with this, more-abundant and less-toxic early transition metals are potential recourses to traditional NMBC's. Specifically, low-valent titanium species are known to mediate key OA and RE stages in reductive coupling reactions.[119-127] Albeit, well-defined reversible OA and RE steps across a titanium center have remained elusive. Such limitation is a possible consequence of the strong electropositive character and preference for high valencies in titanium.[4, 128] However, strategies that circumvent these chemical and redox constrains in favor of unusual, yet useful catalytic reactions have been developed.[129] For instance, our group previously reported a low-coordinated and highly-reducing titanium complex **1.1** that exhibits NMBC-type chemistry in the form of catalytic hydrogen transfer chemistry[51] plus a wide array of small molecule activation. Herein, we expand upon such unique titanium redox chemistry to perform other challenging transformations reminiscent of NMBC's.

The ring opening of THP's [(THP's = thiophene (THP), benzothiophene (BTP), and, dibenzothiophene (DBT)] (eq. 2.1), a formal two-electron reaction, has critical implications in hydrodesulfurization,[130-132] medicinal chemistry,[133-134] and material science.[135-139] Several transition metal complexes react with THP's to generate well-defined ring opened adducts (Mo,[140-141] W,[142] Co,[143-144] Ni[145-146] Ru,[147-148] Ir,[149-150] Rh,[151-160] Pt,[161] Os[162]), but, reversible C-S bond

cleavage and formation has only been observed in the thermally induced intramolecular isomerization of 2-methylbenzothiophene (2-MBTP) in the rhodium complex $(C_5Me_5)Rh(PMe_3)(2\text{-MBTP})$[160] and partial hydrogenation of BTP mediated by the rhodium and iridium-based catalysts $[M(COD)(PPh_3)_2]PF_6$ (COD = 1,5-Cyclooctadiene M = Rh, Ir),[163] and, [(triphos)RhH] (triphos = Bis(2-diphenylphosphinoethyl)phenylphosphine).[164]

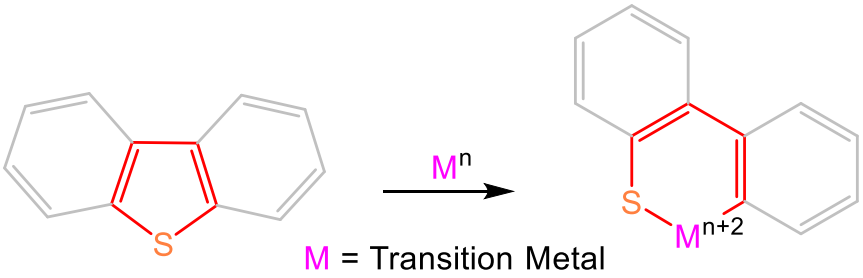

(eq 2.1)

Herein, we report the first example of reversible C-S bond cleavage and formation in THP mediated by a titanium complex. Specifically, **1.1** oxidatively adds a THP molecule to cleanly generate the corresponding ring-opened product $[(Imid^{dipp}N)(^{Ket}Guan)Ti(\kappa^2\text{-}(SCH)(CH)_3)$ (**2.1**). Interestingly, this transformation is reversible under UV light irradiation (280 nm) as **2.1** reductively eliminates THP with concomitant regeneration of **1.1**.

2.1 is thermally labile as heating induces ligand-based C-H bond activation through intramolecular cyclometallation with a ^{Ket}Guan ligand and THP deprotonation to generate the α-thiophenyl titanium-complex $(ImDippN)[(2,6\text{-}^iPr_2C_6H_3N)(2\text{-}^iPrC_6H_3\text{-}6\text{-}(\eta^2\text{-}CH_3CHCH_2)N)C(NC^tBu_2)]Ti[(\eta^1\text{-}(CH)S(CH)_3)$ (**2.2**) via the formal loss of H_2.

2.2 RESULTS AND DISCUSSIONS

We observed that treating dark-brown solutions of **1.1** with one equivalent of THP in C_6D_6 effect an instantaneous change to orange color (eq 2.2). An ^{1}H NMR analysis of this experiment reveals full consumption of both starting materials and clean formation of a new product that

features a set of four different proton environments from 5.83 to 7.31 ppm integrating in a 1:1:1:1 ratio suggestive of an expanded-ring thiophene unit (Figure 2.1) in addition to the typical resonances of titanium-complexed Imid^{dipp}N and ^{Ket}Guan ligands.

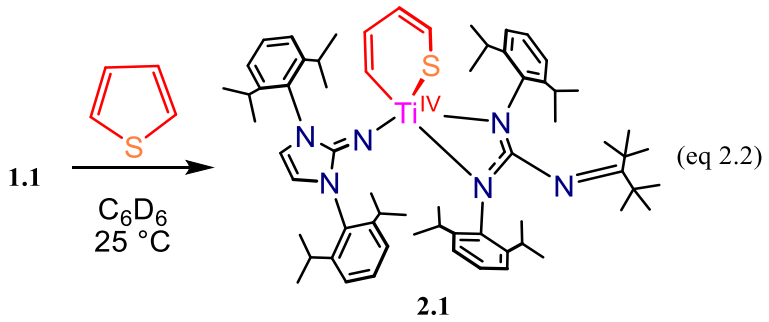

2.1

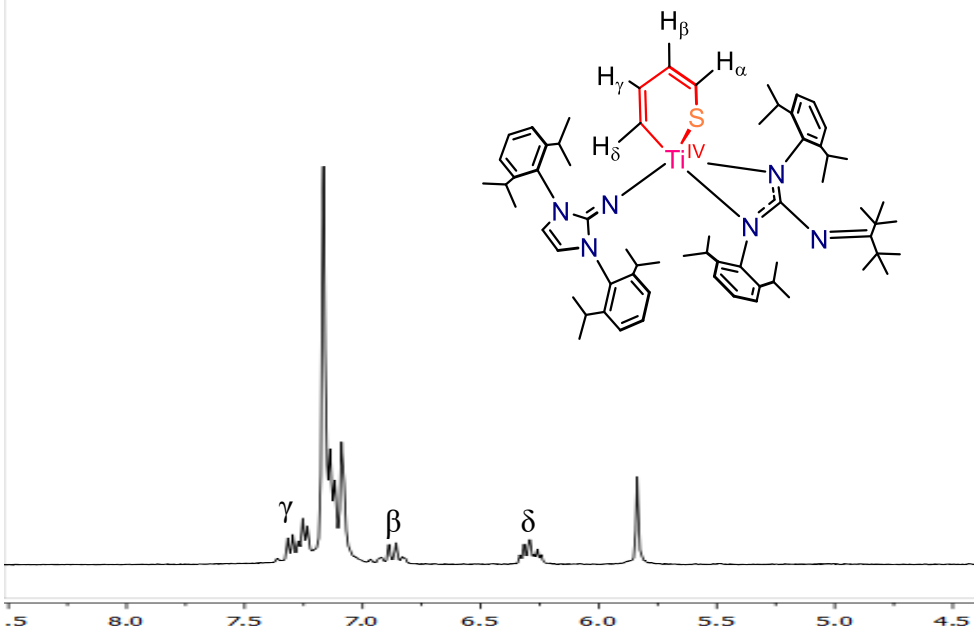

Figure 2.1: Proton resonances for the THP ligand in **2.1**

Such assessment is corroborated by a solid-state structure obtained from an X-ray diffraction experiment performed on single orange crystals of **2.1** grown from concentrated toluene solutions stored at –25 ºC for 4 d. Figure 2.2 shows the first example of a titanium complex supporting a ring expanded THP moiety. This transformation has a negligible effect on the bond

lengths and angles within the supporting ligands Imid^{dipp}N and ^{Ket}Guan and titanium since there are no significant deviations from previously reported 5-coordinated complex such as **1.18**. Furthermore, the thiophene ligand chelates titanium in a κ^2-*CS* fashion through single titanium sulfur and carbon bonds (Ti1-S1 = 2.405(4) Å, Ti1-C4 = 2.037(1) Å, C4-Ti1-S1 = 41.55º)). Inspection of the bond metrics within the THP ligand reveal an almost planar ring with carbon-carbon bond lengths in accordance with a 1,3-butadiene canonical form (C1-C2 = 1.376(2) Å, C2-C3 = 1.499(2) Å, C3-C4 = 1.308(2) Å, C1-S1 = 1.701(1) Å). Overall, this analysis is congruent with a non-activated THP ring as observed in the molybdenum complex [$Me_2Si(C_5Me_4)_2$]Mo(κ^2-(*SC*H)$(CH)_3$)].[140]

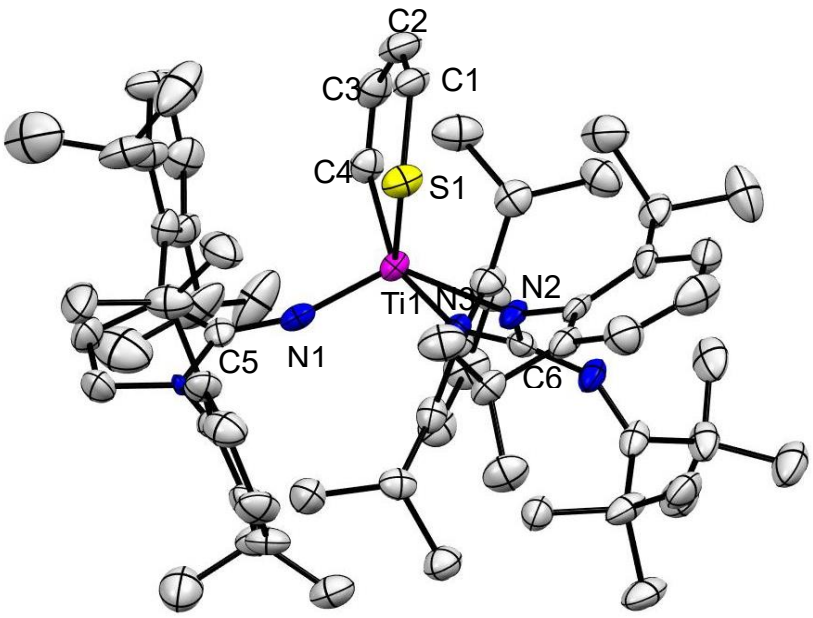

Figure 2.2: Solid-state structure for **2.1** with 50% probability ellipsoids. Selected bond lengths (Å) and angles (º) for **2.1**. T1-N1 = 1.832(4), T1-N2 = 2.115(1), T1-N3 = 2.152 (9), T1-S1 = 2.405(4), T1-C4 = 2.037(1), S1-C1 = 1.701(1), C1-C2 = 1.376(2), C2-C3 = 1.499(2), C3-C4 = 1.308(2), Ti1-N1-C5 = 161.2(9), N2-C6-N3 = 115.5(1), S1-Ti1-C4 = 86.9(4).

Moreover, we encountered that in routine preparative synthesis **2.1**, and subsequent analysis via ^{1}H NMR spectroscopy, equimolar amounts of **1.1** and free THP were frequently detected (5-10%). This outcome is unexpected because during the reaction work-up dynamic vacuum was applied to the reaction vessel to ensure removal of all volatiles (THP = b.p. 84 ºC)[165] prior to recording NMR spectra.

It was reasoned that exposure of **2.1** to light was presumably causing the reductive elimination of THP and generation of **1.1**. Indeed, synthesis and characterization procedures where **2.1** was minimally exposed to light inhibited the production of **1.1** and free THP. Conversely, UV light irradiation (280 nm) of **2.1** solutions (0.010 mM, C_6D_6) induces complete formation of **1.1** and free THP over a period of 2 h (Figure 2.3). Furthermore, the THP ligand in **2.1** is readily displaced by CO (1 atm) to cleanly form **1.4**.

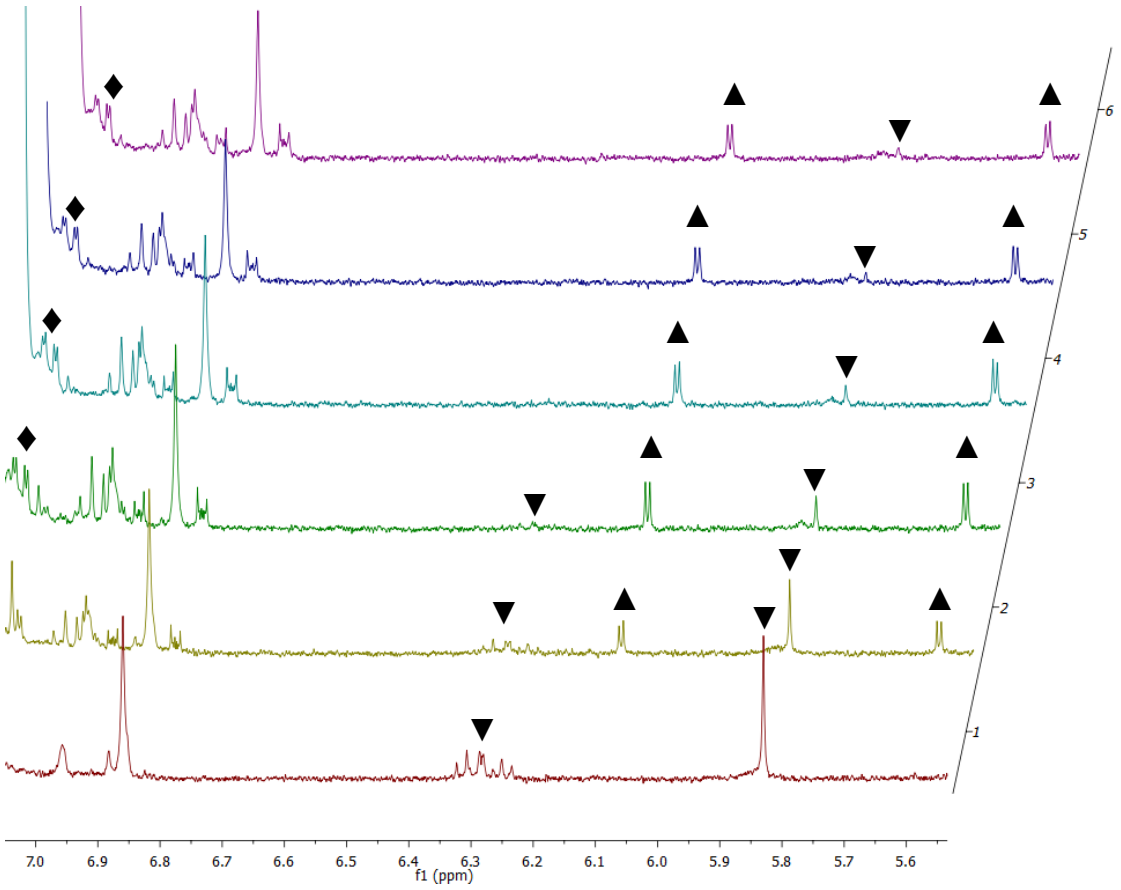

Figure 2.3: Photo-induced reductive elimination of **2.1** (▼) to **1.1** (▲) and THP (♦).

To test if the observed reversibility is temperature dependent or the THP ligand is prone to further activation, a C_6D_6 solution of **2.1** was heated at 60 ºC for 12 h. Under heat, **2.1** transforms to a lower-symmetry product (**2.2**) with no noticeable production of free THP through ^{1}H NMR spectroscopy. **2.2** is more conveniently obtained in 5 min from the reaction between **1.3** and excess THP (Figure 2.4) (Scheme 2.1).

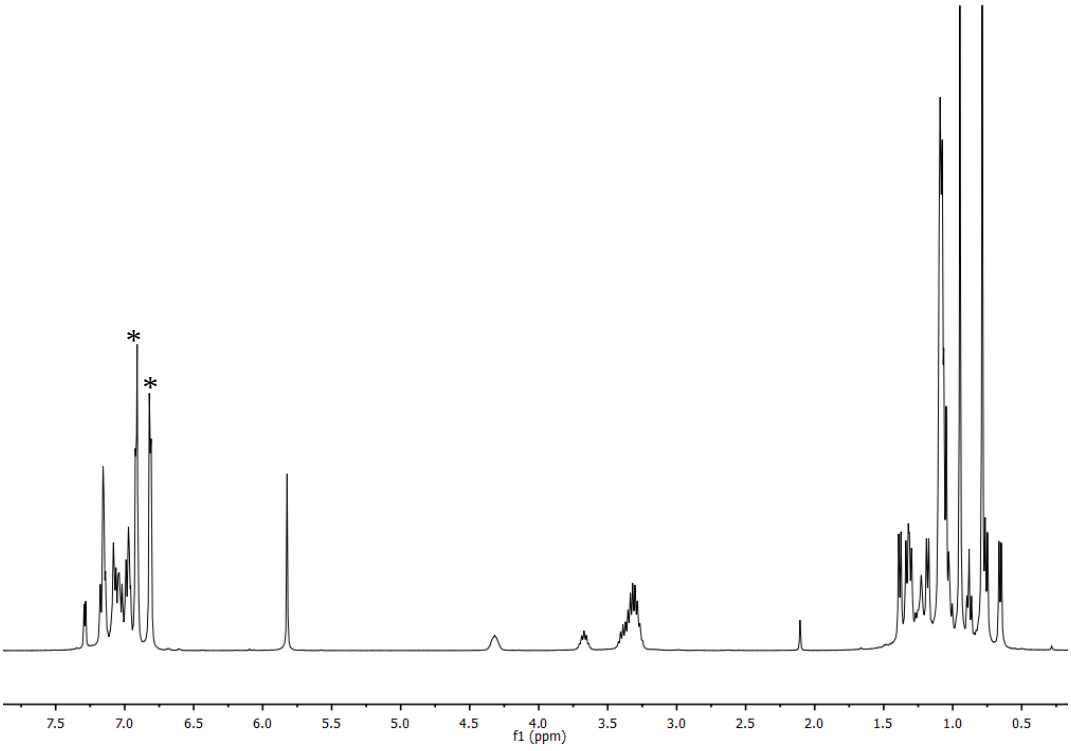

Figure 2.4: ^{1}H NMR spectrum of the reaction between **1.3** and stoichiometric excess of THP in C_6D_6. Asterix (*) denote the presence of unreacted THP.

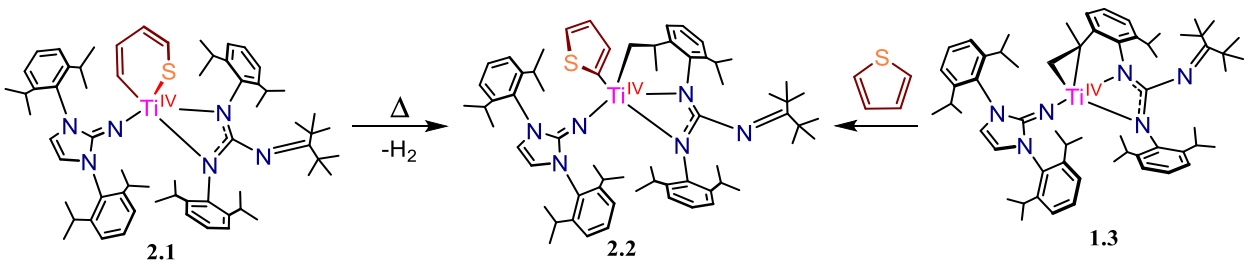

Scheme 2.1 Thermal reactivity of **2.1** and its facile synthesis from **1.3** and THP.

The connectivity of **2.2** was definitively established via an X-Ray diffraction experiment on crystals grown form concentrated Et_2O solutions stored at −25 ºC for 3d. Figure 2.5 depicts a six-membered metallacycle formed between the titanium center and a pending carbon in ^{Ket}Guan (Ti-C15 = 2.132(6)Å) which induces the rearrangement of the THP unit into an apical α-thiophenyl ligand (Ti-C15 = 2.151(6)Å) via the formal of H_2.

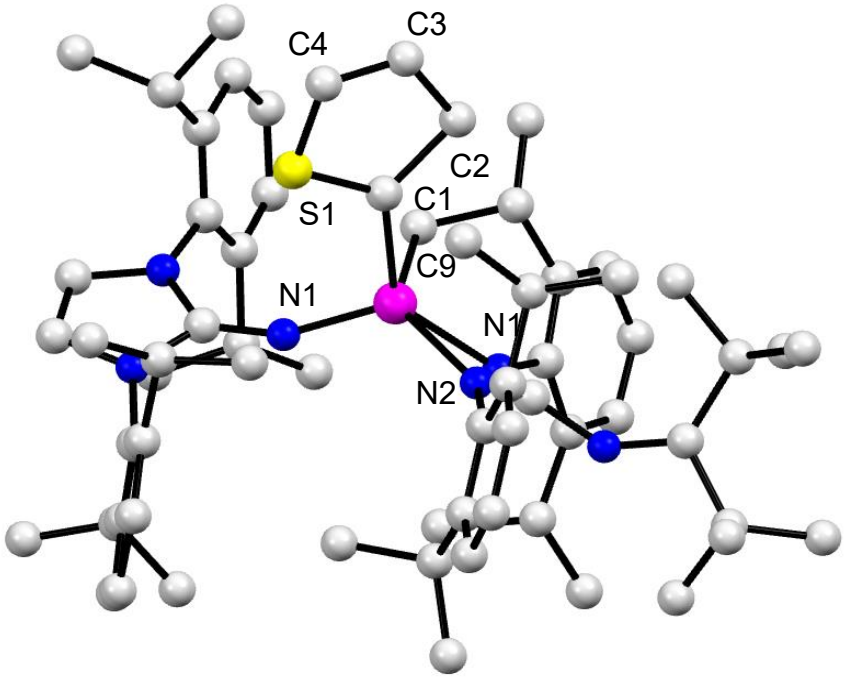

Figure 2.5: Ball and stick model for **2.2** with 50% probability ellipsoids. Selected bond lengths (Å) and angles (º) for. T1-N1 = 1.830(2), T1-N2 = 2.182(2), T1-N3 = 2.193 (2), T1-C1 = 2.151(2), T1-C9 = 2.127(3) Å, S1-C1 = 1.701(1), C1-C2 = 1.648(2), C2-C3 = 1.595(1), C3-C4 = 1.360(1) Å, S1-C4 = 1.602(2), S1-C1 = 1.676(2), Ti1-N1-C5 = 157.462(9), N2-C6-N3 = 111.5(1), Ti1-C9-C8 = 112.5(4).

Interestingly, **2.2** is photolitically inert and unreactive towards H_2 in C_6D_6 at 60 ºC, which stands in stark contrast to the titanacycle **1.3**.

2.3 CONCLUSION

The ring opening of THP by **1.1** in a reversible fashion is further evidence that by implementation of a low-coordinating and electron-releasing ligand scaffold late-metal type reactivity can be promoted in early-metals. Current efforts are devoted towards the development of a catalytic system for THP's activation based on **1.1**. The sustainability advantages of early-metals over noble-metal are undeniable. However, our endeavors might be limited by the propensity of **2.1** towards intramolecular C-H bond activation to form **2.2**. Indeed, **2.2** accounts for the fifth example of intramolecular C-H bond activation in the ^{ket}Guan ligand. Our strategies to prevent this outcome are presented in the following chapter.

2.4 EXPERIMENTAL SECTION

2.4.1 General Considerations

All air and moisture-sensitive operations were performed in a M. Braun dry box under an atmosphere of purified nitrogen or using high vacuum standard Schlenk techniques. Benzene, Et_2O, hexanes, pentane, toluene and THF were dried using a Pure Process Technology Solvent Purification System and subsequently stored under a dinitrogen atmosphere over activated 4 Å molecular sieves. All deuterated solvents were purchased from Cambridge Isotope Laboratories Inc. The deuterated solvents and THP were degassed by three freeze-pump-thaw cycles and were dried over activated 4 Å molecular sieves for 24 h prior to use. The Celite and the 4 Å molecular sieves were heated to 150℃ for at least 24 h and then cooled under vacuum. All other reagents were purchased from commercial sources and used as received. NMR spectra were recorded on a Bruker AVANCE III 400 MHz spectrometer. Resonance assignments in the ^{13}C NMR spectra were based upon ^{1}H – ^{13}C HSQC 2D correlation spectra. ^{1}H NMR and ^{13}C NMR spectra are referenced

to the residual ^{1}H solvent peaks as internal standards or the characteristic ^{13}C resonances of the solvent. ^{19}F NMR spectra were referenced to external α,α,α-trifluorotoluene (-63.72 ppm relative to $CFCl_3$ at 0 ppm). Single crystal X-ray studies for reported structures **2.1**, and **2.2** were carried out using a Bruker 3-axis platform diffractometer equipped with an APEX I CCD detector using a graphite monochromator with a Mo Kα X-ray source (λ = 0.71073 Å) at 100(2) K under a flow of nitrogen gas during data collection. Data collection and cell parameter determination were conducted using the SMART program. Integration of the data and final cell parameter refinements were performed using SAINT software with data absorption correction implemented through SADABS. Structure solutions and structure refinements were completed using direct methods determinations in SHELXTL or Olex2 crystallographic packages. All hydrogen atom positions were idealized and treated as riding on the parent atom. A summary of relevant crystallographic data is presented in Table 2.1.

Synthesis of [(Imid^{dipp}N)(^{Ket}Guan)Ti(κ^2-(*S*CH)(CH)$_3$) (2.1).

A foil-wrapped 20 mL scintillation vial was loaded with **1.1** (0.100 g, 0.104 mmol) and benzene (5 mL), forming a dark brown solution. The solution was frozen at 5 ºC. To this thawing solution, THP (0.042 g, 0.040 mL, 0.520 mmol) was added in one portion via a micropipette. The addition was accompanied by an instantaneous chance to orange color. After 5 min, all volatiles were removed via reduced pressure until an orange solid was obtained. Solid was washed with 5 ml of hexanes (3×) and dried under dynamic vacuum to give a pale orange solid (0.084g, 0.083 mmol 81%). X-Ray quality crystals can be obtained using a concentrated toluene solution (1 mL) followed by storage at –25 ºC for two days. ^{1}H NMR (25 ºC, 400 MHz, C_6D_6): 0.89 (s, 9H, *Me*$_3$C), 1.19 (d, 6H, J_{HH} = 7 Hz, *Me*$_2$CH), 1.22 (d, 18H, J_{HH} = 7 Hz, overlapping *Me*$_2$CH), 1.43 (m, 24H, J_{HH} = 8 Hz, overlapping *Me*$_2$CH), 3.27 (sept, 2H, J_{HH} = 7 Hz, Me$_2$C*H*), 3.38 (sept, 2H, J_{HH} = 7 Hz,

Me_2CH), 3.46 (bs, 2H, Me_2CH), 3.75 (sept, 2H, J_{HH} = 7 Hz, Me_2CH) 5.91 (s, 2H, ImidN*H*), 6.33 (m, 2H, J_{HH} = 7 Hz, overlapping β and γ-THP), 6.93 (q, 1H, J_{HH} = 11 Hz, α-THP), 7.15-7.33 (12H, *aryl*), 7.38 (d, 8H, J_{HH} = 11 Hz, δ-THP). $^{13}C\{^1H\}$ NMR (25 ºC, 101 MHz, C_6D_6): 22.15 (Me_2CH), 23.32 (Me_2CH), 23.42, 24.60, 24.95 Me_3C, 25.84, 26.11, 26.79, 28.02, 29.68, 30.59, 36., 43.83, 44.38, 116.48 (Imid *C*=*C*), 123.47 (aryl), 124.76 (aryl), 124.84 (aryl), 125.02, 125.31 (β-THP), 126.82, 130.22, 131.76 (γ-THP), 135.25, 141.35¸ 144.07, 144.16, 144.75, 145.35, 147.57 ($^tBu_2C$=N), 148.12 (CN_3), 164.76 (α-THP), 181.33.

Table 2.1**:** X-ray crystallographic data for **2.2** – **2.2**.

	(2.1)	**(2.2)**
empirical formula	$C_{65}H_{92}N_6STi$	$C_{63}H_{92}N_6STi$
crystal habit, color	Orange Blocks	Orange Plates
crystal size (mm)	0.2 × 0.2 × 0.1	0.2 × 0.1 × 0.1
crystal system	Monoclinic	Triclinic
space group	P 2_1/n	P-1
Volume (Å^3)	7070.4(11)	3150.0(7)
a	19.0303(17)	12.594(15)
b	16.7435(15)	14.043(17)
c	23.660(2)	20.15(3)
α	90	74.67(3)
β	110.308(2)	87.34(3)
γ	90	66.739(14)
Z	6	4
F_w (g/mol)	1037	1035
density (calcd) (Mg/m^3)	0.925	1.1454
abs coeff (mm^{-1})	0.191	0.213
F_{000}	1960.0	1175.2

total no. of reflns	42561	11307
unique reflns	7494	9554
final *R* indices [$I > 2\sigma(I)$]	R1 = 0.1589, wR2 = 0.4162	R1 = 0.1001, wR2 = 0.2669
largest diff peak and hole (e/ Å^3)	1.72 and -0.65	3.07 and -1.65
GOF	2.746	0.893

Chapter 3: Ligand Modifications

3.1 INTRODUCTION

Coordination and organometallic chemists commonly explore ligand modifications to delineate trends in the electronic, geometrical, and reactivity profile of structurally-related transition metal complexes.[94] This approach has been particularly useful in the chemistry of low valent early-transition metals since ligand degradation pathways can be circumvented in favor of metal-centered reactivity. For instance, the two-electron chemical reduction of the niobium complex $Nb(I)_2(N[^tBu]Ar)_3$ (Ar = 3,5-dimethylphenyl) with $Mg(THF)_3$(anthracene) leads to ligand-based de-alkylation ($^tBu\cdot$) to form the niobium(III) dimer $[(\mu\text{-}N\text{Ar})Nb(N[^tBu]Ar)_2]_2$.[28] In contrast, the $Mg(THF)_3$(anthracene) reduction of the homologated neopentyl (Np) (Np = $-CH_2(CH_3)_3$) anilide complex $Nb(I)_2(N[Np]Ar)_3$ results in the formation of the niobaziridine $Nb(H)(\eta^2\text{-}^tBu(H)C{=}N(Ar))(N[Np]Ar)_2$ adduct through C-H bond oxidative addition of a pending ligand methylene group.[28] In contrast to $[(\mu\text{-}N\text{Ar})Nb(N[^tBu]Ar)_2]_2$, $Nb(H)(\eta^2\text{-}^tBu(H)C{=}N(Ar))(N[Np]Ar)_2$ is an excellent platform for the activation of a wide range of small molecules,[165-166] including sophisticated forms of P_4 functionalization.[167-169]

In the present work we have encountered that the ^{Ket}Guan ligand is susceptible to C-H bond activation to render different cyclometalated adducts. Thus, the access to a related [(Imid^{dipp}N)(^{Ket}Guan)Ti(II)] synthon where the ^{i}Pr groups in the ^{Ket}Guan are absent is a tantalizing avenue to direct novel reactivity by preventing the recurrence of cyclometallation chemistry.

3.2 RESULTS AND DISCUSSIONS

We have synthesized an intramolecularly-capped titanium complex [(xylyl^{ket}guan)(η^6-Im^{Dipp}N)Ti] (**3.1**) where the formal dipp-substitution pattern on the ^{Ket}Guan ligand was replaced for 2,5-dimethylphenyl (xylyl) moieties. **3.1** is readily obtained in good yields (40-50%) from the

low-temperature chemical reduction of the titanium dichloride complex (xylyl^{ket}guan)(η^6-Im^{Dipp}N)Ti(Cl)$_2$ **3.2** with two eq of KC_8 (eq 3.1).

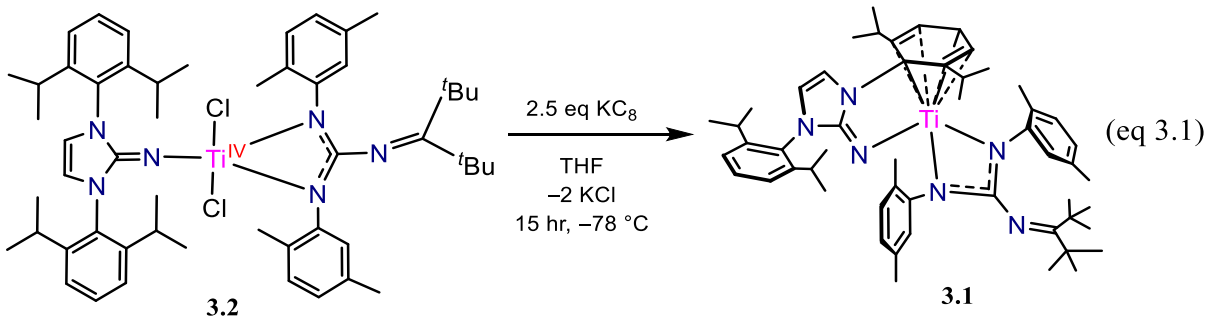

3.2 **3.1** (eq 3.1)

Similar to **1.1**, the ^{1}H NMR spectrum of **3.1** in C_6D_6 shows the de-aromatized *meta* and *para* proton resonances of the capping ring in the olefinic region (4.12 and 2.53 ppm, respectively) (Figure 3.1).

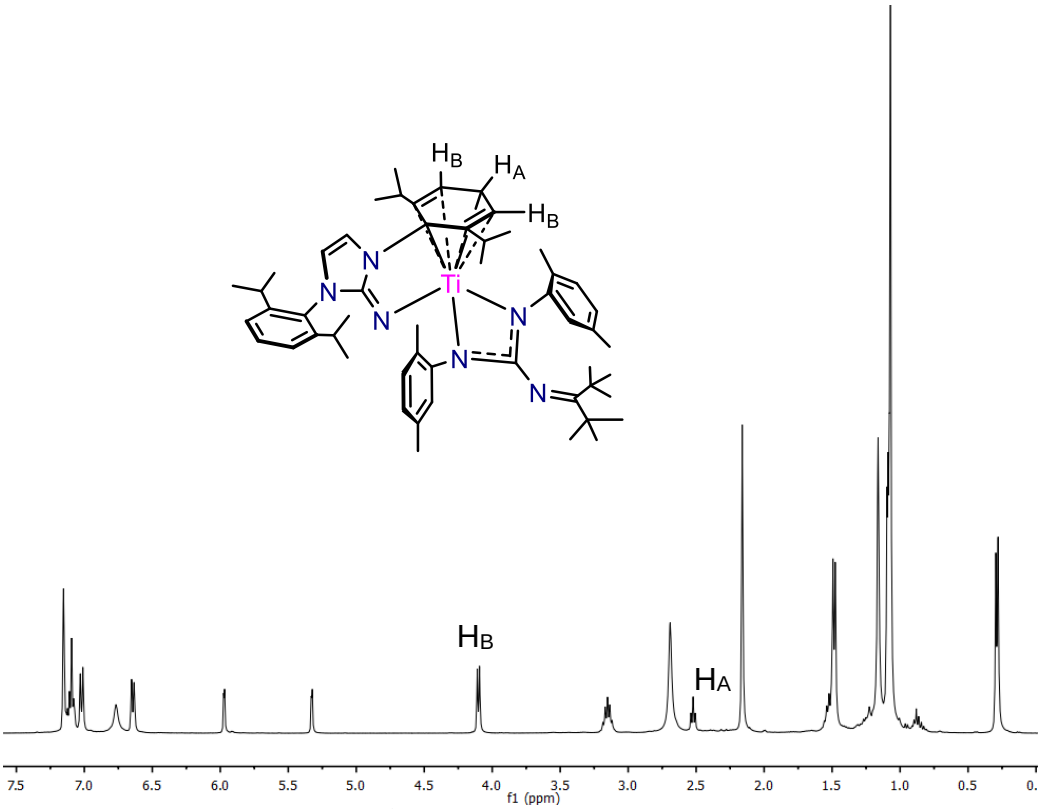

Figure 3.1: ^{1}H NMR spectrum of **3.1** in C_6D_6.

The X-ray structure obtained for **3.1 from** concentrated toluene solutions stored at –25 ºC for 7 d further corroborate the observed spectroscopic features (Figure 3.2). The bond metrics and angles of **3.1** are similar to those of **1.1**. For instance, the capping ring exhibits cyclohexadienyl dianionic character (C7-C8 = 1.445(8) Å, C8-C9 = 1.380(2) Å, C9-C10 = 1.414(2) Å, C10-C11 = 1.393(2) Å, C11-C12 = 1.347(1) Å, C12-C7 = 1.451(9) Å) and the Ti-Im^{Dipp}N angle is bent (Ti1-N1-C5 = 118.6(4)º). With **3.1** in hand, we set to explore and contrast the THP activation chemistry with respect to **1.1**.

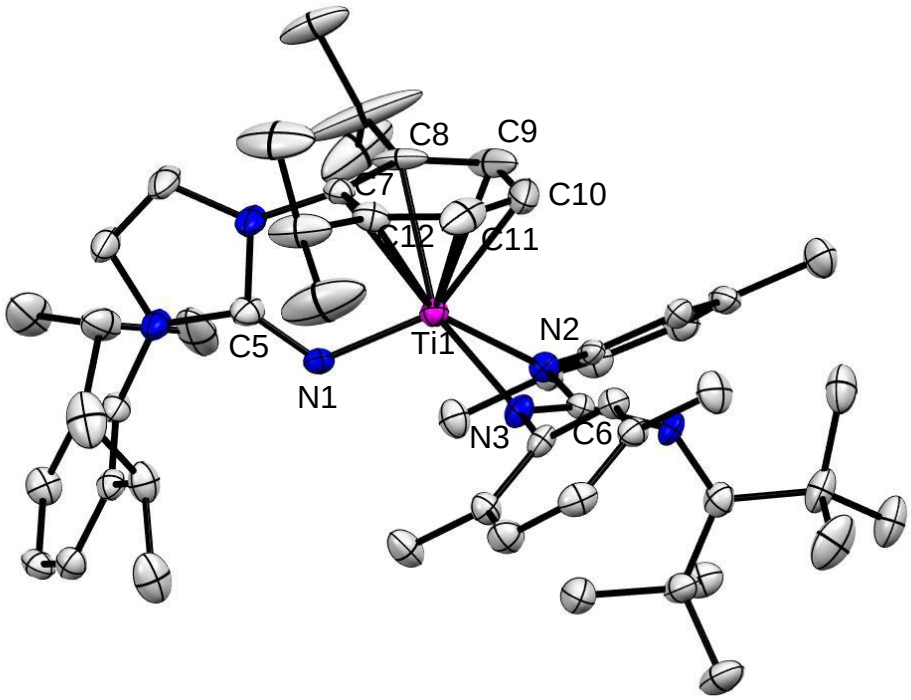

Figure 3.2: Solid-state structure of **3.1** with 50% thermal ellipsoids. Selected bond lengths (Å) and angles (º). T1-N1 = 1.917(2), T1-N2 = 2.116(2), T1-N3 = 2.133 (5), T1-C7 = 2.281(6), T1-C8 = 2.385(7), T1-C9 = 2.375(9), T1-C10 = 2.307(9), T1-C11 2.399(8), T1-C12 2.372(7), C7-C8 = 1.445(8), C8-C9 = 1.380(2), C9-C10 = 1.414(2), C10-C11 = 1.393(2), C11-C12 = 1.347(1), C12-C7 = 1.451(9), Ti1-N1-C5 = 118.6(4), N2-C6-N3 = 111.6(6).

3.2.1 New Thiophene Activation

Besides the spectroscopic and structural resemblance between **1.1** and **3.1**, the later also mediates the ring-opening of THP's, although at higher temperatures. Heating equimolar mixtures of **3.1** and THP at 60 ºC in C_6H_6 cleanly produces [(Imid^{dipp}N)(xylyl^{ket}Guan)Ti(κ^2-(*S*CH)(CH)$_3$) (**3.3**) as a dark-red solid upon reaction work-up. The ^{1}H NMR spectrum of **3.3** shows a solution C_s symmetric molecule with well-defined resonances for the ring-opened THP unit (6.54-7.79 ppm) (Figure 3.3).

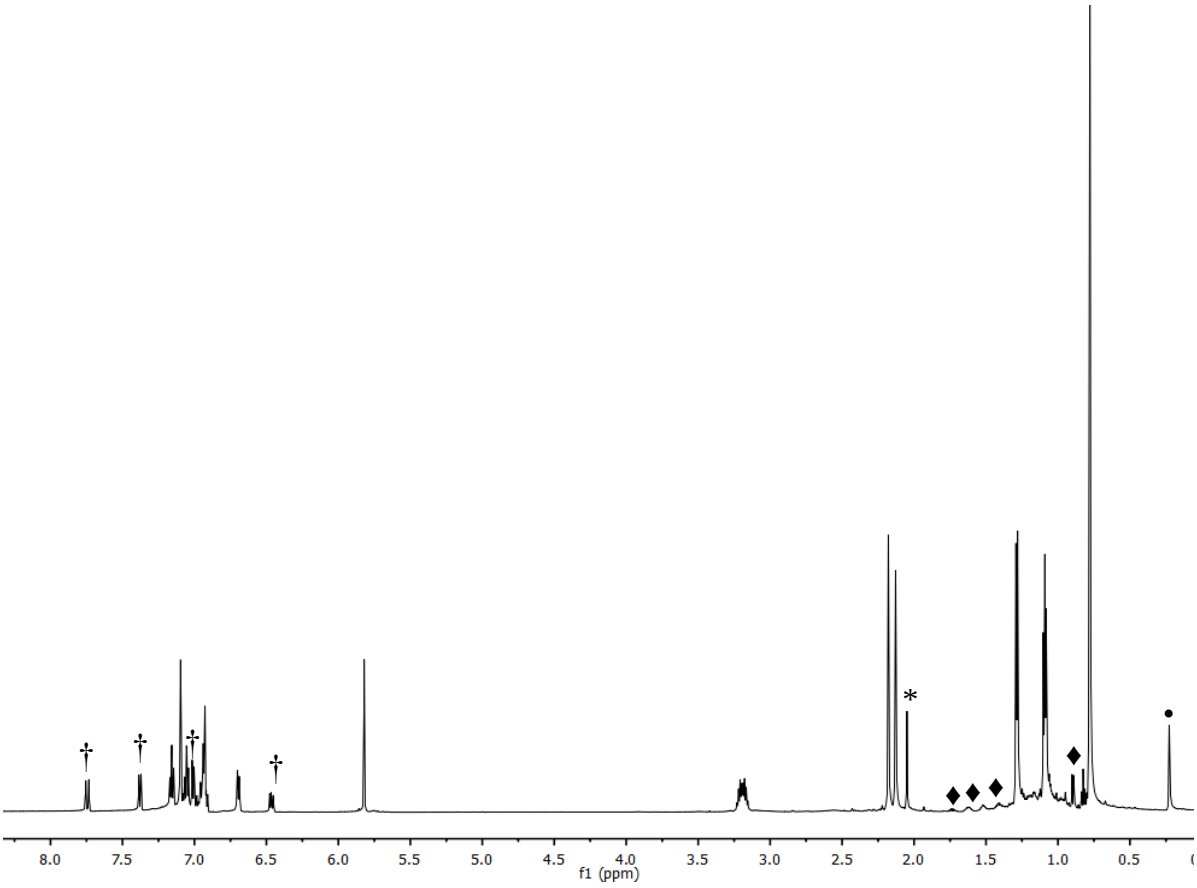

Figure 3.3: ^{1}H NMR spectrum of **3.3** in C_6D_6. Dagger (†) denotes the ring-opened THP ligand resonances. Asterix (*) denotes the presence of residual toluene. Dot (•) denotes the presence of residual silicone grease. Diamond (♦) denotes the presence of residual hexanes.

Figure 3.4 depicts the solid-state structure obtained from an X-ray diffraction experiment of red crystals of **3.3** grown from concentrated toluene solutions stored at –27 ºC for 7d. The disorder of the sulfur atoms over the 1 and 5 positions impede a detailed bond metric analysis of the titanium-THP interactions, but other bond lengths are informative. While the ^{Ket}Guan/ Im^{Dipp}N-titanium bond metrics exhibit negligible changes in comparison to bulkier **2.1**, the THP ring in **3.3** is considerably bent (Ti-S2-C19 = 106.5º (3)). This might be a consequence of crystal packing forces.

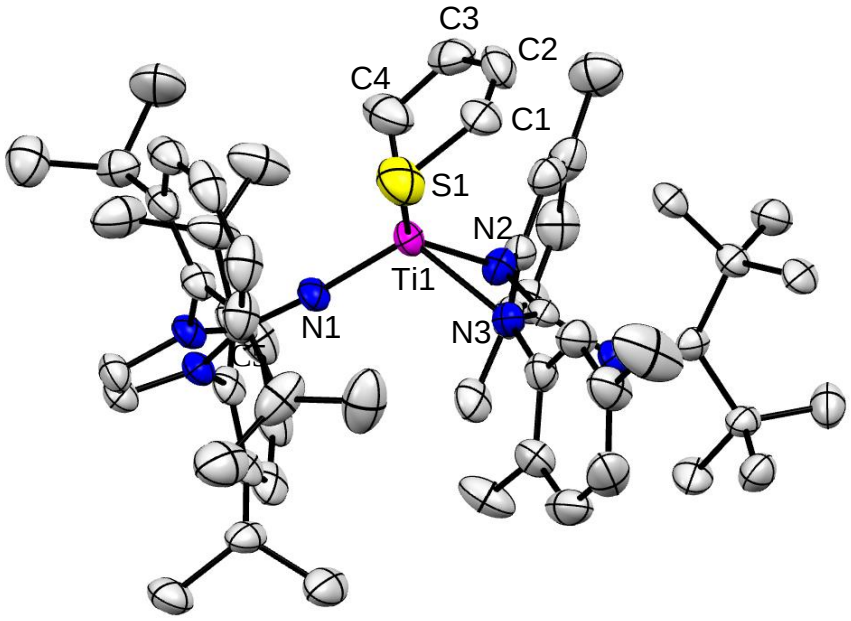

Figure 3.4: Solid-state structure of **3.3** with 50% thermal ellipsoids. Selected bond lengths (Å) and angles (º). T1-N1 = 1.796(3), T1-N2 = 2.128(4), T1-N3 = 2.133(1), T1-S1 = 2.405(4), T1-C4 = 2.037(1), S1-C1 = 1.701(1), C1-C2 = 1.378(2), C2-C3 = 1.429(8), C3-C4 = 1.308(2), Ti1-N1-C5 = 167.0(3), N2-C6-N3 = 112.8(4), S1-Ti1-C4 = 86.9(4).

Furthermore, **3.1** also cleaves the C-S bond of BTP to generate [(Imid^{dipp}N)(xylyl^{ket}Guan)Ti(κ^2-*S*(CH)$_2$C(CH)$_4$*C*] (**3.4**) at 60 ºC in C_6H_6. Finally, the C-S bond cleavage of DBT by **3.1** under identical conditions to that of THP and BTP completes the family THP's ring opened products [(Imid^{dipp}N)(xylyl^{ket}Guan)Ti(κ^2-*S*C(CH)$_4$C(CH)$_4$*C*] (**3.5**). The ^{1}H NMR spectra of **3.4** and **3.5** is reminiscent of **3.3** (Figures 3.5-3.6). Noteworthy, cyclometallation products were not observed nor isolated at 60 ºC.

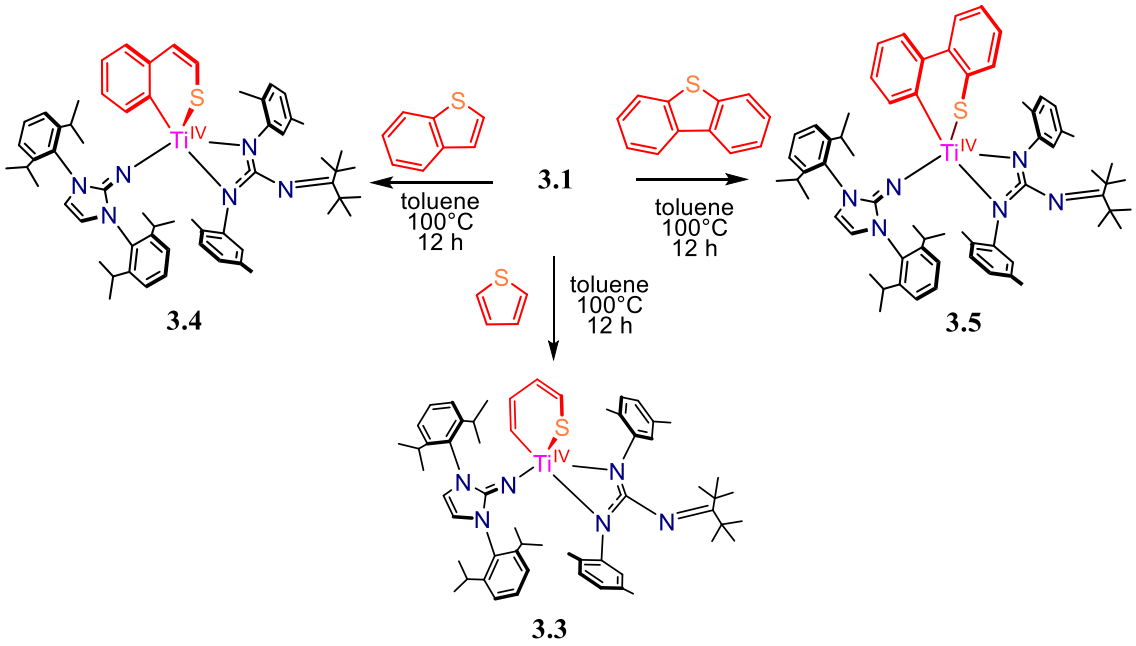

Scheme 3.1: Ring opening of THP, BTP and DBT by **3.1**.

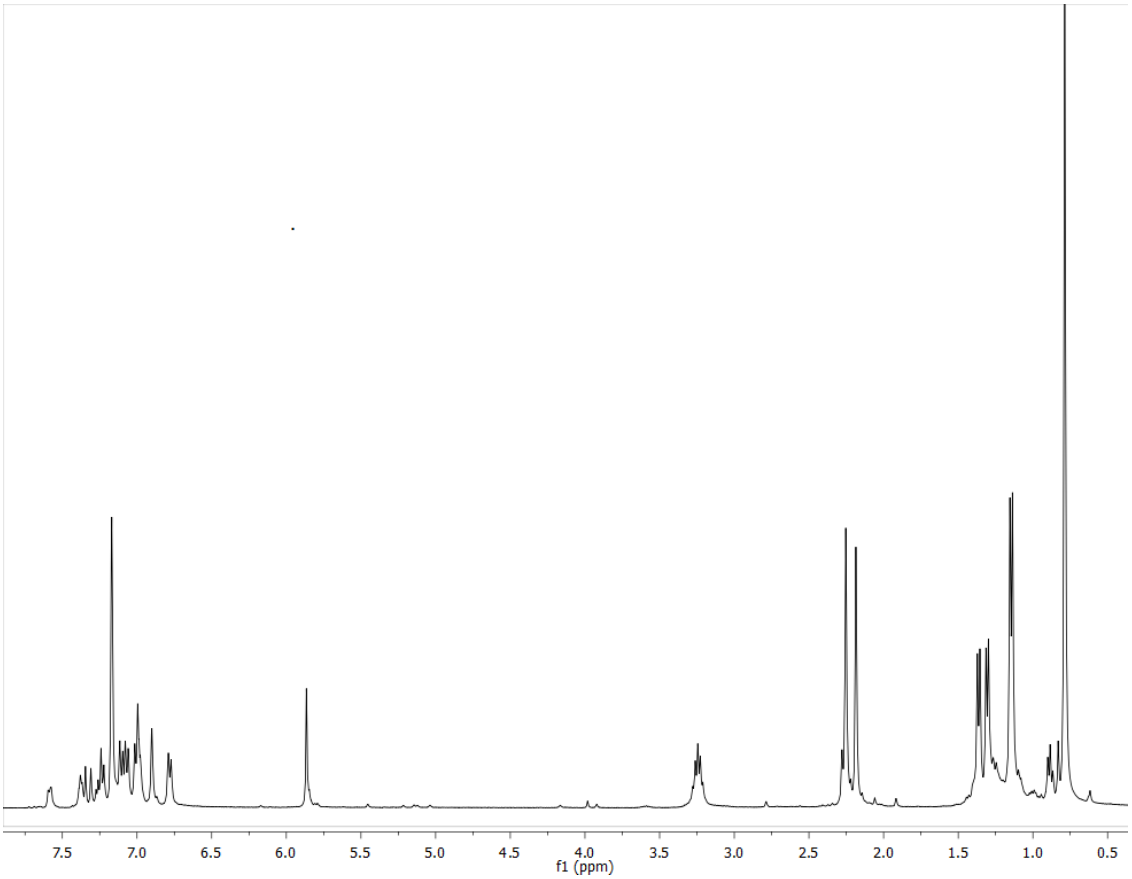

Figure 3.5: ^{1}H NMR spectrum of **3.4** in C_6D_6.

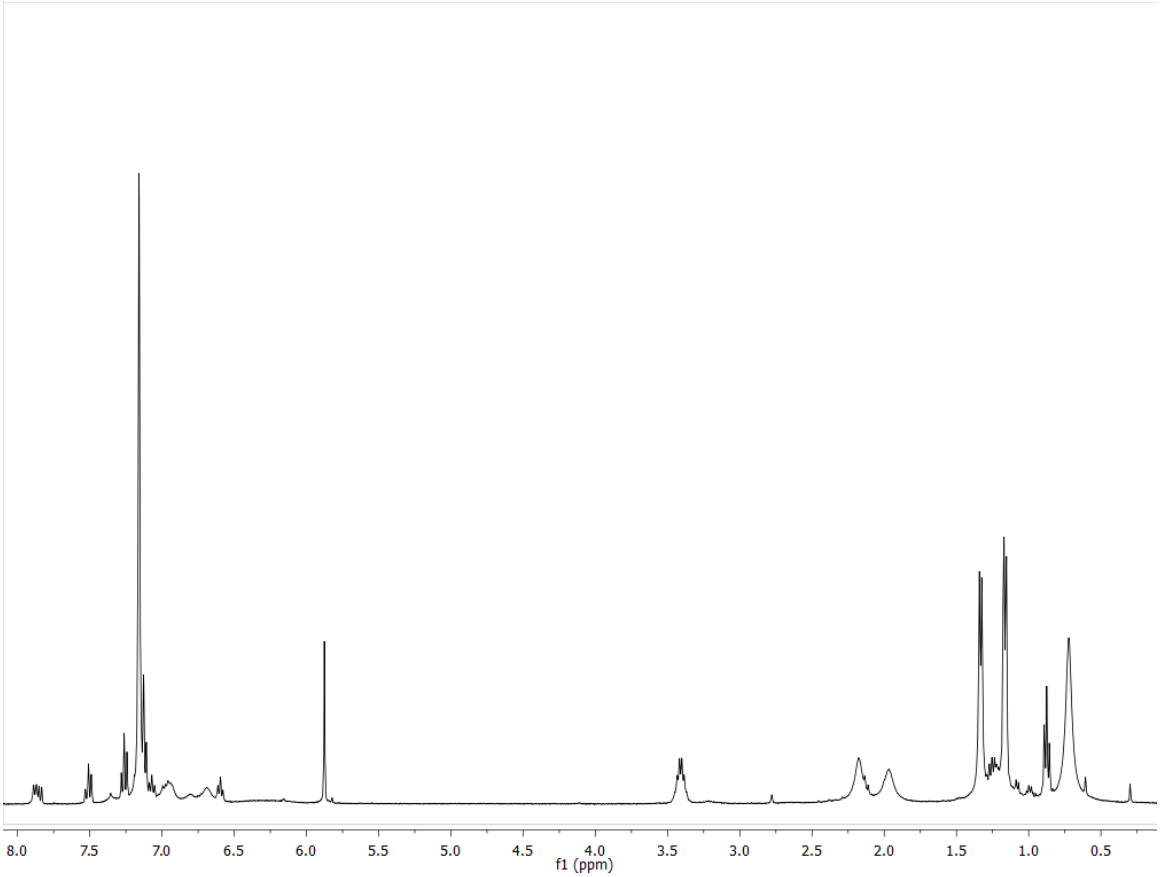

Figure 3.6: ^{1}H NMR spectrum of **3.5** in C_6D_6.

3.2.2 Thiophene photo reactivity

In virtue of the propensity of **2.1** to reductive eliminate THP under UV light irradiation, we set to explore the effect of ligand modifications on **3.3** for THP photoactivation. The UV photolysis of **3.3** was monitored through ^{1}H NMR spectroscopy. This experiment shows gradual consumption of starting materials and production of a major compound over a period of 4 d. Importantly, no free THP resonances were recorded (Figure 3.7). This outcome highlights the dipp substituents as key moieties for photoinduced reductive elimination of THP. At present, the identity of the photoproduct is uknown and further characterization work is ongoing, specifically, to establish definitive connectivity of **3.6** through X-Ray crystallography (eq 3.2).

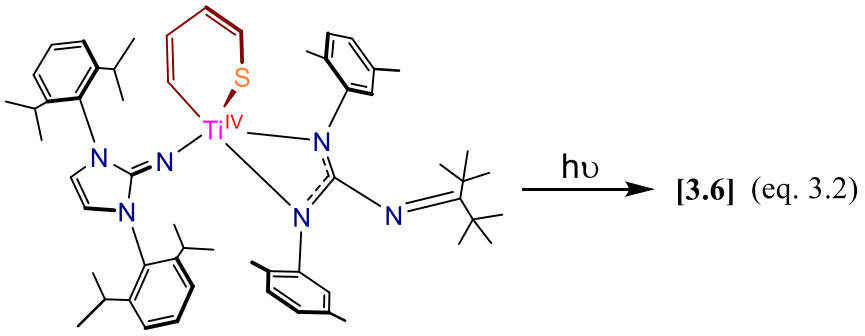

3.3

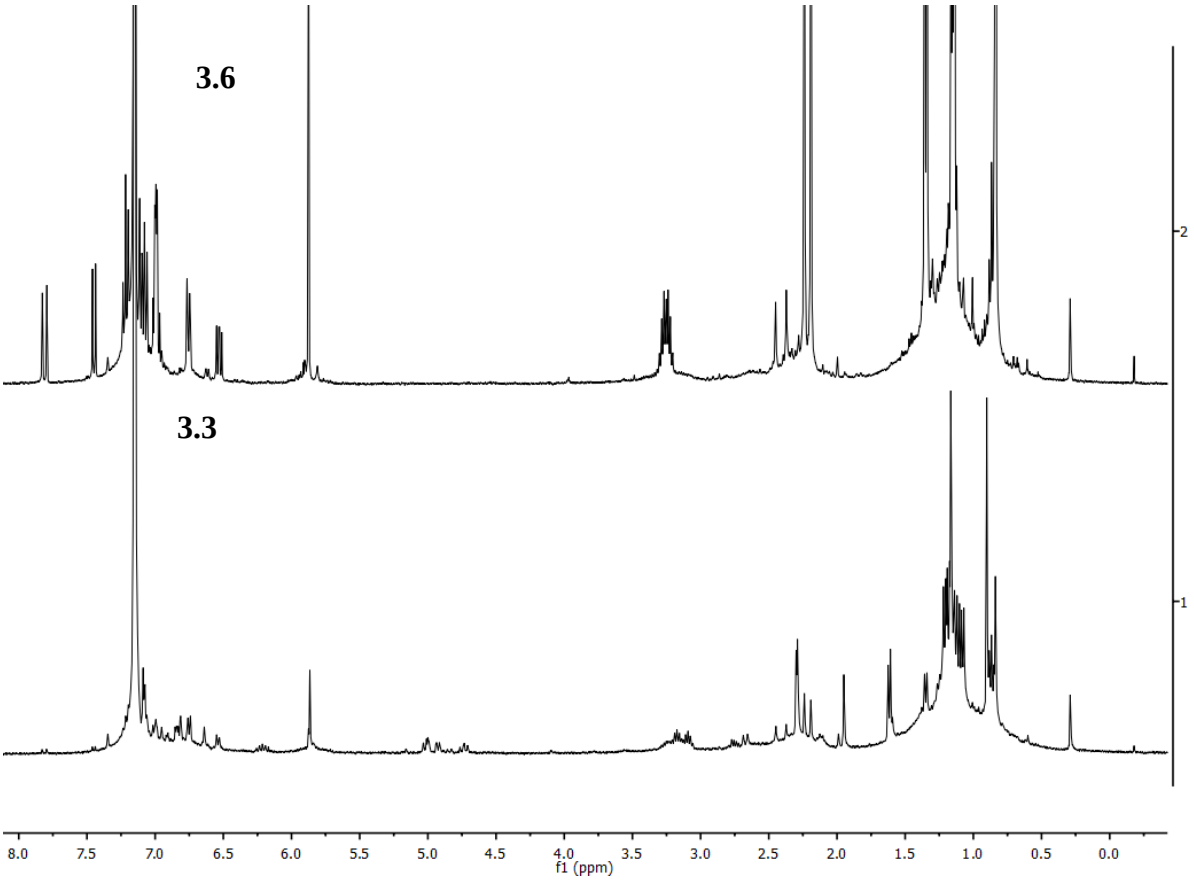

Figure 3.7: ^{1}H NMR spectra showing the photolysis of **3.5** after 4d to produce **3.6**.

Next, **3.4** was photolyzed with UV light under identical conditions to that of **3.1**. Tracking the evolution of this reaction via ^{1}H NMR spectroscopy over 3 d shows consumption of **3.4**, production of a new molecule (**3.7**), and no observable resonances for free DBT (Figure 3.8). If the photolysis is performed in C_6D_{12}, orange crystals of this new complex gradually form over a period of 7 d (eq 3.3).

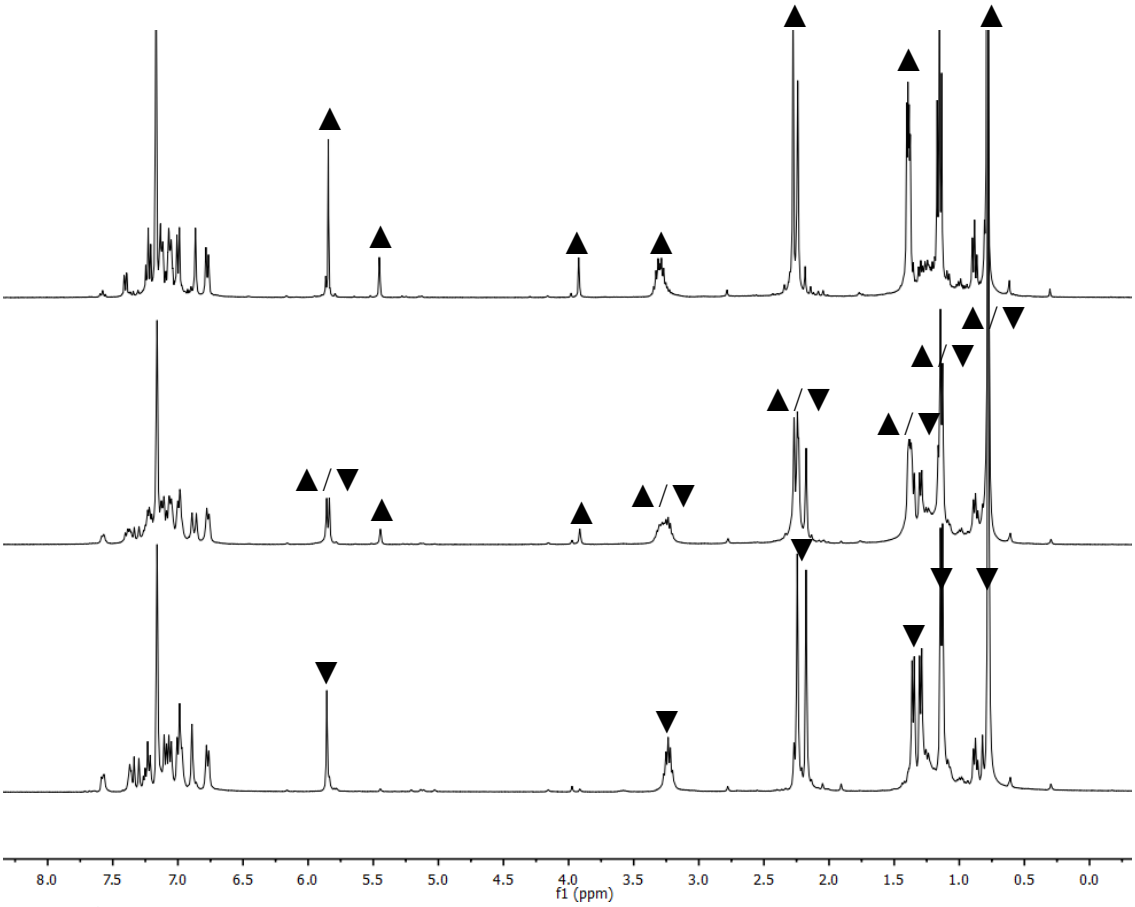

Figure 3.8: ^{1}H NMR spectra showing the photolysis of **3.1** (▼) over 4d to produce **3.7** (▲).

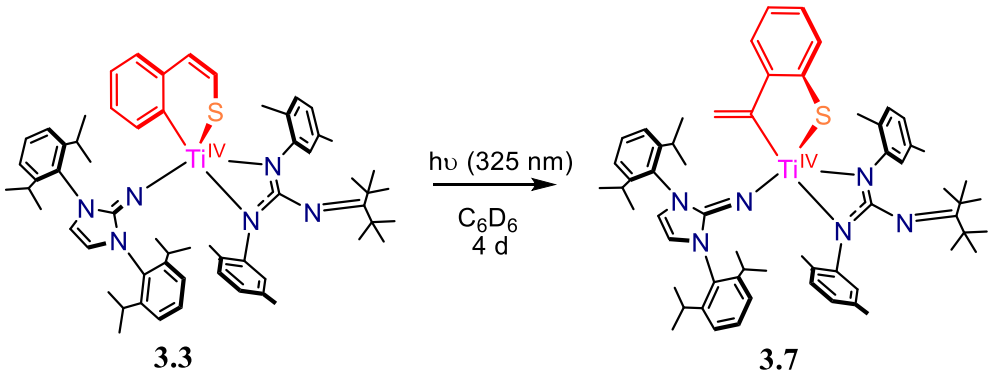

3.3 **3.7** (eq. 3.3)

Crystallographic analysis of this material reveals an unobserved form of BTP activation by a transition metal [(Imid^{dipp}N)(xylyl^{Ket}Guan)Ti(κ^2-*S*C(CH)$_4$C*C*CH$_2$] **3.7** in the P-1 space group. Figure 3.9 depicts a titanium center supporting a benzothiete-type ligand derived from a ring-

contracted BTP moiety. Interestingly, the exocyclic methylene unit has a particularly short C=C bond (C16-C17 = 1.218(7) Å).

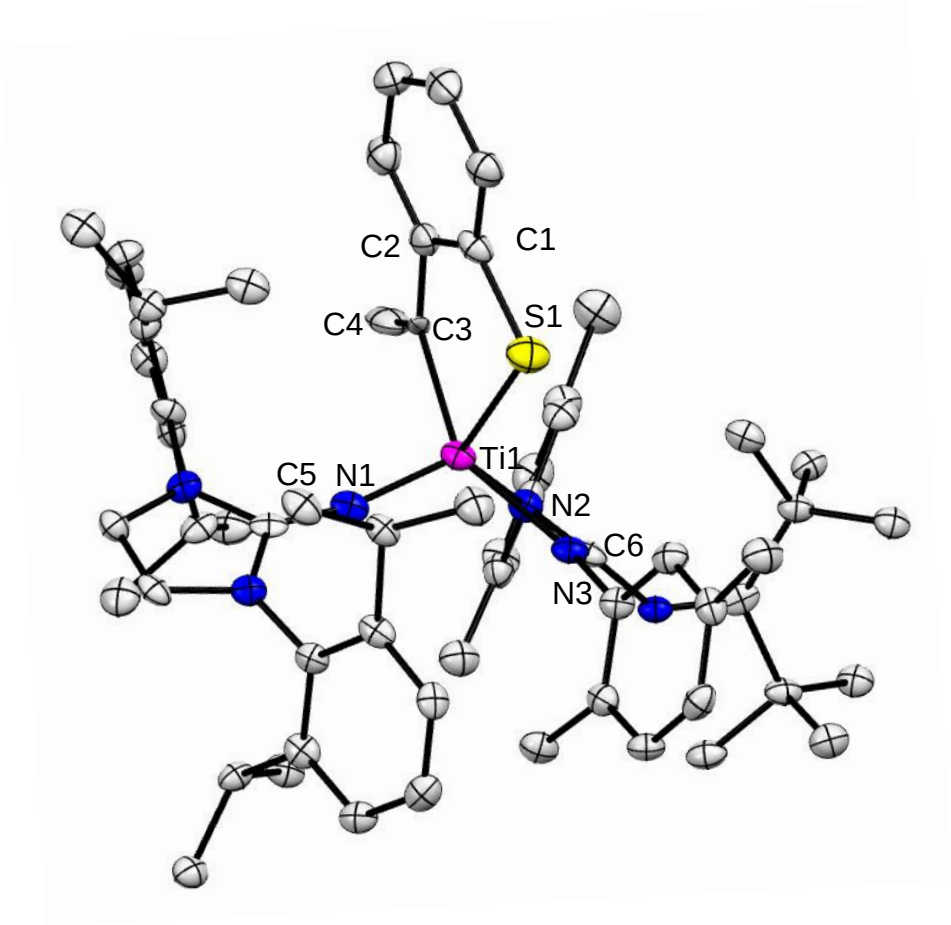

Figure 3.9: Solid state structure of **3.7** with 50% probability ellipsoids. Selected bond lengths (Å) and angles (º). T1-N1 = 1.798(3) Å, T1-N2 = 2.134(3), T1-N3 = 2.072(4), T1-S1 = 2.367(2) Å, T1-C2 = 2.185(4) Å, S1-C1 = 1.701(1), C1-C2 = 1.406(3), C2-C3 = 1.528(7), C3-C4 = 1.218(2) Å, Ti1-N1-C5 = 161.8(3), N2-C6-N3 = 111.2(4), S1-Ti1-C4 = 82.9(1).

Lastly, UV irradiation of **3.5** in C_6D_6 leads to DBT reductive elimination and formation of an intermolecularly-capped titanium complex [(Imid^{dipp}N)(xylyl^{Ket}Guan)Ti(η^6-C_6D_6)] (**3.8**)

(Section 3.X.1) (eq 3.3) (Figure 3.8). A similar reaction was reported by Rauchfuss, where the titanium complex $(Cp)_2TiSC_{12}H_8$ reductively eliminates DBT upon photolysis in a CO atmosphere to produce $(Cp)_2Ti(CO)_2$.[170] Noteworthy, the $SC_{12}H_8$ unit in $(Cp)_2TiSC_{12}H_8$ was installed through a lithium chloride (LiCl) elimination reaction between $(Cp)_2TiCl_2$ and 2,2'-$Li(LiS)C_{12}H_8$. Additionally, there is no reaction between $(Cp)_2Ti(CO)_2$ and DBT.

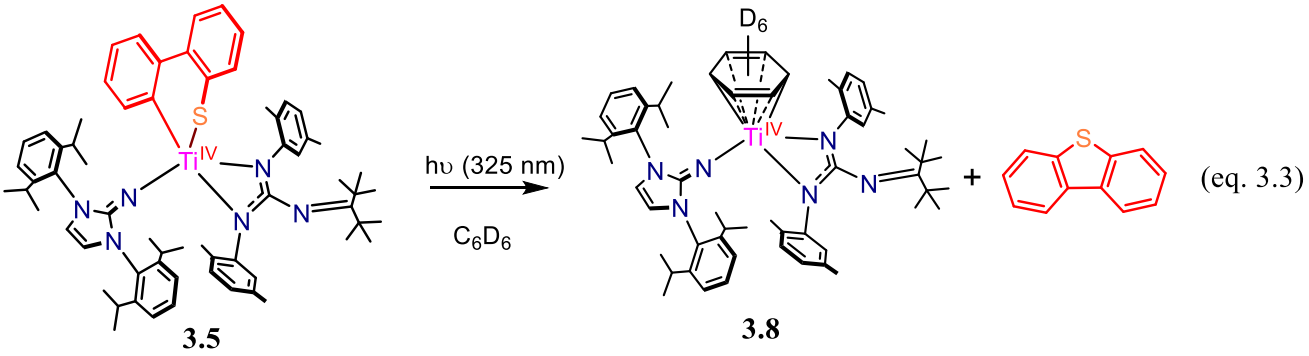

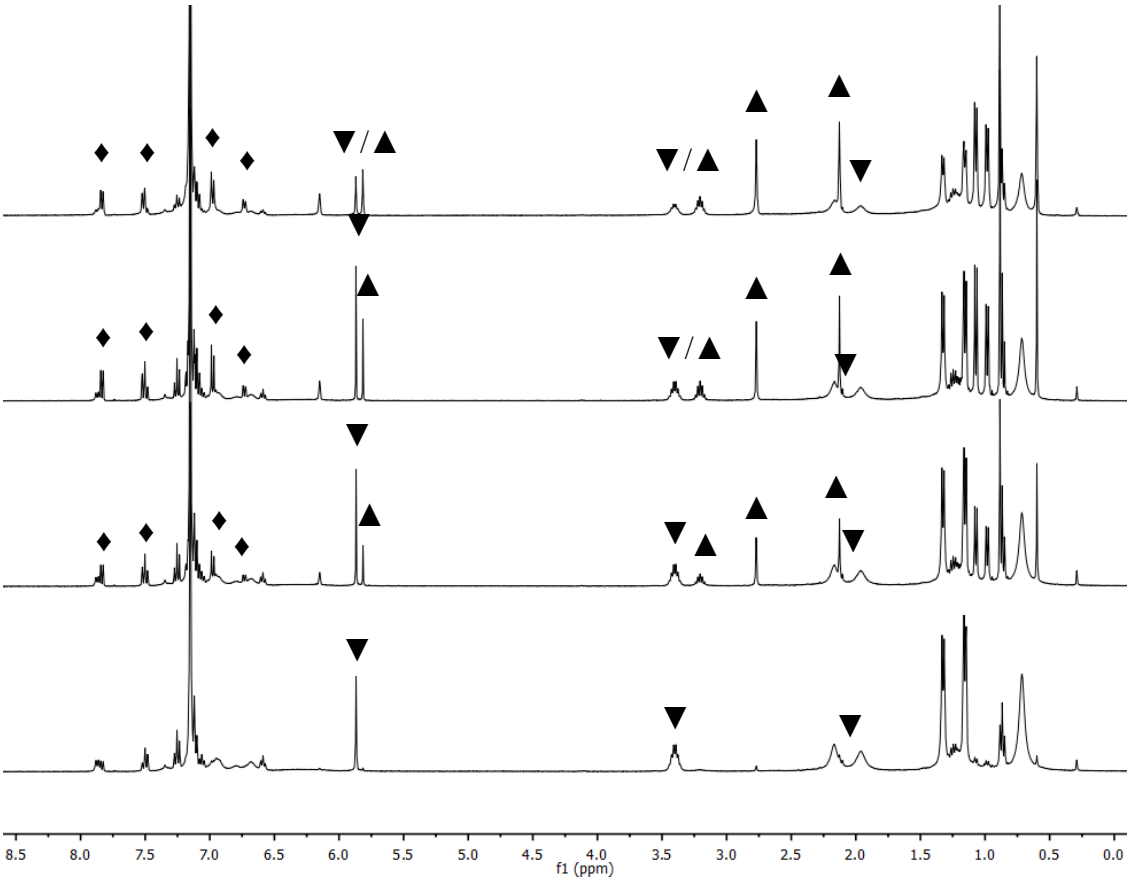

Figure 3.10: ^{1}H NMR spectra showing the photolysis of **3.5** (▼) over 4 d to produce **3.8** (▲) and DBT (♦).

3.2.3 Bis(pentafluorophenyl)borane insertion

The unsaturations of the THP ligand in **3.3** are possible entry points for functionality introduction apart from just hydrogenation. We selected bis(pentafluorophenyl)borane $[(C_6F_5)_2BH]_2$ as a hydroborylation reagent for the coordinated THP moiety of **3.3**, given the well-established reactivity of $[(C_6F_5)_2BH]_2$ towards a range of alkenes and alkynes.[171-173] Moreover, $(C_6F_5)_2BH$ is an potent Lewis acid in the ring opening of epoxides and cyclic ethers,[113] a property that might be suitable to further functionalize the THP ligand in **3.3**.

We found that mixing equimolar amounts of **3.3** and $[(C_6F_5)_2BH]_2$ in C_6H_6 produces a new, dark red compound , which can be recrystallized from Et_2O solutions stored at −25 ºC for 4 d. Analysis of these crystals by synchrotron radiation reveal formation of a titanium-supported thiaboracyclohex-4-enyl ring derived from the insertion of boron from $[(C_6F_5)_2BH]_2$ across a C-S bond [(Imid^{dipp}N)(xylyl^{Ket}Guan)Ti[(η^3-*S*(*C*H)$_2$CHCH$_2$B(C_6F_5)$_2$] (**3.9**) (eq 3.4).

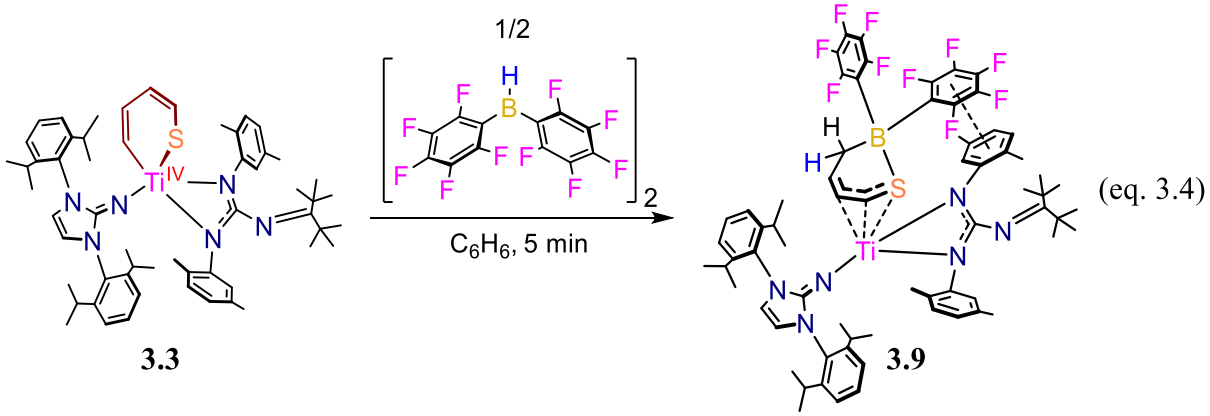

(eq. 3.4)

The bond metrics of the expanded THP unit support the thiaboracyclohexenyl resonance form (C54-S1 = 1.748(4) Å, C54-C55 = 1.425(5) Å,C55-C56 = 1.354(5) Å, C56-C57 = 1.496(4) Å, C56-B1 = 1.614(5) Å), although, the B-S bond in the thioboracycle (S1-B1 = 2.006(3) Å) is significantly longer than a single B-S bond (ca. 1.8 Å)[174-175] suggesting a S→B dative interaction. The η^3 interactions are consistent with single Ti-S,[94, 176-177] and Ti-C bonds[178] (Ti-S = 2.471(9) Å,

Ti-C54 = 2.139(3) Å, Ti-C55 = 2.478(3) Å)). Possibly, the shortening of the Ti-Cγ bond is due to steric effects and puckering of the thiaboracycle ring. Furthermore, a flanking 2,5-xylyl ring of the ^{Ket}Guan ligand is arranged in a coplanar mode with a pending perfluorinated arene ring through π-π stacking interactions (xylyl-C_6F_6 = 3.672 Å (avg)) (Figure 3.11).[179-180]

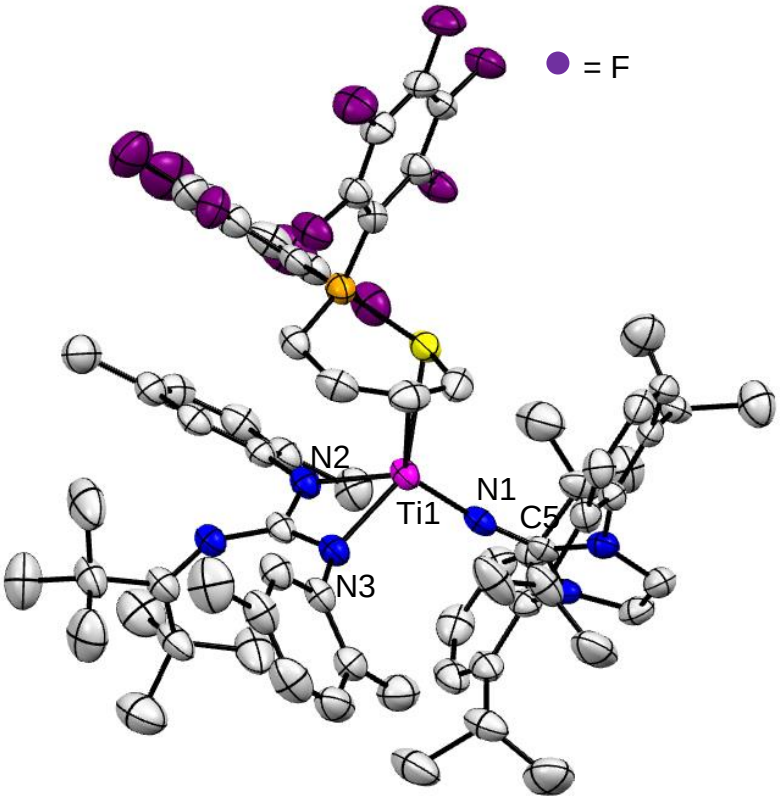

Figure 3.11: Solid state structure of **3.9** with 50% probability ellipsoids. Selected bond lengths (Å) and angles (º). T1-N1 = 1.811(3) Å, T1-N2 = 2.082(2) Å, T1-N3 = 2.112 (2) , T1-S1 = 2.471(9), Ti-C54 = 2.139(3), Ti-C55 = 2.487(3), C54-S1= 1.748(4), C54-C55 = 1.425(5),C55-C56 = 1.354(5), C56-C57 = 1.496(4), C57-B1 1.614(5), S1-B1 = 2.006(3), xylyl-C_6F_6 = 3.672 (avg), Ti1-N1-C5 = 164.2(2), N2-C6-N3 = 112.1(2)º, S1-B1-C57 = 105.1(2).

This interaction is preserved in solution since the ^{19}F NMR shows two sets of resonances in a 2:1:2 ratio each, corresponding to the meta, para, ortho, fluorine nuclei in the locked ring (xylyl-C_6F_5) and the unbonded B-C_6F_5 moiety (Figure 3.12). Additionally, the protons of the thiaboracyclohexenyl ligand appear as inequivalent, yet, well-defined resonances (Figure 3.13).

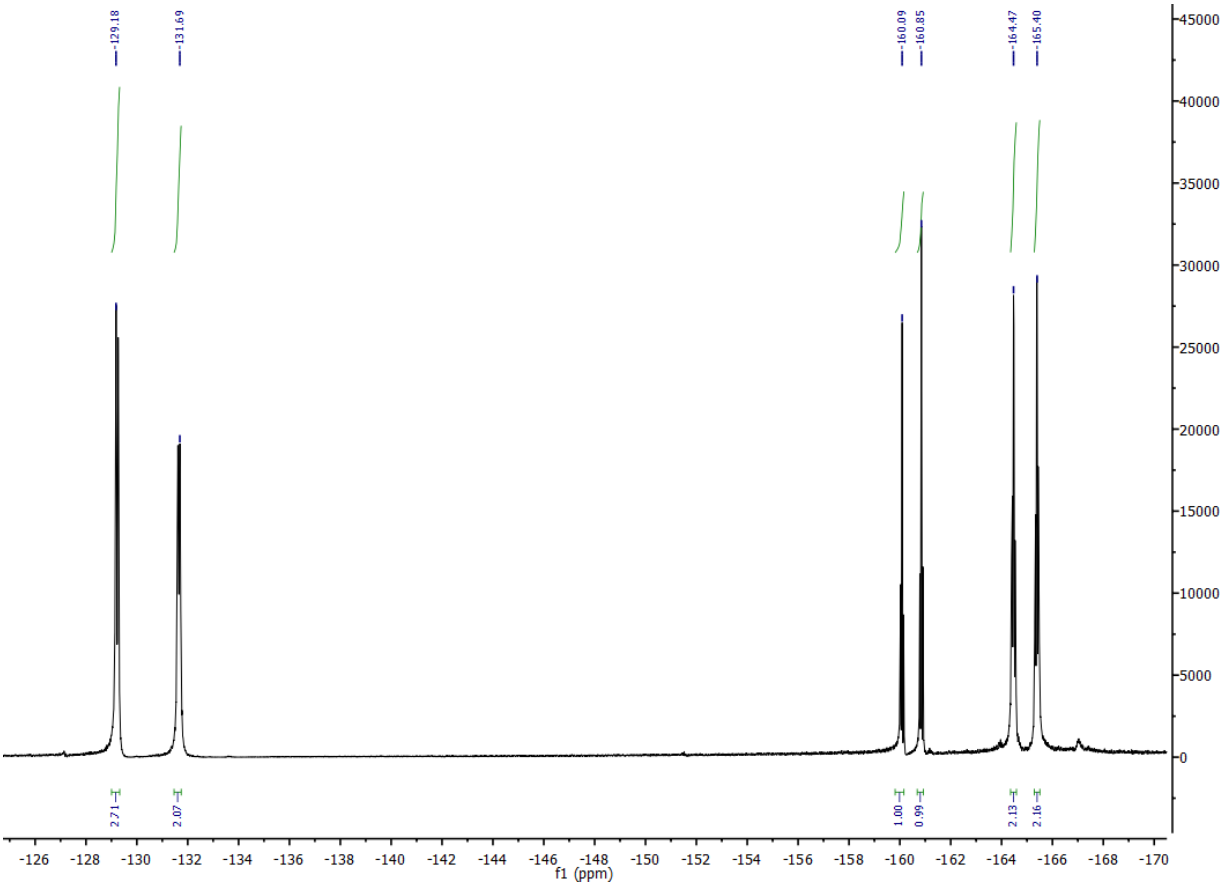

Figure 3.12: $^{19}F\{H/C\}$ NMR spectrum for **3.9**.

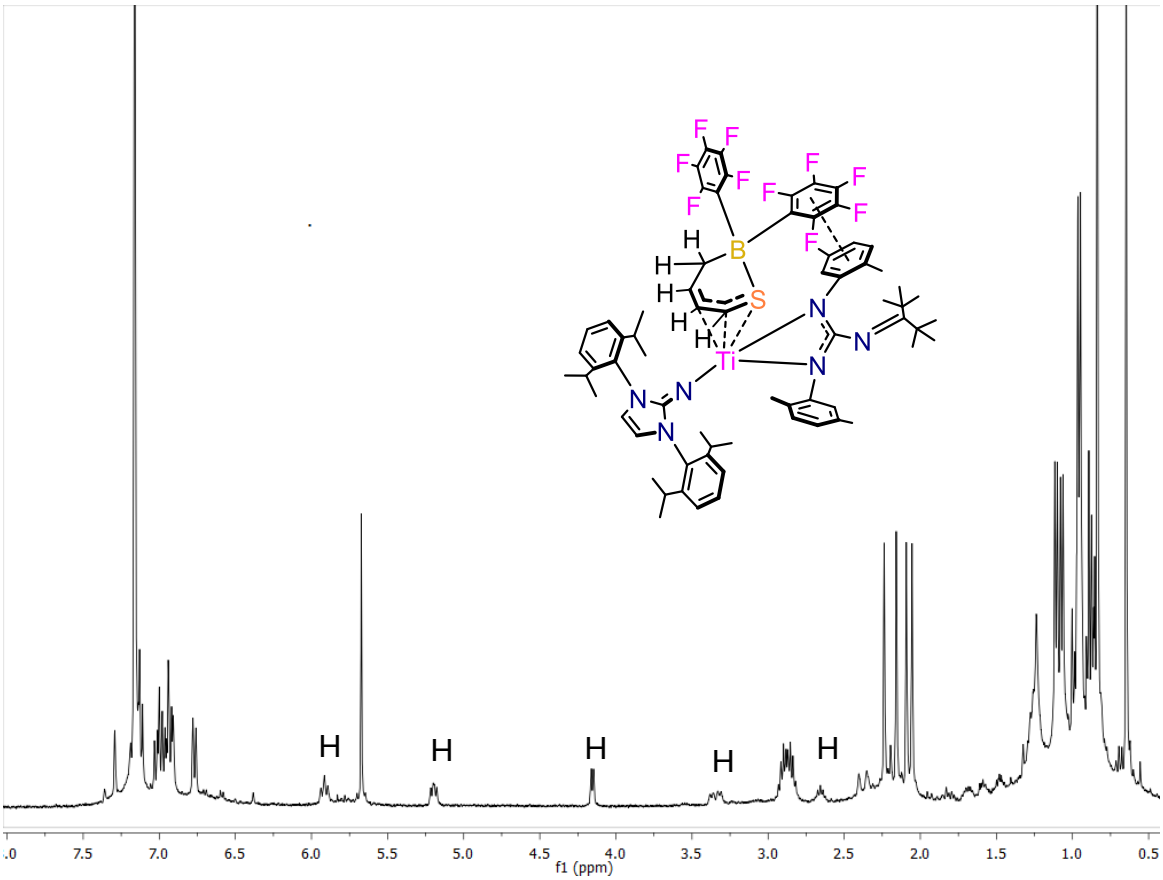

Figure 3.13: Proton resonances for the THP ligand in **3.9**.

To our knowledge, the synthesis of thiaboracyclohexenes-type rings has only been reported by Tokitoh in the reaction of [(Tbt)B-μ-η^2:η^2-*S*$_2$-SnPh$_2$] (Tbt = 2,4,6-tris[bis(trimethylsilyl)methyl]phenyl) with different 1,2-butadienes.[181] As such, the presented work might open new avenues for the synthesis of these novel and interesting types of heterocycles. Currently, we are exploring the reactivity of [(C$_6$F$_5$)$_2$BH]$_2$ towards **3.4** and **3.5**.

3.2.4 Borane-Arene Adduct

The reaction between **3.3** and [(C$_6$F$_5$)$_2$BH]$_2$ exemplifies that molecules such as THP are prone to novel forms of activation upon coordination to the [[(Imid^{dipp}N)(xylyl^{ket}Guan)Ti] system. In the same vein, the doubly-reduced capping ring in **3.1** might serve as a preliminary platform to

develop functionalization methods for de-aromatized systems.[182-183] To test this hypothesis, we selected $[(C_6F_5)_2BH]_2$ given its singular reactivity with **3.3**, strong Lewis-acid character, and, hydroborylating properties.

The mixing of **3.1** and one equiv of $[(C_6F_5)_2BH]_2$ generates a vibrant-green mixture in C_6D_6 (eq. 3.5). The ^{1}H NMR spectrum of this new molecule displays well-defined resonances from 0.55 to 6.99 ppm consistent with diamagnetic species (**3.10**).

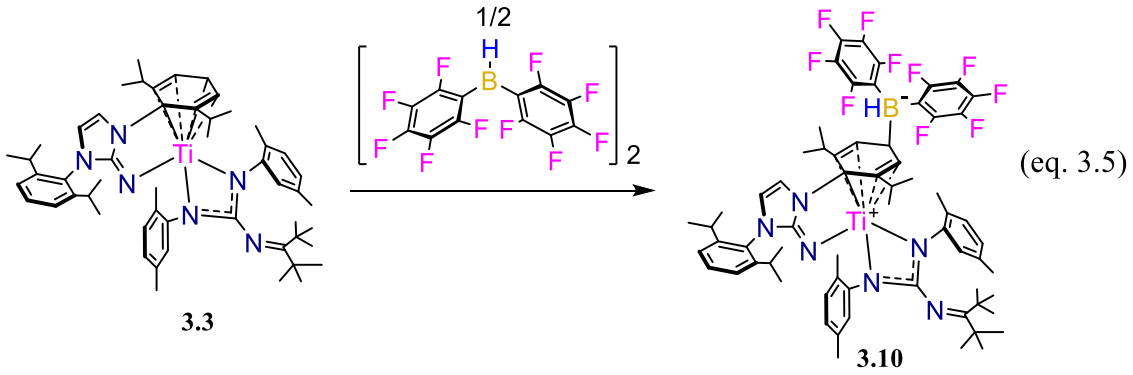

(eq. 3.5)

Concentrated toluene solutions of this material were stored at −25 ºC for 1 d to produce X-ray diffraction quality green crystals. The solid-state structure of this compound shows the addition of one $[(C_6F_5)_2BH]_2$ molecule to the masking ring of the titanium center (Imid^{dipp}N)(xylyl^{ket}Guan)Ti(η^5-(*C*H)$_5$CH-BH(C_6F_5)$_2$) **3.10 (Figure 3.14)**. The capping ring adopts a half-chair conformation with bond metrics in accordance to 1,2-cyclohedienyl species (C16-C17 = 1.400(2) Å, C17-C18 = 1.372(1) Å, C18-C19 = 1.538(2) Å, C19-C20 = 1.520(2) Å, C20-C21 = 1.440(2) Å). The aryl-borane interaction replaces one of the titanium-arene bonds decreasing the hapticity of the masking ring from η^6 to η^5 (Ti1-C16 = 2.231(1) Å, Ti1-C17 = 2.375(1) Å, Ti1-C18 = 2.384(1) Å, Ti1-C20 = 2.375(2) Å, Ti1-C21 = 2.369(1) Å). The masking ring-borane C-B bond is longer (C19-B1 = 1.711(2) Å) than single C-B bonds (1.6 Å (avg)).{Weast, 1984 #188}

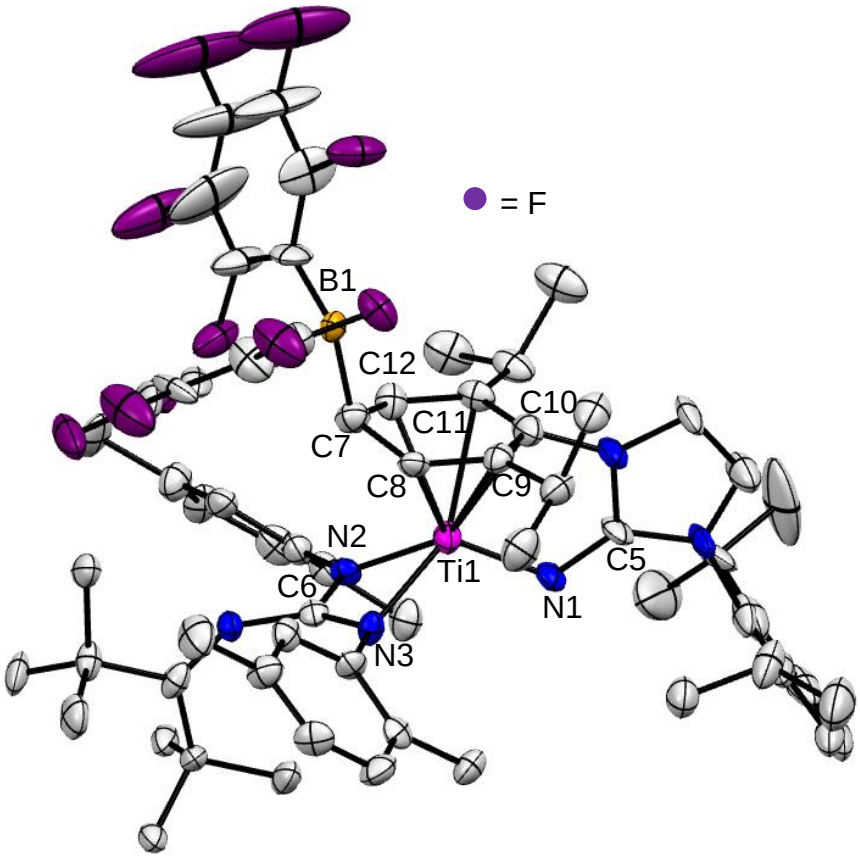

Figure 3.14: Solid state structure of **3.10** with 50% probability ellipsoids. Selected bond lengths (Å) and angles (º). T1-N1 = 1.860(7), T1-N2 = 2.073(9), T1-N3 = 2.087 (9), T1-C8 = 2.384(9), Ti-C9 = 2.368(9), Ti-C10 = 2.231(9) Å, Ti-C11 = 2.369(9), Ti-C12 = 2.375(9) Å, C7-B1 = 1.711(9), C56-C57 = 1.496(4), C57-B1 1.614(5), S1-B1 = 2.006(3), Ti1-N1-C5 = 119.8(8), N2-C6-N3 = 112.1(8).

To our knowledge, **3.10** is the first example of a structurally characterized de-aromatized ring coordinated to a Lewis acid. Currently, we are trying to translate this novel reactivity pattern of $[(C_6F_5)_2BH]_2$ into an intermolecular context, specifically for the synthesis of aryl boranes.

3.2.4 Benzene Hydrogenation

The formation of the intermolecularly-capped titanium complex **3.8** was described in (Section 3.2.2). **3.8** is also obtained from the photolysis of **3.1** in C_6D_6 over a period of 1 d (60%

spectroscopic yield) (Figure 3.15). Similarly, **3.8** is obtained via the thermolysis of **3.1** in C_6D_6, reaching equilibrium after 2 d (40% spectroscopic yield). Importantly, no cyclometallation or metal-hydride resonances are observed under these conditions.

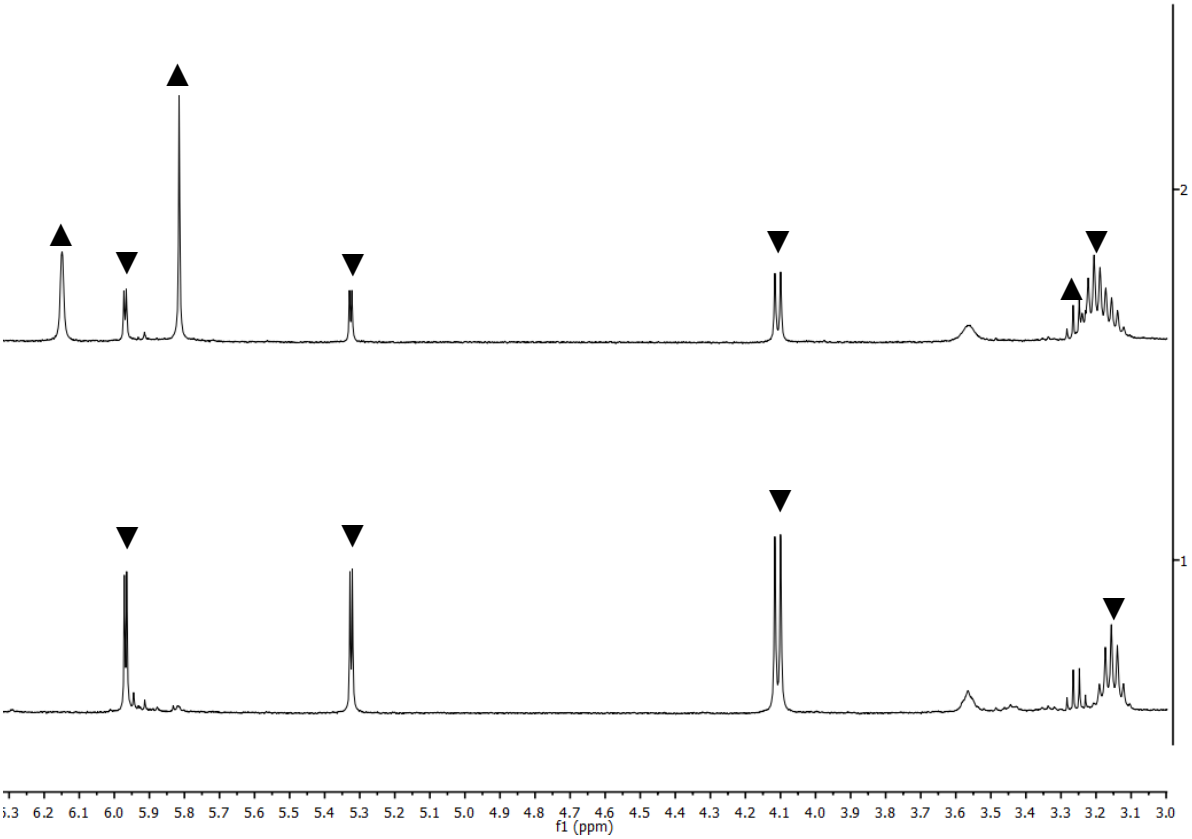

Figure 3.15: ^{1}H NMR spectra showing the photolysis of **3.1** (▼) over 4d to produce **3.8** (▲).

The hydrogen isotopologue [(Imid^{dipp}N)(xylyl^{Ket}Guan)Ti(η^6-C_6H_6) (**3.11**) is more conveniently synthesized in preparative scales via the two-electron KC_8 reduction of **3.2** in THF/C_6H_6 (30:1) mixtures at –78 ºC (eq 3.5).

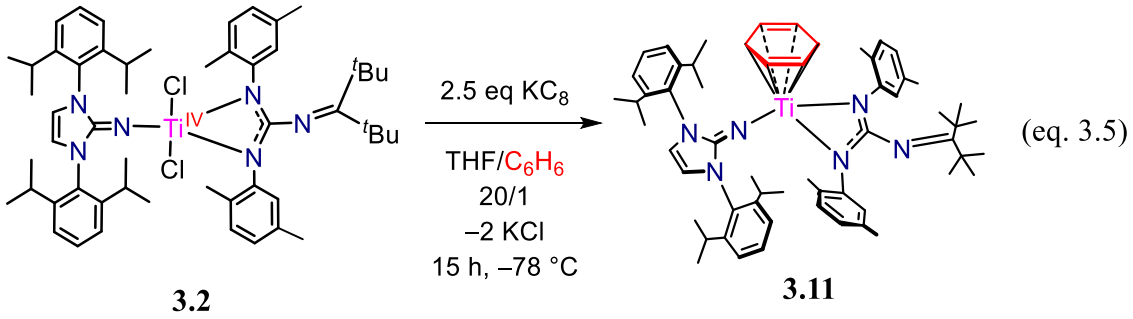

3.2 **3.11** (eq. 3.5)

With **3.11** in hand, its reactivity towards H_2 was investigated to compare the effect of the xylyl^{ket}guan ligand versus the dipp-type substitution in **1.1**.

The heating (80 ºC) of pressurized H_2 (8 atm) C_6D_6 solutions of **3.11** leads to the catalytic hydrogenation of C_6D_6 into $C_6H_6D_6$ over a period of 6 d (TON = 8). This new hydrogenation profile might be a consequence of employing the less encumbering xylyl^{Ket}guan ligand which permits the coordination of benzene because no arene hydrogenation chemistry by the bulkier **1.1** system has been observed under identical conditions. Noteworthy, other early transition-metals catalyze the hydrogenation of different arenes,[184-186] but no titanium-based examples are precedented. Thus, this outcome represents another chemical consequence of subtle structural modifications on the metal's secondary coordination sphere in reactivity.

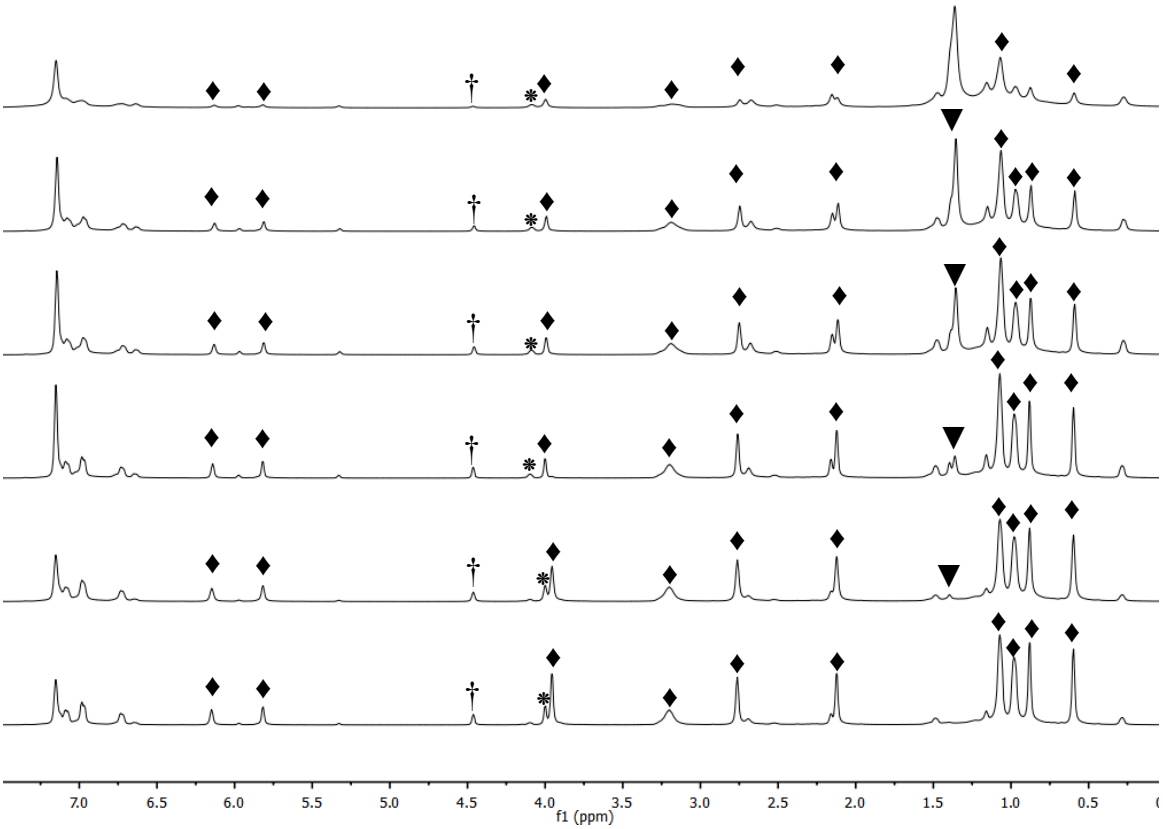

Figure 3.16: ^{1}H NMR spectra showing the hydrogenation of C_6D_6 to $C_6D_6H_6$ (▼) by **3.11** (♦), H_2 (⁕), Fc (†). Experiment performed with the help of Alejandra Gomez.

3.2.4 Toluene Coordination and N_2 Activation

Encouraged by the effects of ligand modifications in the reactivity at titanium, we synthesized a system where the aliphatic moieties on the ortho positions on the ^{ket}Guan ligand are nonexistent. In comparison to **1.1** and **3.1**, this new molecular design renders a more exposed titanium center and opens new possibilities up for different chemistries.

A 4-^{t}Bu-phenyl ^{ket}Guan ligand [(4-^{t}BuPh^{ket}guan = (^{t}BuC=N)C(N4-^{t}BuPh)$_2$] satisfies this criterion, and, moreover, the ^{t}Bu groups serve as excellent electron-donating substituents and spectroscopic manifolds.

The starting point for this reductions chemistry is the titanium dichloride [(Imid^{dipp}N)(4-^{t}BuPh^{ket}Guan)Ti(Cl)$_2$ (**3.12**) readily obtained from a metathesis reaction between (Imid^{dipp}N)TiCl$_3$

and (4-^{t}BuPh^{ket}guan)Li. The low-temperature (–78 ºC) reduction of **3.12** with two equiv of KC_8 in THF gives a new diamagnetic product which has not been characterized via X-Ray diffraction methods (**3.13**).

Under similar conditions but using toluene instead of THF as the reaction solvent, an intractable product mixture is obtained. However, if 1,4,7,10,13,16-hexaoxacyclooctadecane (18-crown-6 = 18C6) is added as a solubilizing agent for KC_8, the toluene-capped titanium complex is produced [(Imid^{dipp}N)(4-^{t}BuPh^{ket}Guan)Ti(η^6-$C_6H_6CH_3$) (**3.14**) (eq 3.6).

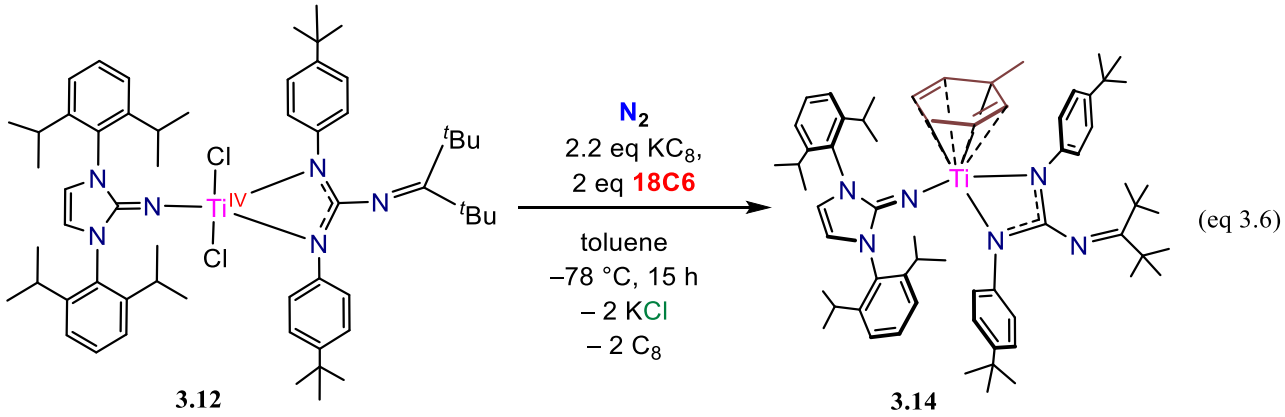

3.12 **3.14** (eq 3.6)

Disorder problems at the capping-ring and 4-^{t}BuPh^{ket}guan ligand preclude a detailed discussion regarding the solid-state structure of **3.14 (Figure 3.17)**, but, connectivity is definitively established. The successful synthesis of **3.14** might provide a new entry to low-valent chemistries assisted by a more exposed titanium center.

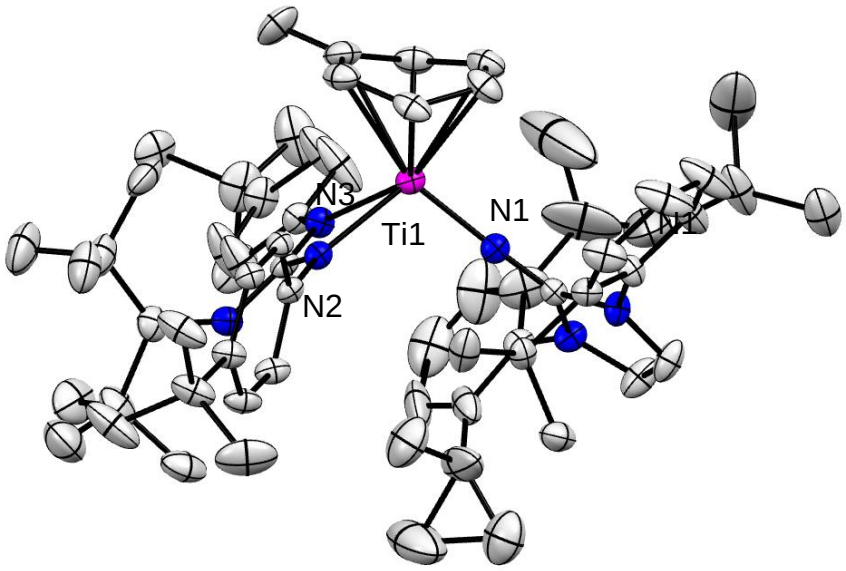

Figure 3.17: Solid state structure of **3.14** with 50% probability ellipsoids. Selected bond lengths (Å) and angles (º). T1-N1 = 1.860(2), T1-N2 = 2.171(2), T1-N3 = 2.155(2) Ti1-N1-C5 = 177.2(2), N2-C6-N3 = 111.4(2)

Additionally, if the reduction of **3.12** is performed with 3.1 eq of KC_8 in THF/toluene solutions (20/1) at –78 ºC a new dark-brown product is generated upon reaction work up. This material produces yellow X-ray quality crystals from pentane solutions stored at –25 ºC for 3 d. The solid-state structure obtained from these crystals depicts a dianionic titanium-dimer with two bridging nitride ligands $[K_2(Imid^{dipp}N)(4\text{-}^{t}BuPh^{ket}Guan)Ti]_2(\mu\text{-}N)_2$ (**3.15**) (Figure 3.18). The planar diamond core Ti_2N_2 features Ti-N bond lengths consistent with complete N_2 splitting[187] (T1-N5 = 1.785(7) Å, T1-N4 = 1.813(6) Å, T1-N13 = 1.872(6) Å, T2-N13 = 1.872(6) Å, T2-N14 = 1.854(6) Å, N13-N14 2.504(1) Å). One of the potassium cations is sandwiched between the flanking aryl rings of the $Imid^{dipp}N$ ligands. The other potassium cation features π-interactions with a flanking $Imid^{dipp}N$ aryl ring and the rest of its coordination sphere is completed through chelation of an N-atom and η^2-arene ring of a ^{Ket}Guan ligand. The only other report of a titanium complex

capable of cleaving the triple bond of N_2 to generate the corresponding bridging nitride was reported by Gambarotta in 2009.[187]

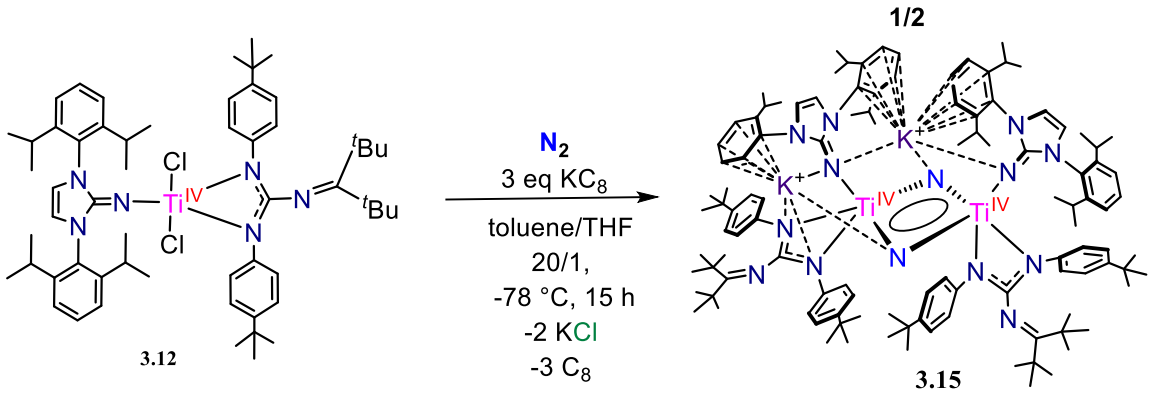

(eq 3.7)

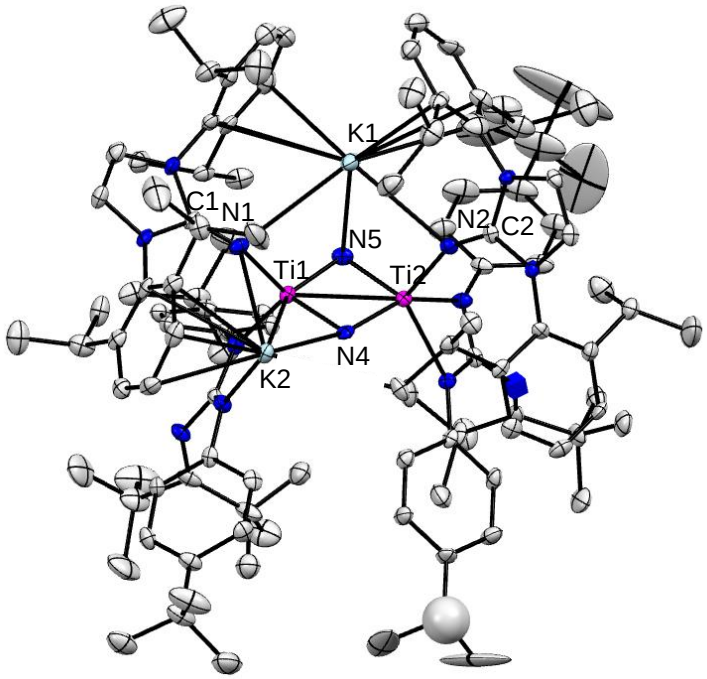

Figure 3.18: Solid state structure of **3.15** with 50% probability ellipsoids. Selected bond lengths (Å) and angles (°).T1-N1 = 2.048(7), T2-N2 = 1.980(7), T1-N4= 1.785(5) Å, T1-N5 = 1.813(6), T2-N4= 1.785(5) Å, T2-N4 = 1.872(6), N4-N4 = 2.504(0). C1-N1-T1 = 146.5(5), C2-N2-T2 = 154.4(6).

3.3 CONCLUSIONS

We have taken advantage of the synthetic modularity found in guandinate-type ligands as reactivity manifolds in the system [(^{ket}guan)(Im^{Dipp}N)Ti]. Specifically, the ortho substituents in the R-groups of the ^{ket}guan [(^{t}BuC=N)C(R)$_2$ R = Dipp, Xylyl, 4-^{t}BuPh)] were systemically varied to test the effect of decreasing the steric encumbrance in the metal's secondary coordination sphere. In comparison to the bulkier Dipp system **1.1**, 3.1 prevents intermolecular cyclometallation, and consequently, different forms of THP's activation and hydrogenation chemistry are attained. Finally, the more exposed titanium system 3.12 system permits the coordination of toluene and gives access to complete N_2 splitting under reducing conditions.

3.4 EXPERIMENTAL SECTION

3.4.1 General Considerations

All air and moisture-sensitive operations were performed in a M. Braun dry box under an atmosphere of purified nitrogen or using high vacuum standard Schlenk techniques. Benzene, Et_2O, hexanes, pentane, toluene and THF were dried using a Pure Process Technology Solvent Purification System and subsequently stored under a dinitrogen atmosphere over activated 4 Å molecular sieves. All deuterated solvents were purchased from Cambridge Isotope Laboratories Inc. The deuterated solvents and THP were degassed by three freeze-pump-thaw cycles and were dried over activated 4 Å molecular sieves for 24 h prior to use. The Celite and the 4 Å molecular sieves were heated to 150℃ for at least 24 h and then cooled under vacuum. $(C_6F_5)_2BH$ was synthesized according to literature procedures.[171] xylyNCNxylyl was synthesized accordioning to a modify literature procedure.[188] All other reagents were purchased from commercial sources and

used as received. Anhydrous BTP and DBT were obtained via sublimation under dynamic vacuum (200 mTorr) at 60 ºC. NMR spectra were recorded on a Bruker AVANCE III 400 MHz spectrometer. Resonance assignments in the ^{13}C NMR spectra were based upon ^{1}H – ^{13}C HSQC 2D correlation spectra. ^{1}H NMR and ^{13}C NMR spectra are referenced to the residual ^{1}H solvent peaks as internal standards or the characteristic ^{13}C resonances of the solvent. ^{19}F NMR spectra were referenced to external α,α,α-trifluorotoluene (-63.72 ppm) relative to $CFCl_3$ at 0 ppm. Single crystal X-ray studies for reported structures **3.1-3.15** were collected at ChemMatCARS located at the Advanced Photon Source (APS), Argonne National Laboratory (ANL), using synchrotron radiation (λ = 0.41328 Å) in conjunction with a Bruker D8 three-circle platform goniometer equipped with Dectris PILATUS 100 detector under a nitrogen cryo-steam at 100(2) K. Crystals were mounted on a glass fiber or on a Mitigen Kapton loop using NVH crystallographic immersion oil. Data was collected using φ and ω scan collection strategies. Data collection and cell parameter determination were conducted using the SMART program. Integration of the data and final cell parameter refinements were performed using SAINT software with data absorption correction implemented through SADABS. Structure solutions and structure refinements were completed using direct methods determinations in SHELXTL or Olex2 crystallographic packages. All hydrogen atom positions were idealized and treated as riding on the parent atom. A summary of relevant crystallographic data is presented in Table 3.1.

Synthesis of [(xylyl^{ket}guan)(η^6-Im^{Dipp}N)Ti] (3.1).

A 500 mL round bottom flask containing a red solution of **3.2** (5.00 g, 5.48 mmol) in THF (250 mL) was cooled to −78 ºC for 1 h with vigorous stirring. In a 20 mL scintillation vial, a bronze slurry of KC_8 (1.85 g, 13.70 mmol) in THF (20 mL) was cooled to −78 ºC for 30 min. To the stirring solution of **3.2**, the KC_8 suspension was added dropwise over a period of 10 min. An immediate color change to dark brown was observed. While maintaining the temperature at −78 ºC, the reaction mixture was stirred for 12 h. Thereafter, the solvent was slowly removed under reduced pressure to afford a dark brown solid. This material was subsequently dissolved in room-temperature hexanes (150 mL) and filtered through a plug of Celite supported on a medium porosity glass frit. The dark brown filter cake was thoroughly washed with hexane (3 × 30 mL) to give a dark colored filtrate. The filter cake was discarded and the volatiles of the filtrate were removed under reduced pressure to give a dark brown solid that was dissolved in 15 mL pentane and stored at −25 ºC for 5 d. A dark brown precipitate formed, and pentane was decanted. Upon drying the dark brown precipitate under dynamic vacuum, a dark-brown solid was obtained. (2 g, 2.38 mmol 43%). This material can be crystallized from a saturated Et_2O solutions stored at −25 ºC for 5 d. ^{1}H NMR (25 ºC, 400 MHz, C_6D_6): δ 0.29 (d, 6H, J_{HH} = 7 Hz, *Me*$_2$C*H*), 1.08 (s, 9H, C*Me*$_3$), 1.10 (m, 12H, two overlapping *Me*$_2$CH, J_{HH} = 3 Hz,), 1.19 (s, 9H, C*Me*$_3$), 1.48 (d, 6H, J_{HH} = 7 Hz, *Me*$_2$CH), 1.53 (sept, 2H, J_{HH} = 7 Hz Me$_2$C*H*) 2.17 (s, 6H, *Me*-xylyl), 2.53 (t, 1H, J_{HH} = 7 Hz, *para*-C*H* η^6-aryl), 2.68 (s, 6H, *Me*-xylyl), 3.15 (sept, 2H, J_{HH} = 7 Hz Me$_2$C*H*), 4.12 (d, 2H, J_{HH} = 6 Hz, *meta*-C*H* η^6-aryl), 5.35 (d, 1H, J_{HH} = 3 Hz, Imid*H*), 6.00 (d, 1H, J_{HH} = 3 Hz, Imid*H*), 7.14-7.18 (9H, aryl), 6.64 (d, 2H, J_{HH} = 8 Hz, *H*-xylyl), 6.78 (s, 2H, *aromatic*), 7.01 (d, 2H, J_{HH} = 8 Hz *H*-xylyl), 7.11 (m, 4H, J_{HH} = 6 Hz, *aromatic*).

Synthesis of [(Imid^{dipp}N)(xylyl^{Ket}Guan)Ti(κ^2-(*S*CH)(CH)$_3$) (3.3).

A 100 mL round bottom Cajon flask was loaded with **3.1** (2.00 g, 2.23 mmol) and THP (0.220 g, 0.210 mL, 2.26 mmol) in benzene (60 mL) which formed a dark-brown solution. The reaction vessel was sealed and heated to an external temperature of 110 ºC. After 15 h, the solution turned to dark-red color and all-volatiles were removed under reduced pressure until a dark-red semisolid formed. This material was triturated in 20 mL of hexanes and subsequently evaporated under reduced pressure until a glossy red solid was obtained. (1.99 g, 2.38 mmol 96%). This material can be crystallized from a saturated toluene solution stored at −25 ºC for 7 d. . ^{1}H NMR (25 ºC, 400 MHz, C_6D_6): 2.85 (s, 9H, C*Me*$_3$), 1.17 (m, 12H, two overlapping *Me*$_2$CH, J_{HH} = 3 Hz), 1.35 (d, 12H, J_{HH} = 7 Hz, *Me*$_2$CH), 3.26 (m, 4H, two-overlapping Me$_2$C*H*, J_{HH} = 7 Hz), 5.90 (s, 2H, Imid*H*), 6.52 (m, 1H, J_{HH} = 6 Hz, *β*-THP), 6.75 (d, 2H, J_{HH} = 8 Hz, *H*-xylyl), 7.13 (m, 5H, J_{HH} = 10 Hz, *aromatic*), 7.17 (s, 1H, , *aromatic*), 7.21 (t, 1H, J_{HH} = 7 Hz, *γ*-THP), 7.43 (d, 1H, J_{HH} = 9 Hz, *α*-THP), 7.79 (d, 1H, J_{HH} = 13 Hz, *δ*-THP).

Synthesis of [(Imid^{dipp}N)(xylyl^{Ket}Guan)Ti(κ^2-*S*(CH)$_2$C(CH)$_4$*C*)] (3.4).

A 50 mL round bottom Cajon flask was loaded with **3.1** (0.50 g, 0.60 mmol) and BTP (0.079 g, 0.60 mmol) in benzene (20 mL) which formed a dark-brown solution. The reaction vessel was sealed and heated to an external temperature of 90 ºC. After 15 h, the solution turned to dark-red color and all-volatiles were removed under reduced pressure until a dark-red semisolid formed. This material was triturated in 20 mL of hexanes and subsequently evaporated under reduced pressure until a dark red solid was obtained. This material was suspended in 10 mL of hexanes and stored at −25 ºC for 2 d. A dark red precipitate formed, and hexanes was decanted. Upon drying of the precipitates under dynamic vacuum, a red solid was obtained (0.220 g, 2.22 mmol 37%). This material can be crystallized from a saturated toluene solutions stored at −25 ºC for 7 d. ^{1}H NMR (25 ºC, 400 MHz, C_6D_6): 0.77 (s, 18H, C*Me*$_3$), 1.13 (d, 12H, J_{HH} = 7 Hz, *Me*$_2$CH), 1.28 (d,

6H, J_{HH} = 7 Hz, *Me*$_2$CH), 1.33 (d, 6H, J_{HH} = 7 Hz, *Me*$_2$CH), 2.17 (s, 6H, *Me*-xylyl), 2.23 (s, 6H, *Me*-xylyl), 3.26 (m, 4H, two-overlapping Me$_2$C*H*, J_{HH} = 7 Hz), 5.86 (s, 2H, Imid*H*), 6.76 (d, 2H, J_{HH} = 8 Hz, *H*-xylyl), 6.89 (s, 2H), 6.99 (m, 4H), 7.07 (m, 4H, J_{HH} = 8 Hz), 7.23 (m, 2H, J_{HH} = 8 Hz), 7.34 (d, 1H, J_{HH} = 8 Hz), 7.37 (m, 1H, J_{HH} = 4 Hz), 7.59 (m, 1H).

Synthesis of [(Imid^{dipp}N)(xylyl^{Ket}Guan)Ti(κ^2-*S*C(CH)$_4$C(CH)$_4$*C*)] (3.5)

A 50 mL round bottom Cajon flask was loaded with **3.1** (0.50 g, 0.60 mmol) and DBT (0.110 g, 0.60 mmol) in benzene (20 mL) which formed a dark-brown solution. The reaction vessel was sealed and heated to an external temperature of 90 ºC. After 15 h, the solution turned to dark-red color and all-volatiles were removed under reduced pressure until a dark-red semisolid formed. This material was triturated in 20 mL of hexanes and subsequently evaporated under reduced pressure until a dark red solid was obtained. This solid was suspended in 10 mL of hexanes and stored at at −25 ºC for 2 d. A dark red precipitate formed, and hexanes was decanted. Upon drying of the precipitates under dynamic vacuum, a red solid was obtained. (.370 g, 0.36 mmol 60%). (0.220 g, 2.22 mmol 37%). This material can be crystallized from a saturated toluene solutions stored at −25 ºC for 7 d. ^{1}H NMR (25 ºC, 400 MHz, C_6D_6): δ 0.72 (s, 18H, C*Me*$_3$), 1.15 (d, 12H, J_{HH} = 7 Hz, *Me*$_2$CH,), 1.33 (d, 12H, J_{HH} = 7 Hz, *Me*$_2$CH,), 1.96 (s, 6H, *Me*-xylyl), 2.17 (s, 6H, *Me*-xylyl), 3.26 (m, 4H, two-overlapping Me$_2$C*H*, J_{HH} = 7 Hz), 3.22 5.88 (s, 2H, Imid*H*), 6.60 (t, 1H, J_{HH} = 7 Hz), 7.07 (t, 1H, J_{HH} = 8 Hz), 7.26 (t, 2H, J_{HH} = 8 Hz), 7.51 (t, 2H, J_{HH} = 8 Hz), 7.51 (t, 2H, J_{HH} = 8 Hz), 7.85 (M, 2H, J_{HH} = 8 Hz).

[(Imid^{dipp}N)(xylyl^{Ket}Guan)Ti(κ^2-*S*C(CH)$_4$C*C*CH$_2$)] (3.7)

An NMR tube with a J-Young type valve was load with **3.5** (.04 g, 0.04 mmol) and C_6D_{12} (0.7 mL) which formed a dark-red solution. The reaction vessel was photolyzed (325 nm) for 7 d. A gradual change to orange color and formation of shinny orange crystal squares was observed (0.010 g, 0.01 mmol, 25%). ^{1}H NMR (25 ºC, 400 MHz, C_6D_6): δ 0.78 (s, 18H, C*Me*$_3$), 1.14. (m,

12H, two-overlapping *Me*$_2$CH, J_{HH} = 7 Hz), 1.14 (m, 12H, two-overlapping *Me*$_2$CH, J_{HH} = 7 Hz), 1.40 (m, 12H, two-overlapping *Me*$_2$CH, J_{HH} = 7 Hz), 2.23 (s, 6H, *Me*-xylyl), 2.27 (s, 6H, *Me*-xylyl), 3.30 (m, 4H, two-overlapping Me$_2$C*H*, J_{HH} = 7 Hz), 3.91 (d, 1H, *H*$_2$C-DBT, J_{HH} = 2 Hz), 5.44 (d, 1H, *H*$_2$C-DBT, J_{HH} = 2 Hz), 5.84 (s, 2H, Imid*H*), 6.76 (d, 2H, J_{HH} = 8 Hz), 6.86 (s, 2H), 7.00 (d, 3H, J_{HH} = 7 Hz), 7.06 (m, 5H, J_{HH} = 7 Hz), 7.40 (m, 4H, J_{HH} = 7 Hz), 7.22 (t, 3H, J_{HH} = 8Hz), 7.40 (dd, 3H, J_{HH} = 2Hz, J_{HH} = 8Hz).

[(Imid^{dipp}N)(xylyl^{Ket}Guan)Ti[(η^3-*S*(*C*H)$_2$CHCH$_2$B(C$_6$F$_5$)$_2$] (3.9)

A 20 mL scintillation vial was loaded with **3.1** (0.50 g, 0.54 mmol) and benzene (15 mL), forming a dark brown solution. Solution was frozen at 5 ºC. To this thawing solution, (C$_6$F$_5$)$_2$BH (0.187g, 0.540 mmol) was added as solid. A gradual chance to a darker red color was observed upon thawing. After 5 min, mixture was filtered through a Celite column (2 cm × 0.5 cm) supported on glasswool to give a very dark red filtrate and a small black plug. All volatiles were removed via reduced pressure until a very dark red solid was obtained. This material was suspended in 10 mL of hexanes and stored at −25 ºC for 2 d. A dark red precipitate formed, and hexanes was decanted. Upon drying of the precipitates under dynamic vacuum, a red solid was obtained (0.470 g, 0.37 mmol 69%). The material was crystallized using a solution of Et$_2$O (2 mL) followed by storage at –25 ºC. ^{1}H NMR (25 ºC, 400 MHz, C$_6$D$_6$): δ 0.64 (s, 9H, C*Me*$_3$),), 0.64 (s, 9H, C*Me*$_3$), 0.84 (s, 9H, C*Me*$_3$), 0.95 (d, 12H, J_{HH} = 7 Hz, *Me*$_2$CH), 1.07 (d, 6H, J_{HH} = 7 Hz, *Me*$_2$CH), 1.12 (d, 6H, J_{HH} = 7 Hz, *Me*$_2$CH), 2.04 (s, 3H, *Me*-xylyl), 2.09 (s, 3H, *Me*-xylyl), 2.16 (s, 3H, *Me*-xylyl), 2.23 (s, 3H, *Me*-xylyl), 2.84 (m, 4H, two-overlapping Me$_2$C*H*, J_{HH} = 7 Hz), 3.29 (dd, 1H, J_{HH} = 9 Hz, J_{HH} = 20 Hz, *H*-THP•BR$_2$), 4.14 (s, 1H, *H*-THP•BR$_2$), 5.19 (t, 1H, J_{HH} = 8 Hz, *H*-THP•BR$_2$), 5.68 (s, 2H, Imid*H*), 5.91 (t, 1H, J_{HH} = 9 Hz, *H*-THP•BR$_2$), 6.77 (d, 2H, J_{HH} = 8 Hz, *H*-xylyl), 6.94 (m, 8H, *aromatic*), 7.13 (d, 2H, J_{HH} = 8 Hz, *H*-xylyl), 7.29 (s, 1H, *aromatic*). ^{19}F{^{1}H] (25 ºC, 376 MHz, C$_6$D$_6$): −165.38 (dt, 2F, J_{FF} = 22 Hz, J_{FF} = 10 Hz, meta-C$_6$*F*$_6$), −164.47 (dt, 2F, J_{FF} = 22 Hz, J_{FF} = 10 Hz, meta-C$_6$*F*$_6$),−160.85 (t, 1F, J_{FF} = 22 Hz, para-C$_6$*F*$_6$),−160.09 (t,

1F, J_{FF} = 22 Hz, para-C_6F_6), −131.69 (d, 2F, J_{FF} = 29 Hz, ortho-C_6F_6),−129.27 (d, 2F, J_{FF} = 29 Hz, ortho-C_6F_6).

Synthesis of [(Imid^{dipp}N)(xylyl^{Ket}Guan)Ti(η^5-(*C*H)$_5$CH-BH(C$_6$F$_5$)$_2$)] (3.10)

A 20 mL scintillation vial was loaded with **3.11** (0.100 g, 0.107 mmol) and benzene (5mL), forming a dark brown solution. Solution was frozen at 5 ºC. To this thawing solution, $(C_6F_5)_2BH$ (0.037g, 0.107 mmol) was added as solid. A gradual chance to a green color was observed upon thawing. After 5 min, mixture was filtered through a Celite column (2 cm × 0.5 cm) supported on glasswool to give a clear red filtrate and a small black plug. All volatiles were removed via reduced pressure until a green solid was obtained. (0.470 g, 0.37 mmol 69%). The material was crystallized using a saturated solution of toluene (2 mL) followed by storage at –25 ºC. (0.081 g, 0.07 mmol, 64%). ^{1}H NMR (25 ºC, 400 MHz, C_6D_6): δ 0.57 (d, 6H, J_{HH} = 7 Hz, *Me*$_2$CH), 0.65 (s, 9H, C*Me*$_3$), 0.94 (d, 6H, J_{HH} = 7 Hz, *Me*$_2$CH), 1.02 (s, 9H, C*Me*$_3$), 1.04 (d, 6H, J_{HH} = 7 Hz, *Me*$_2$CH), 1.21 (d, 6H, J_{HH} = 7 Hz, *Me*$_2$CH), 1.90 (sept, 2H, J_{HH} = 6 Hz, Me$_2$C*H*), 2.39 (s, 6H, *Me*-xylyl), 2.56 (s, 6H, *Me*-xylyl), 2.62 (sept, 2H, J_{HH} = 7 Hz, Me$_2$C*H*), 3.25 (s, 1H, B*H*(C$_6$F$_5$)$_2$), 5.41 (s, 1H, Imid*H*), 5.45 (s, *aromatic*), 6.23 (s, 1H, Imid*H*), 6.77 (d, 2H, J_{HH} = 8 Hz, *H*-xylyl), 6.91 (d, 2H, J_{HH} = 8 Hz, *aromatic*), 7.01 (d, 2H, J_{HH} = 8 Hz, *aromatic*).

Synthesis of [(Imid^{dipp}N)(xylyl^{Ket}Guan)Ti(η^6-*C*$_6$H$_6$)] (3.11)

A 100 mL round bottom flask containing a red solution of **3.2** (1.00 g, 0.110 mmol) in THF (40 mL) and C_6H_6 (5 mL) was cooled to −78 ºC for 1 h with vigorous stirring. In a 20 mL scintillation vial, a bronze slurry of KC_8 (0.37 g, 0.274 mmol) in THF (5 mL) was cooled to −78 ºC for 30 min. To the stirring solution of 2.2, the KC_8 suspension was added dropwise over a period of 10 min. An immediate color change to dark brown was observed. While maintaining the temperature at −78 ºC, the reaction mixture was stirred for 12 h. Thereafter, the solvent was slowly

removed under reduced pressure to afford a dark brown solid. This material was subsequently dissolved in room-temperature hexanes (50 mL) and filtered through a plug of Celite supported on a medium porosity glass frit. The dark brown filter cake was thoroughly washed with hexane (3 × 30 mL) to give a dark colored filtrate. The filter cake was discarded and the volatiles of the filtrate were removed under reduced pressure to give a dark brown solid that was dissolved in pentane (10 mL) and stored at −25 ºC for 3 d. A dark brown precipitate formed, and pentane was decanted. Upon drying the dark brown precipitate under dynamic vacuum, a dark-brown solid was obtained. (0.49 g, 2.38 mmol 43%). This material can be crystallized from a saturated Et_2O solutions stored at −25 ºC for 5 d. ^{1}H NMR (25 ºC, 400 MHz, C_6D_6): δ 0.61 (s, 9H, C*Me*$_3$), 0.89 (s, 9H, C*Me*$_3$), 0.84 (s, 9H, C*Me*$_3$), 0.98 (d, 12H, J_{HH} = 7 Hz, *Me*$_2$CH), 1.09 (d, 12H, J_{HH} = 7 Hz), 2.14 (s, 6H, *Me*-xylyl), 2.78 (s, 6H, *Me*-xylyl), 3.20 (sept, 4H, J_{HH} = 7 Hz, Me$_2$C*H*), 3.98 (s, 6H, η^6-C$_6$*H*$_6$), 5.82 (s, 2H, Imid*H*), 6.16 (s, 2H, *aryl*), 6.73 (d, 2H, J_{HH} = 8 Hz, *H*-xylyl), 7.00 (d, 4H, J_{HH} = 8 Hz, *aryl*), 7.11 (d, 4H, J_{HH} = 8 Hz, *aryl*).

Synthesis of K$_2$(Imid^{dipp}N)(4-^{t}BuPh ^{Ket}Guan)Ti]$_2$(μ-N)$_2$ (3.15).

A 20 mL scintillation vial was loaded with **3.14** (0.200 g, 0.214 mmol), toluene (4 mL), and THF (0.5 ml) forming a dark-red solution. The mixture was cooled to −78 ºC for 30 m with vigorous stirring. In another 20 mL scintillation vial, a bronze slurry of KC_8 (0.089 g, 0.665 mmol) in toluene (3 mL) was cooled to −78 ºC for 30 min. To the stirring solution of **2.2**, the KC_8 suspension was added dropwise over a period of 10 min. An immediate color change to dark brown was observed. While maintaining the temperature at −78 ºC, the reaction mixture was stirred for 12 h. Thereafter, the solvent was slowly removed under reduced pressure to afford a dark brown solid. This material was subsequently dissolved in room-temperature pentanes (10 mL) and filtered through a Celite column (2 cm × 0.5 cm) supported on glasswool to give a clear brown filtrate

and a small black plug (C_8). The filtrate was concentrated to 2 ml and stored at –25 ºC producing yellow crystals after 4 d. (0.125 g, 0.068 mmol, 63%). ^{1}H NMR (25 ºC, 400 MHz, C_6D_6): δ 0.94 (s, 9H, C*Me*$_3$), 1.14 (m, 12H, two-overlapping *Me*$_2$CH, J_{HH} = 6 Hz), 1.30 (s, 9H, C*Me*$_3$), 0.94 (s, 9H, C*Me*$_3$), 1.30 (s, 18H, 4-*Me*$_3$CPh), 3.42 (sept, 4H, J_{HH} = 6 Hz, Me$_2$C*H*), 5.96 (s, 1H, Imid*H*), 6.89 (t, 2H, J_{HH} = 8 Hz, *dipp*-aromatic), 6.98 (d, 4H, J_{HH} = 7 Hz, *dipp*-aromatic), 7.30 (d, 2H, J_{HH} = 8 Hz, 4-^{t}BuPh*H*), 7.44 (d, 2H, J_{HH} = 8 Hz, 4-^{t}BuPh*H*)

Table 3.1**:** X-ray crystallographic data for **3.1** – **3.15**.

	(**3.1**)	(**3.3**)	(**3.7**)
empirical formula	$C_{53}H_{72}N_6Ti$	$C_{57}H_{76}N_6STi$	$C_{62}H_{81}STi$
crystal habit, color	Ambar Plates	Orange Plates	Orange Plates
crystal size (mm)	0.1 × 0.1 × 0.05	0.2 × 0.2 × 0.1	0.4 × 0.3 × 0.1
crystal system	Monoclinic	Monoclinic	Triclinic
space group	P 2_1/n	P 2_1	P-1
Volume (Å^3)	5318.4(18)	5423.0(11)	5438.8(11)
a	21.111(4)	11.0761(13)	10.7244(11)
b	10.583(2)	18.325(2)	18.722(2)
c	24.640(5)	26.718(3)	27.733(3)
α	90	90	89.834(3)
β	104.962(4)	90	89.968(2)
γ	90	90	77.621(2)
Z	4	4	4
F_w (g/mol)	1038.73	1046.54	2098.3
density (calcd) (Mg/m^3)	1.237	1.148	1.910
abs coeff (mm^{-1})	0.236	0.251	0.240
F_{000}	1972.0	1866.0	2098.3
total no. of reflns	63369	103729	45217
unique reflns	10807	10476	14028
final *R* indices [$I > 2\sigma(I)$]	R1 = 0.1483, wR2 = 0.3752	R1 = 0.0715, wR2 = 0.1654	R1 = 0.0589, wR2 = 0.1490

largest diff peak and hole (e/ Å^3)	1.89 and -0.75	0.47 and -0.72	0.57 and -0.88
GOF	2.015	1.039	1.055

	(**3.9**•Et_2O)	(**3.10**•Et_2O)	(**3.14**)
empirical formula	$C_{73}H_{84}BF_{10}N_6OSTi$	$C_{69}H_{81}BF_{10}N_6OTi$	$C_{64}H_{86}N_6Ti$
crystal habit, color	Purple Blocks	Green Blocks	Ambar Plates
crystal size (mm)	0.4 × 0.3 × 0.1	0.5 × 0.2 × 0.01	0.2 × 0.2 × 0.05
crystal system	Orthorhombic	Monoclinic	Triclinic
space group	$C2/_C$	C2	P-1
Volume (Å^3)	14440.8(14)	12749(6)	3048.7(2)
a	23.0502(10)	16.412(5)	10.6292(5)
b	24.8235(19)	20.605(5)	11.6371(5)
c	26.718(3)	27.1216(11)	24.8921(11)
α	90	90	91.7800(10)
β	132.4676(7)	115.6330(10)	96.9260(10)
γ	90	90	93.4590(10)
Z	8	12	2
F_w (g/mol)	4400	965	987
density (calcd) (Mg/m^3)	1.057	1.170	1.573
abs coeff (mm^{-1})	0.122	0.202	0.202
F_{000}	4400.0	5776.0	1516.0
total no. of reflns	54443	74574	74574
unique reflns	8108	14729	23854
final *R* indices [$I > 2\sigma(I)$]	R1 = 0.0502, wR2 = 0.1732	R1 = 0.0652, wR2 = 0.1653	R1 = 0.1112, wR2 = 0.3174
largest diff peak and hole (e/ Å^3)	0.90 and -0.47	0.55 and -0.41	1.96 and -0.72
GOF	1.596	1.020	1.397

	(**3.15**)
empirical formula	$C_{111}H_{144}K_2N_{14}Ti_2$
crystal habit, color	Yellow Squares
crystal size (mm)	0.5 × 0.5 × 0.1
crystal system	Monoclinic
space group	C2/c
Volume ($Å^3$)	25872(3)
a	20.7048(13)
b	27.8769(18)
c	45.796(3)
α	90
β	101.8220(10)
γ	90
Z	24
F_w (g/mol)	1848
density (calcd) (Mg/m^3)	0.910
abs coeff (mm^{-1})	0.286
F_{000}	7019.0
total no. of reflns	77606
unique reflns	12768
final *R* indices [$I > 2\sigma(I)$]	R1 = 0.1080, wR2 = 0.3213
largest diff peak and hole (e/ $Å^3$)	2.07 and -0.81
GOF	2.642

References

(1) Hilt, G.; Punner, F.; Mobus, J.; Naseri, V.; Bohn, M. A., A Lewis Acidity Scale in Relation to Rate Constants of Lewis Acid Catalyzed Organic Reactions. *Eur. J. Org. Chem.* **2011,** (30), 5962-5966.

(2) Xiu, W.; Zhenhua, W.; Zhang, G.; Zhang, W.; Wu, Y.; Gao, Z., Tunable Titanocene Lewis Acid Catalysts for Selective Friedel–Crafts Reaction of Indoles and N-Sulfonylaldimines. *Eur. J. Org. Chem.* **2016,** *2016* (3), 502-507.

(3) Klosin, J.; Fontaine, P. P.; Figueroa, R., Development of Group IV Molecular Catalysts for High Temperature Ethylene-α-Olefin Copolymerization Reactions. *Acc. Chem. Res.* **2015,** *48* (7), 2004-2016.

(4) Beaumier, E. P.; Pearce, A. J.; See, X. Y.; Tonks, I. A., Modern applications of low-valent early transition metals in synthesis and catalysis. *Nature Reviews Chemistry* **2019,** *3* (1), 15-34.

(5) Okamoto, S., Synthetic Reactions Using Low-valent Titanium Reagents Derived from Ti(OR)4 or CpTiX3 (X = O-i-Pr or Cl) in the Presence of Me3SiCl and Mg. *The Chemical Record* **2016,** *16* (2), 857-872.

(6) Chirik, P. J.; Bouwkamp, M. W., 4.03 - Complexes of Titanium in Oxidation States 0 to II - Mingos, D. Michael P. In *Comprehensive Organometallic Chemistry III*, Crabtree, R. H., Ed. Elsevier: Oxford, **2007**; pp 243-279.

(7) Buchwald, S. L.; Nielsen, R. B., Group-4 Metal-Complexes of Benzynes, Cycloalkynes, Acyclic Alkynes, and Alkenes. *Chem. Rev.* **1988,** *88* (7), 1047-1058.

(8) Lenoir, D., The Application of Low-Valent Titanium Reagents in Organic-Synthesis. *Synthesis-Stuttgart* **1989,** (12), 883-897.

(9) Furstner, A., Chemistry of and with Highly Reactive Metals. *Angew. Chem. Int. Ed.* **1993,** *32* (2), 164-189.

(10) Aleandri, L. E.; Bogdanovic, B.; Gaidies, A.; Jones, D. J.; Liao, S. J.; Michalowicz, A.; Roziere, J.; Schott, A., [$Ti(MgCl)_2(THF)_x$] - a Reagent for the Mcmurry Reaction and a Novel Inorganic Grignard Complex. *J. Organomet. Chem.* **1993,** *459* (1-2), 87-93.

(11) Mori, M., Activation of nitrogen for organic synthesis. *Journal of Organometallic Chemistry* **2004,** *689* (24), 4210-4227.

(12) Ozerov, O. V.; Patrick, B. O.; Ladipo, F. T., Highly Regioselective [2 + 2 + 2] Cycloaddition of Terminal Alkynes Catalyzed by η^6-Arene Complexes of Titanium Supported by Dimethylsilyl-Bridged p-tert-Butyl Calix[4]arene Ligand. *J. Am. Chem. Soc.* **2000,** *122* (27), 6423-6431.

(13) Rosenthal, U.; Pellny, P.-M.; Kirchbauer, F. G.; Burlakov, V. V., What Do Titano- and Zirconocenes Do with Diynes and Polyynes? *Acc. Chem. Res.* **2000,** *33* (2), 119-129.

(14) Suzuki, N.; Tsuchiya, T.; Aihara, N.; Iwasaki, M.; Saburi, M.; Chihara, T.; Masuyama, Y., Synthesis and Structure of Seven-Membered Metallacycloalkynes. *Eur. J. Inorg. Chem.* **2013,** *2013* (3), 347-356.

(15) Cohen, S. A.; Auburn, P. R.; Bercaw, J. E., Structure and reactivity of bis(pentamethylcyclopentadienyl)(ethylene)titanium(II), a simple olefin adduct of titanium. *Journal of the American Chemical Society* **1983,** *105* (5), 1136-1143.

(16) Cohen, S. A.; Bercaw, J. E., Titanacycles derived from reductive coupling of nitriles, alkynes, acetaldehyde, and carbon dioxide with bis(pentamethylcyclopentadienyl)(ethylene)titanium(II). *Organometallics* **1985,** *4* (6), 1006-1014.

(17) Otten, E.; Batinas, A. A.; Meetsma, A.; Hessen, B., Versatile Coordination of Cyclopentadienyl-Arene Ligands and Its Role in Titanium-Catalyzed Ethylene Trimerization. *J. Am. Chem. Soc.* **2009,** *131* (14), 5298-5312.
(18) Sato, F.; Urabe, H.; Okamoto, S., Synthesis of Organotitanium Complexes from Alkenes and Alkynes and Their Synthetic Applications. *Chem. Rev.* **2000,** *100* (8), 2835-2886.
(19) You, Y. J.; Girolami, G. S., Mono(cyclopentadienyl)titanium(II) complexes with hydride, alkyl, and tetrahydroborate ligands: Synthesis, crystal structures, and ethylene dimerization and trimerization catalysis. *Organometallics* **2008,** *27* (13), 3172-3180.
(20) Fürstner, A.; Bogdanović, B., New Developments in the Chemistry of Low-Valent Titanium. *Angew. Chem. Int. Ed.* **1996,** *35* (21), 2442-2469.
(21) McMurry, J. E., Carbonyl-coupling reactions using low-valent titanium. *Chem. Rev.* **1989,** *89* (7), 1513-1524.
(22) Hashimoto, Y.; Mizuno, U.; Matsuoka, H.; Miyahara, T.; Takakura, M.; Yoshimoto, M.; Oshima, K.; Utimoto, K.; Matsubara, S., Structural Studies of the Low-Valent Titanium "Solution": What Goes on in the Pinacol Coupling Reaction? *J. Am. Chem. Soc.* **2001,** *123* (7), 1503-1504.
(23) Lapointe, R. E.; Wolczanski, P. T.; Mitchell, J. F., Carbon-Monoxide Cleavage by $(Silox)_3Ta$ (Silox = $^tBu_3SiO$). *J. Am. Chem. Soc.* **1986,** *108* (20), 6382-6384.
(24) Knobloch, D. J.; Lobkovsky, E.; Chirik, P. J., Dinitrogen cleavage and functionalization by carbon monoxide promoted by a hafnium complex. *Nature Chemistry* **2009,** *2*, 30.
(25) Crescenzi, R.; Solari, E.; Floriani, C.; Chiesi-Villa, A.; Rizzoli, C., Binding of a meso-Octaethyl Tris(pyrrole)−Mono(pyridine) Ligand to Titanium(III) and Titanium(IV): A Monomeric Titanium(IV) Oxo Bis(pyridine)−Bis(pyrrole) Complex Derived from the C−O Bond Cleavage of Carbon Monoxide. *Organometallics* **1996,** *15* (26), 5456-5458.
(26) Steffey, B. D.; Chamberlain, L. R.; Chesnut, R. W.; Chebi, D. E.; Fanwick, P. E.; Rothwell, I. P., Intramolecular Activation of Aliphatic and Aromatic Carbon-Hydrogen Bonds by Tantalum(III) Metal Centers - Synthesis and Structure of the Bis-Metalated Compounds $Ta(OC_6H_3Bu^tMe_2CH_2)_2Cl$ and $Ta(OC_6H_3PhC_6H_4)_2(OAr\text{-}2,6\text{-}Ph_2)$ ($OAr\text{-}2,6\text{-}Ph_2$ = 2,6-Diphenylphenoxide). *Organometallics* **1989,** *8* (6), 1419-1423.
(27) Yu, J. S.; Fanwick, P. E.; Rothwell, I. P., Intramolecular Alkane Dehydrogenation and Functionalization at Niobium Metal Centers. *J. Am. Chem. Soc.* **1990,** *112* (22), 8171-8172.
(28) Figueroa, J. S.; Piro, N. A.; Mindiola, D. J.; Fickes, M. G.; Cummins, C. C., Niobaziridine Hydrides. *Organometallics* **2010,** *29* (21), 5215-5229.
(29) Tayebani, M.; Feghali, K.; Gambarotta, S.; Yap, G., Molecular Rearrangements of a Low-Valent Niobium Amide: Ligand C−H Bond Oxidative Addition and Reductive Elimination. *Organometallics* **1998,** *17* (19), 4282-4290.
(30) Riley, P. N.; Clark, J. R.; Fanwick, P. E.; Rothwell, I. P., Synthesis and structure of niobium and tantalum derivatives of bis(dicyclohexylphosphino)methane (dcpm). *Inorganica Chimica Acta* **1999,** *288* (1), 35-39.
(31) Messerle, L., Metal-metal bonded dinuclear and organodimetallic complexes of the early transition metals (Groups 4 and 5): synthesis, structure, and reactivity. *Chemical Reviews* **1988,** *88* (7), 1229-1254.
(32) LaPointe, R. E.; Wolczanski, P. T.; Mitchell, J. F., Carbon monoxide cleavage by $(silox)_3Ta$ (silox = *t*-Bu_3SiO-). *Journal of the American Chemical Society* **1986,** *108* (20), 6382-6384.
(33) Bercaw, J. E.; Bell, L. G.; Brintzinger, H.; Marvich, R. H., Titanocene as an Intermediate in Reactions Involving Molecular-Hydrogen and Nitrogen. *J. Am. Chem. Soc.* **1972,** *94* (4), 1219-&.

(34) Brintzinger, H.; Bercaw, J. E., Nature of so-called titanocene, $(C_{10}H_{10}Ti)_2$. *J. Am. Chem. Soc.* **1970,** *92* (21), 6182-6185.
(35) Fryzuk, M. D., Activation and functionalization of molecular nitrogen by metal complexes. *Chem. Rec.* **2003,** *3* (1), 2-11.
(36) Shima, T.; Hu, S. W.; Luo, G.; Kang, X. H.; Luo, Y.; Hou, Z. M., Dinitrogen Cleavage and Hydrogenation by a Trinuclear Titanium Polyhydride Complex. *Science* **2013,** *340* (6140), 1549-1552.
(37) Tayebani, M.; Feghali, K.; Gambarotta, S.; Yap, G., Molecular rearrangements of a low-valent niobium amide: Ligand C-H bond oxidative addition and reductive elimination. *Organometallics* **1998,** *17* (19), 4282-4290.
(38) Araya, M. A.; Cotton, F. A.; Matonic, J. H.; Murillo, C. A., An Efficient Reduction Process Leading to Titanium(II) and Niobium(II): Preparation and Structural Characterization of trans-$MCl_2(py)_4$ Compounds, M = Ti, Nb, and Mn. *Inorganic Chemistry* **1995,** *34* (22), 5424-5428.
(39) Edema, J. J. H.; Duchateau, R.; Gambarotta, S.; Hynes, R.; Gabe, E., Novel titanium(II) amine complexes L_4TiCl_2[L = 1/2 N,N,N',N'-tetramethylethylenediamine (TMEDA), 1/2 N,N,N'-trimethylethylenediamine, pyridine, 1/2 2,2'-bipyridine]: synthesis and crystal structure of monomeric trans-$(TMEDA)_2TiCl_2$. *Inorganic Chemistry* **1991,** *30* (2), 154-156.
(40) Wijeratne, G. B.; Zolnhofer, E. M.; Fortier, S.; Grant, L. N.; Carroll, P. J.; Chen, C.-H.; Meyer, K.; Krzystek, J.; Ozarowski, A.; Jackson, T. A.; Mindiola, D. J.; Telser, J., Electronic Structure and Reactivity of a Well-Defined Mononuclear Complex of Ti(II). *Inorganic Chemistry* **2015,** *54* (21), 10380-10397.
(41) Snead, T. E., Dicarbonylbis(cyclopentadienyl)titanium. In *Encyclopedia of Reagents for Organic Synthesis*, John Wiley & Sons, Ltd: 2001.
(42) Kool, L. B.; Rausch, M. D.; Alt, H. G.; Herberhold, M.; Thewalt, U.; Wolf, B., $[Cp_2Ti(PMe_3)_2]$—A Versatile Source of Titanocene Derivatives. *Angew. Chem. Int. Ed.* **1985,** *24* (5), 394-401.
(43) Spencer, M. D.; Wilson, S. R.; Girolami, G. S., Butadiene Complexes of Titanium(II) and Titanium(0): Synthesis, Butadiene Dimerization Catalysis, and Crystal Structures of $TiMe_2(\eta^4$-1,4-$C_4H_4Ph_2)$(dmpe) and $Ti(\eta^4$-$C_4H_6)_2$(dmpe). *Organometallics* **1997,** *16* (13), 3055-3067.
(44) Boynton, J. N.; Guo, J.-D.; Grandjean, F.; Fettinger, J. C.; Nagase, S.; Long, G. J.; Power, P. P., Synthesis and Characterization of the Titanium Bisamide $Ti\{N(H)Ar^{iPr6}\}2$ (Ar^{iPr6} = C_6H_3-2,6-$(C_6H_2$-2,4,6-$^iPr_3)_2$ and Its $TiCl\{N(H)Ari^{Pr6}\}_2$ Precursor: Ti(II) → Ti(IV) Cyclization. *Inorganic Chemistry* **2013,** *52* (24), 14216-14223.
(45) Hagadorn, J. R.; Arnold, J., Tethered Bis-Amidinates as Supporting Ligands: A Concerted Elimination/σ–π Rearrangement Reaction Forming an Unusual Titanium Arene Complex. *Angew. Chem. Int. Ed.* **1998,** *37* (12), 1729-1731.
(46) Nakanishi, Y.; Ishida, Y.; Kawaguchi, H., Synthesis and reactions of a zirconium naphthalene complex bearing a tetraanionic C-capped triaryloxide ligand. *Dalton Transactions* **2016,** *45* (40), 15879-15885.
(47) Tsai, Y.-C.; Wang, P.-Y.; Lin, K.-M.; Chen, S.-A.; Chen, J.-M., Synthesis and reactions of β-diketiminato divanadium(i) inverted-sandwich complexes. *Chemical Communications* **2008,** (2), 205-207.
(48) Watanabe, T.; Ishida, Y.; Matsuo, T.; Kawaguchi, H., Syntheses and structures of zirconium(iv) complexes supported by 2,6-di-adamantylaryloxide ligands and formation of arene-bridged dizirconium complexes with an inverse sandwich structure. *Dalton Transactions* **2010,** *39* (2), 484-491.

(49) Huang, W.; Dulong, F.; Wu, T.; Khan, S. I.; Miller, J. T.; Cantat, T.; Diaconescu, P. L., A six-carbon 10π-electron aromatic system supported by group 3 metals. *Nature Communications* **2013,** *4*, 1448.
(50) Graham, T. W.; Kickham, J.; Courtenay, S.; Wei, P.; Stephan, D. W., Reduction of Titanium(IV)-Phosphinimide Complexes: Routes to Ti(III) Dimers, Ti(IV)-Metallacycles, and Ti(II) Species. *Organometallics* **2004,** *23* (13), 3309-3318.
(51) Aguilar-Calderón, J. R.; Metta-Magaña, A. J.; Noll, B.; Fortier, S., C(sp^3)−H Oxidative Addition and Transfer Hydrogenation Chemistry of a Titanium(II) Synthon: Mimicry of Late-Metal Type Reactivity. *Angew. Chem. Int. Ed.* **2016,** *55* (45), 14101-14105.
(52) Spannenberg, A.; Tillack, A.; Arndt, P.; Kirmse, R.; Kempe, R., Homoleptic trisaminopyridinato M-III complexes (M = Ti, V and Cr), synthesis, structure and EPR investigations. *Polyhedron* **1998,** *17* (5-6), 845-850.
(53) Bailey, B. C.; Basuli, F.; Huffman, J. C.; Mindiola, D. J., Terminal titanium(IV) (trimethylsilyl)imides prepared by oxidatively induced trimethylsilyl abstraction. *Organometallics* **2006,** *25* (11), 2725-2728.
(54) Haas, I.; Hubner, C.; Kretschmer, W. P.; Kempe, R., A Highly Efficient Titanium Catalyst for the Synthesis of Ultrahigh-Molecular-Weight Polyethylene (UHMWPE). *Chem. Eur. J.* **2013,** *19* (28), 9132-9136.
(55) Shannon, R. D., Revised Effective Ionic-Radii and Systematic Studies of Interatomic Distances in Halides and Chalcogenides. *ActaActa Cryst. A Cryst. A* **1976,** *32* (Sep1), 751-767.
(56) Mullins, S. M.; Duncan, A. P.; Bergman, R. G.; Arnold, J., Reactivity of a Titanium Dinitrogen Complex Supported by Guanidinate Ligands: Investigation of Solution Behavior and a Novel Rearrangement of Guanidinate Ligands. *Inorganic Chemistry* **2001,** *40* (27), 6952-6963.
(57) Hagadorn, J. R.; Arnold, J., Low-valent chemistry of titanium benzamidinates leading to new Ti μ-N_2, μ-O, alkyl derivatives, and the cyclometalation of TMEDA. *J. Am. Chem. Soc.* **1996,** *118* (4), 893-894.
(58) Loh, Y. K.; Ángeles Fuentes, M.; Vasko, P.; Aldridge, S., Successive Protonation of an N-Heterocyclic Imine Derived Carbonyl: Superelectrophilic Dication Versus Masked Acylium Ion. *Angew. Chem. Int. Ed.* **2018,** *57* (50), 16559-16563.
(59) Xian Wu, M. T., Transition metal complexes supported by highly basic imidazolin-2-iminato and imidazolin-2-imine N-donor ligands. *Coordination Chemistry Reviews* **2014,** *260*, 116.
(60) Connelly, N. G.; Geiger, W. E., Chemical Redox Agents for Organometallic Chemistry. *Chemical Reviews* **1996,** *96* (2), 877-910.
(61) Basuli, F.; Kilgore, U. J.; Brown, D.; Huffman, J. C.; Mindiola, D. J., Terminal Zirconium Imides Prepared by Reductive C−N Bond Cleavage. *Organometallics* **2004,** *23* (26), 6166-6175.
(62) Basuli, F.; Huffman, J. C.; Mindiola, D. J., Reductive C–N bond cleavage of the NCCCN β-diketiminate backbone: A direct approach to azabutadienyl and alkylidene-anilide scaffolds. *Inorganica Chimica Acta* **2007,** *360* (1), 246-254.
(63) Cotton, F. A.; Daniels, L. M.; Murillo, C. A.; Wang, X. P., Cleavage of formamidinate ligands on a Ta=Ta double bond: Formation of HxC-NAryl (x = 0 and 1) and arylimido-bridged complexes. *Inorg. Chem.* **1997,** *36* (5), 896-901.
(64) Hagadorn, J. R.; Arnold, J., Titanium(II), -(III), and -(IV) Complexes Supported by Benzamidinate Ligands. *Organometallics* **1998,** *17* (7), 1355-1368.
(65) Bailey, B. C.; Basuli, F.; Huffman, J. C.; Mindiola, D. J., Oxidatively induced alpha-hydrogen abstraction. A mild protocol to generate terminal titanium alkylidenes containing a beta-hydrogen. *Organometallics* **2006,** *25* (16), 3963-3968.

(66) Ferreira, M. J.; Matos, I.; Ascenso, J. R.; Duarte, M. T.; Marques, M. M.; Wilson, C.; Martins, A. M., Alkylation, cation formation, and insertion reactions in titanium tris(ketimide) complexes. *Organometallics* **2007,** *26* (1), 119-127.
(67) Jensen, B. S.; Parker, V. D., Reversible anion radical–dianion redox equilibria involving ions of simple aromatic compounds. *Journal of the Chemical Society, Chemical Communications* **1974,** (10), 367-368.
(68) Bouwkamp, M. W.; Budzelaar, P. H. M.; Meetsma, A.; Hessen, B., Reactivity of cationic decamethylmetallocene complexes towards ketones. *Journal of Organometallic Chemistry* **2011,** *696* (9), 1920-1924.
(69) Cole, S. C.; Coles, M. P.; Hitchcock, P. B., Transition-metal imido-boroxide complexes: a structural and spectroscopic investigation of the influence of boron. *Journal of the Chemical Society, Dalton Transactions* **2002,** (22), 4168-4174.
(70) Fleischer, E. B.; Sung, N.; Hawkinson, S., Crystal structure of benzophenone. *The Journal of Physical Chemistry* **1968,** *72* (12), 4311-4312.
(71) Lam, C. P.; Anthon, C.; Heinemann, F. W.; O'Connor, J. M.; Meyer, K., Structural and spectroscopic characterization of a charge-separated uranium benzophenone ketyl radical complex. *Journal of the American Chemical Society* **2008,** *130* (20), 6567-6576.
(72) Matson, E. M.; Kiernicki, J. J.; Anderson, N. H.; Fanwick, P. E.; Bart, S. C., Isolation of a uranium(III) benzophenone ketyl radical that displays redox-active ligand behaviour. *Dalton Transactions* **2014,** *43* (48), 17885-17888.
(73) Hou, Z.; Jia, X.; Fujita, A.; Tezuka, H.; Yamazaki, H.; Wakatsuki, Y., Alkali and Alkaline-Earth Metal Ketyl Complexes: Isolation, Structural Diversity, and Hydrogenation/Protonation Reactions. *Chem. Eur. J.* **2000,** *6* (16), 2994-3005.
(74) Covert, K. J.; Wolczanski, P. T.; Hill, S. A.; Krusic, P. J., Ketyl Complexes of $(silox)_3Ti$ (silox = $^tBu_3SiO$-). *Inorganic Chemistry* **1992,** *31* (1), 66-78.
(75) Lewis, R. A.; MacLeod, K. C.; Mercado, B. Q.; Holland, P. L., Geometric and redox flexibility of pyridine as a redox-active ligand that can reversibly accept one or two electrons. *Chemical Communications* **2014,** *50* (76), 11114-11117.
(76) Durfee, L. D.; Fanwick, P. E.; Rothwell, I. P.; Folting, K.; Huffman, J. C., Reductive elimination pathways to low valent titanium aryl oxide complexes. *Journal of the American Chemical Society* **1987,** *109* (15), 4720-4722.
(77) Kisko, J. L.; Hascall, T.; Parkin, G., Multiple bonding of titanium and vanadium to the heavier chalcogens: Syntheses and structures of the terminal selenido and tellurido complexes [η^4-Me_8taa]M=E (M=Ti, V; E=Se, Te). *Journal of the American Chemical Society* **1997,** *119* (32), 7609-7610.
(78) Allen, J. M.; Ellis, J. E., Synthesis and characterization of titanium tetraisocyanide complexes, $[CpTi(CNXyl)_4E]$, E = I, $SnPh_3$, and $SnMe_3$. *Journal of Organometallic Chemistry* **2008,** *693* (8-9), 1536-1542.
(79) Kool, L. B.; Rausch, M. D.; Herberhold, M.; Alt, H. G.; Thewalt, U.; Honold, B., Diamagnetic Isocyanide Complexes of Titanium, Zirconium, and Hafnium. *Organometallics* **1986,** *5* (12), 2465-2468.
(80) Reiss, F.; Altenburger, K.; Hollmann, D.; Spannenberg, A.; Jiao, H. J.; Arndt, P.; Rosenthal, U.; Beweries, T., Redox-Disproportionation of a Decamethyltitanocene(III) Isonitrile Alkynyl Complex. *Chem. Eur. J* **2017,** *23* (33), 7891-7895.
(81) Cuenca, T.; Gomez, R.; Gomezsal, P.; Royo, P., Synthesis and Characterization of Ansa-Dimethylsilylbiscyclopentadienyl Titanium(II) Complexes - Crystal-Structure of

[Ti($Me_2Si(C_5H_4)_2$)(CN(2,6-$Me_2C_6H_3$))$_2$]. *Journal of Organometallic Chemistry* **1993,** *454* (1-2), 105-111.
(82) Greidanus-Strom, G.; Carter, C. A. G.; Stryker, J. M., Migratory insertion of isonitriles into titanacyclobutane complexes. A novel stereocontrolled synthesis of substituted cyclobutanimines. *Organometallics* **2002,** *21* (6), 1011-1013.
(83) Entley, W. R.; Treadway, C. R.; Wilson, S. R.; Girolami, G. S., The hexacyanotitanate ion: Synthesis and crystal structure of $[NEt_4]_3$[Ti-III$(CN)_6$]center·4MeCN. *Journal of the American Chemical Society* **1997,** *119* (27), 6251-6258.
(84) Brown, A.; Saber, M.; Van den Heuvel, W.; Schulte, K.; Soncini, A.; Dunbar, K. R., Titanium(III) Member of the Family of Trigonal Building Blocks with Scorpionate and Cyanide Ligands. *Inorganic Chemistry* **2017,** *56* (3), 1031-1035.
(85) Thewalt, U.; Nuding, W., Titanium(IV) compounds with cyano ligands: Crystal structures of $Cp_2Ti(CN)(OCH_3)$ and $[Cp_2(Ti(CN)]_2O$. *Journal of Organometallic Chemistry* **1996,** *512* (1-2), 127-130.
(86) Carbo, J. J.; Garcia-Lopez, D.; Gonzalez-del Moral, O.; Martin, A.; Mena, M.; Santamaria, C., Carbon-Nitrogen Bond Construction and Carbon-Oxygen Double Bond Cleavage on a Molecular Titanium Oxonitride: A Combined Experimental and Computational Study. *Inorganic Chemistry* **2015,** *54* (19), 9401-9412.
(87) Klouras, N.; Nastopoulos, V.; Tzavellas, N.; Leban, I., Cyano Derivatives of Bis(Cyclopentadienyl)Titanium(IV) - the Crystal and Molecular Structure of μ-Oxo-Bis[Bis(Cyclopentadienyl)Cyanotitanium(IV)], $[(\eta^5\text{-}C_5H_5)_2TiCN]_2O$. *Zeitschrift Fur Anorganische Und Allgemeine Chemie* **1995,** *621* (10), 1767-1770.
(88) Gambarotta, S.; Floriani, C.; Chiesi-Villa, A.; Guastini, C., Decamethylvanadocene chemistry: synthesis, structure, and reactions of vanadium(II) and vanadium(III) derivatives with carbon monoxide and isocyanides. *Inorganic Chemistry* **1984,** *23* (12), 1739-1747.
(89) Martins, A. M.; Marques, M. M.; Ascenso, J. R.; Dias, A. R.; Duarte, M. T.; Fernandes, A. C.; Fernandes, S.; Ferreira, M. J.; Matos, I.; Oliveira, M. C.; Rodrigues, S. S.; Wilson, C., Titanium and zirconium ketimide complexes: synthesis and ethylene polymerisation catalysis. *Journal of Organometallic Chemistry* **2005,** *690* (4), 874-884.
(90) Basuli, F.; Watson, L. A.; Man, J. C. H.; Mindiola, D. J., Phosphaazaallene and phosphinylimide complexes stemming from a terminal and four-coordinate titanium phosphinidene. *Dalton Trans.* **2003,** (22), 4228-4229.
(91) Mullane, K. C.; Cheisson, T.; Nakamaru-Ogiso, E.; Manor, B. C.; Carroll, P. J.; Schelter, E. J., Reduction of Carbonyl Groups by Uranium(III) and Formation of a Stable Amide Radical Anion. *Chem. Eur. J.* **2018,** *24* (4), 826-837.
(92) Gianetti, T. L.; Bergman, R. G.; Arnold, J., Carbon-fluorine bond cleavage in fluoroarenes via a niobium(iii) imido complex: from stoichiometric to catalytic hydrodefluorination. *Chemical Science* **2014,** *5* (6), 2517-2524.
(93) Smith, M. R.; Matsunaga, P. T.; Andersen, R. A., Preparation of Monomeric $(Me_5C_5)_2VO$ and $(Me_5C_5)_2Ti(O)(L)$ and Their Decomposition to $(Me_5C_5)M_4(\mu\text{-}O)_6$. *Journal of the American Chemical Society* **1993,** *115* (15), 7049-7050.
(94) Sweeney, Z. K.; Polse, J. L.; Bergman, R. G.; Andersen, R. A., Dihydrogen Activation by Titanium Sulfide Complexes. *Organometallics* **1999,** *18* (26), 5502-5510.
(95) Howard, W. A.; Parkin, G., Interconversion of Hydrosulfido and Sulfido Ligands in Permethylzirconocene Complexes. *Organometallics* **1993,** *12* (6), 2363-2366.

(96) Howard, W. A.; Parkin, G., Terminal oxo, sulfido, selenido, and tellurido complexes of zirconium, (.eta.5-C5Me4R)2Zr(E)(NC5H5): comparison of terminal Zr-E single and Zr:E double-bond lengths. *Journal of the American Chemical Society* **1994,** *116* (2), 606-615.
(97) Kayal, A.; Kuncheria, J.; Lee, S. C., Bis[hydrotris(pyrazol-1-yl)borato]titanium(II): a stable Tp_2M complex of singular reactivity. *Chemical Communications* **2001,** (23), 2482-2483.
(98) Mendiratta, A.; Figueroa, J. S.; Cummins, C. C., Synthesis of a four-coordinate titanium(iv) oxoanion via deprotonation and decarbonylation of complexed formate. *Chemical Communications* **2005,** (27), 3403-3405.
(99) Hazari, N.; Mountford, P., Reactions and Applications of Titanium Imido Complexes. *Accounts of Chemical Research* **2005,** *38* (11), 839-849.
(100) Hagadorn, J. R.; Arnold, J., Preparation of complexes containing Ti=E, $Ti_2(\mu\text{-}E_2)$ and $Ti(\eta^2\text{-}E_2)$ (E=O, S) functionalities from a reactive titanium dinitrogen complex. *Inorganic Chemistry* **1997,** *36* (14), 2928-2929.
(101) Hanna, T. E.; Keresztes, I.; Lobkovsky, E.; Bernskoetter, W. H.; Chirik, P. J., Synthesis of a Base-Free Titanium Imido and a Transient Alkylidene from a Titanocene Dinitrogen Complex. Studies on TiNR Hydrogenation, Nitrene Group Transfer, and Comparison of 1,2-Addition Rates. *Organometallics* **2004,** *23* (14), 3448-3458.
(102) Hanna, T. E.; Lobkovsky, E.; Chirik, P. J., Dihydrogen and Silane Addition to Base-Free, Monomeric Bis(cyclopentadienyl)titanium Oxides. *Inorganic Chemistry* **2007,** *46* (7), 2359-2361.
(103) Duchateau, R.; Williams, A. J.; Gambarotta, S.; Chiang, M. Y., Carbon-carbon double-bond formation in the intermolecular acetonitrile reductive coupling promoted by a mononuclear titanium(II) compound. Preparation and characterization of two titanium(IV) imido derivatives. *Inorganic Chemistry* **1991,** *30* (25), 4863-4866.
(104) Muller, U.; Krug, V., $[TiSCl_4]^{2-}$ and $[Ti_3O(S_2)_3Cl_6]^{2-}$, a Multinuclear Complex with a Structure Typical for Clusters. *Angew. Chem. Int. Edit.*
1988, *27* (2), 293-294.
(105) Hsu, S. H.; Chang, J. C.; Lai, C. L.; Hu, C. H.; Lee, H. M.; Lee, G. H.; Peng, S. M.; Huang, J. H., Terminal titanium-ligand multiple bonds. Cleavages of C = O and C = S double bonds with Ti imido complexes. *Inorganic Chemistry* **2004,** *43* (21), 6786-6792.
(106) Lundmark, P. J.; Kubas, G. J.; Scott, B. L., Formation of an anionic titanium(IV) sulfide dimer, $\{Na_2[CpTi(\mu\text{-}S)(S)]_2\cdot 4THF\}_2$, by elimination of CpH and H_2 from $Cp_2Ti(SH)_2$ upon deprotonation with NaH. *Organometallics* **1996,** *15* (17), 3631-3633.
(107) Komuro, T.; Matsuo, T.; Kawaguchi, H.; Tatsumi, K., Palladium dimethylsilanedithiolato complex: a precursor for Ti-Pd and $Ti\text{-}Pd_2$ heterometallic complexes. *Chemical Communications* **2002,** (9), 988-989.
(108) Sweeney, Z. K.; Polse, J. L.; Andersen, R. A.; Bergman, R. G.; Kubinec, M. G., Synthesis, structure, and reactivity of monomeric titanocene sulfido and disulfido complexes. Reaction of H_2 with a terminal M=S bond. *Journal of the American Chemical Society* **1997,** *119* (19), 4543-4544.
(109) Ratti, C.; Richard, P.; Tabard, A.; Guilard, R., Synthesis and characterization of a new series of titanium(IV) porphyrins co-ordinated to a disulphur or a diselenium ligand. *Journal of the Chemical Society, Chemical Communications* **1989,** (2), 69-70.
(110) Darwish, W.; Schlecht, S.; Schaper, A.; Froba, M.; Harms, K.; Massa, W.; Sundermeyer, J., Synthesis and Crystal Structures of Axially Substituted Titaniumphthalocyanines and Preparation of PcTi@SBA-15 and PcTi&TiOx@SBA-15 Materials. *Zeitschrift Fur Anorganische Und Allgemeine Chemie* **2009,** *635* (8), 1215-1224.

(111) Verma, A. K.; Chou, J. H.; Rauchfuss, T. B., A polymeric binary titanium(IV) sulfide and its conversion to molecular Lewis base adducts. *Inorganic Chemistry* **1998,** *37* (22), 5960-+.
(112) See, X. Y.; Beaumier, E. P.; Davis-Gilbert, Z. W.; Dunn, P. L.; Larsen, J. A.; Pearce, A. J.; Wheeler, T. A.; Tonks, I. A., Generation of Ti-II Alkyne Trimerization Catalysts in the Absence of Strong Metal Reductants. *Organometallics* **2017,** *36* (7), 1383-1390.
(113) Zhang, J.; Park, S.; Chang, S., Piers' borane-mediated hydrosilylation of epoxides and cyclic ethers. *Chemical Communications* **2018,** *54* (52), 7243-7246.
(114) Hartwig, J. F., *Organotransition metal chemistry : from bonding to catalysis*. University Science Books: Sausalito, 2010.
(115) House, J. E., Chapter 22 - Coordination Compounds in Catalysis. In *Inorganic Chemistry (Second Edition)*, House, J. E., Ed. Academic Press: 2013; pp 747-772.
(116) Arévalo, R.; Chirik, P. J., Enabling Two-Electron Pathways with Iron and Cobalt: From Ligand Design to Catalytic Applications. *Journal of the American Chemical Society* **2019**.
(117) Egorova, K. S.; Ananikov, V. P., Which Metals are Green for Catalysis? Comparison of the Toxicities of Ni, Cu, Fe, Pd, Pt, Rh, and Au Salts. *Angewandte Chemie International Edition* **2016,** *55* (40), 12150-12162.
(118) Egorova, K. S.; Ananikov, V. P., Toxicity of Metal Compounds: Knowledge and Myths. *Organometallics* **2017,** *36* (21), 4071-4090.
(119) Ozerov, O. V.; Patrick, B. O.; Ladipo, F. T., Highly Regioselective [2 + 2 + 2] Cycloaddition of Terminal Alkynes Catalyzed by η6-Arene Complexes of Titanium Supported by Dimethylsilyl-Bridged p-tert-Butyl Calix[4]arene Ligand. *Journal of the American Chemical Society* **2000,** *122* (27), 6423-6431.
(120) Kablaoui, N. M.; Hicks, F. A.; Buchwald, S. L., Diastereoselective Synthesis of γ-Butyrolactones from Enones Mediated or Catalyzed by a Titanocene Complex. *Journal of the American Chemical Society* **1996,** *118* (24), 5818-5819.
(121) Kablaoui, N. M.; Hicks, F. A.; Buchwald, S. L., Titanocene-Catalyzed Cyclocarbonylation of o-Allyl Aryl Ketones to γ-Butyrolactones. *Journal of the American Chemical Society* **1997,** *119* (19), 4424-4431.
(122) He, X.; Hartwig, J. F., True Metal-Catalyzed Hydroboration with Titanium. *Journal of the American Chemical Society* **1996,** *118* (7), 1696-1702.
(123) Gilbert, Z. W.; Hue, R. J.; Tonks, I. A., Catalytic formal [2+2+1] synthesis of pyrroles from alkynes and diazenes via TiII/TiIV redox catalysis. *Nature Chemistry* **2015,** *8*, 63.
(124) Pearce, A. J.; See, X. Y.; Tonks, I. A., Oxidative nitrene transfer from azides to alkynes via Ti(ii)/Ti(iv) redox catalysis: formal [2+2+1] synthesis of pyrroles. *Chemical Communications* **2018,** *54* (50), 6891-6894.
(125) Davis-Gilbert, Z. W.; Wen, X.; Goodpaster, J. D.; Tonks, I. A., Mechanism of Ti-Catalyzed Oxidative Nitrene Transfer in [2 + 2 + 1] Pyrrole Synthesis from Alkynes and Azobenzene. *Journal of the American Chemical Society* **2018,** *140* (23), 7267-7281.
(126) Davis-Gilbert, Z. W.; Yao, L. J.; Tonks, I. A., Ti-Catalyzed Multicomponent Oxidative Carboamination of Alkynes with Alkenes and Diazenes. *Journal of the American Chemical Society* **2016,** *138* (44), 14570-14573.
(127) Davis-Gilbert, Z. W.; Tonks, I. A., Titanium redox catalysis: insights and applications of an earth-abundant base metal. *Dalton Transactions* **2017,** *46* (35), 11522-11528.
(128) Heins, S. P.; Wolczanski, P. T.; Cundari, T. R.; MacMillan, S. N., Redox non-innocence permits catalytic nitrene carbonylation by (dadi)Ti□NAd (Ad = adamantyl). *Chemical Science* **2017,** *8* (5), 3410-3418.

(129) Sánchez-Delgado, R. A., *Organometallic Modeling of the Hydrodesulfurization and Hydrodenitrogenation Reactions*. **2002**.
(130) T.Kabe, A. I., W.Qian, *Hydrodesulfurization and Hydrodenintrogenation: Chemistry and Engineering*. **2000**.
(131) Bianchini, C.; Meli, A., Hydrogenation, Hydrogenolysis, and Desulfurization of Thiophenes by Soluble Metal Complexes: Recent Achievements and Future Directions. *Accounts of Chemical Research* **1998,** *31* (3), 109-116.
(132) Lednicer, D., *The Organic Chemistry of Drug Synthesis*. **1998,** *6*.
(133) Gramec, D.; Peterlin Mašič, L.; Sollner Dolenc, M., Bioactivation Potential of Thiophene-Containing Drugs. *Chemical Research in Toxicology* **2014,** *27* (8), 1344-1358.
(134) Barbarella, G.; Zangoli, M.; Di Maria, F., Chapter Three - Synthesis and Applications of Thiophene Derivatives as Organic Materials. In *Advances in Heterocyclic Chemistry*, Scriven, E. F. V.; Ramsden, C. A., Eds. Academic Press: 2017; Vol. 123, pp 105-167.
(135) Perepichka, D. F.; Perepichka, I. F., *Handbook of thiophene-based materials : applications in organic electronics and photonics*. Wiley: Chichester, 2009; Vol. Vol. 2.
(136) Meng, H.; Zheng, J.; Lovinger, A. J.; Wang, B.-C.; Van Patten, P. G.; Bao, Z., Oligofluorene−Thiophene Derivatives as High-Performance Semiconductors for Organic Thin Film Transistors. *Chemistry of Materials* **2003,** *15* (9), 1778-1787.
(137) Zhang, F.; Wu, D.; Xu, Y.; Feng, X., Thiophene-based conjugated oligomers for organic solar cells. *Journal of Materials Chemistry* **2011,** *21* (44), 17590-17600.
(138) Barbarella, G.; Melucci, M.; Sotgiu, G., The Versatile Thiophene: An Overview of Recent Research on Thiophene-Based Materials. *Advanced Materials* **2005,** *17* (13), 1581-1593.
(139) Churchill, D. G.; Bridgewater, B. M.; Parkin, G., Modeling Aspects of Hydrodesulfurization at Molybdenum: Carbon−Sulfur Bond Cleavage of Thiophenes by Ansa Molybdenocene Complexes. *Journal of the American Chemical Society* **2000,** *122* (1), 178-179.
(140) Sattler, A.; Janak, K. E.; Parkin, G., Modeling aspects of hydrodesulfurization by molybdenum hydride compounds: Desulfurization of thiophene and benzothiophene and C–S bond cleavage of dibenzothiophene. *Inorganica Chimica Acta* **2011,** *369* (1), 197-202.
(141) Jones, W. D.; Chin, R. M.; Crane, T. W.; Baruch, D. M., Carbon-Sulfur Bond Cleavage in Thiophene by Group 6 Metallocenes. *Organometallics* **1994,** *13* (11), 4448-4452.
(142) Jones, W. D.; Chin, R. M., Thiophene carbon-sulfur bond cleavage by cobalt. Synthesis, structure, and dynamics of [(C5Me5)Co]2(C4H4S). *Organometallics* **1992,** *11* (7), 2698-2700.
(143) Jones, W.; M. Chin, R., *Thiophene carbon-sulfur bond cleavage by cobalt. Synthesis, structure, and dynamics of [(C5Me5)Co]2(C4H4S)*. 1992; Vol. 11.
(144) Vicic, D. A.; Jones, W. D., Modeling the Hydrodesulfurization Reaction at Nickel. Unusual Reactivity of Dibenzothiophenes Relative to Thiophene and Benzothiophene. *Journal of the American Chemical Society* **1999,** *121* (33), 7606-7617.
(145) Vicic, D. A.; Jones, W. D., Room-Temperature Desulfurization of Dibenzothiophene Mediated by [(i-Pr2PCH2)2NiH]2. *Journal of the American Chemical Society* **1997,** *119* (44), 10855-10856.
(146) Dailey, K. M. K.; Rauchfuss, T. B.; Rheingold, A. L.; Yap, G. P. A., A New Pathway for Thiophene Ring Opening by Transition Metals. *Journal of the American Chemical Society* **1995,** *117* (23), 6396-6397.
(147) Jones, W.; Martin Chin, R.; L. Hoaglin, C., *Cleavage of the Carbon−Sulfur Bonds in Thiophenes by a Binuclear Ruthenium Complex*. 1999; Vol. 18.

(148) Selnau, H. E.; Merola, J. S., Reactions of iridium complex [Ir(COD)(PMe3)3]Cl with benzene, pyridine, furan, and thiophene: carbon-hydrogen cleavage vs. ring opening. *Organometallics* **1993,** *12* (5), 1583-1591.
(149) Bianchini, C.; Meli, A.; Peruzzini, M.; Vizza, F.; Frediani, P.; Herrera, V.; Sánchez-Delgado, R., *Opening, desulfurization, and hydrogenation of thiophene at iridium. An experimental study in a homogeneous phase*. 1993; Vol. 115.
(150) Jones, W. D.; Dong, L., Insertion of rhodium into the carbon-sulfur bond of thiophene. Mechanism of a model for the hydrodesulfurization reaction. *Journal of the American Chemical Society* **1991,** *113* (2), 559-564.
(151) Dong, L.; Duckett, S. B.; Ohman, K. F.; Jones, W. D., A model for homogeneous hydrodesulfurization. The importance of .eta.2-coordination and sulfur coordination in carbon-hydrogen and carbon-sulfur bond cleavage reactions of thiophene. *Journal of the American Chemical Society* **1992,** *114* (1), 151-160.
(152) Chin, R. M.; Jones, W. D., Dimerization of Thiophene to Give a Linear S(CH)8S Fragment with [(C5Me5)Rh(C2H4)2]. *Angewandte Chemie International Edition in English* **1992,** *31* (3), 357-358.
(153) Jones, W. D.; Chin, R. M., Mechanism of formation of carbon-carbon bonds in the ring opening and coupling of thiophene by rhodium complex, (C5Me5)Rh(C2H4)2. *Journal of the American Chemical Society* **1992,** *114* (25), 9851-9858.
(154) Jones, W. D.; Vivic, D. A.; Martin Chin, R.; Roache, J. H.; Myers, A. W., Homogeneus models of thiophene HDS reactions. Selectivity in thiophene C□S cleavage and thiophene reactions with dinuclear metal complexes. *Polyhedron* **1997,** *16* (18), 3115-3128.
(155) Myers, A. W.; Dong, L.; Ateşin, T. A.; Skugrud, R.; Flaschenriem, C.; Jones, W. D., Bond cleavage reactions in substituted thiophenes by a rhodium complex. *Inorganica Chimica Acta* **2008,** *361* (11), 3263-3270.
(156) Grochowski, M. R.; Brennessel, W. W.; Jones, W. D., Carbon−Sulfur Bond Cleavage of Methyl-Substituted Thiophenes with Iridium(III). *Organometallics* **2009,** *28* (9), 2661-2667.
(157) Oster, S. S.; Grochowski, M. R.; Lachicotte, R. J.; Brennessel, W. W.; Jones, W. D., Carbon−Sulfur Bond Activation of Dibenzothiophenes and Phenoxythiin by [Rh(dippe)(μ-H)]2 and [Rh2(dippe)2(μ-Cl)(μ-H)]. *Organometallics* **2010,** *29* (21), 4923-4931.
(158) Willems, S. T. H.; Budzelaar, P. H. M.; Moonen, N. N. P.; de Gelder, R.; Smits, J. M. M.; Gal, A. W., Coordination and Oxidative Addition at a Low-Coordinate Rhodium(I) β-Diiminate Centre. *Chemistry – A European Journal* **2002,** *8* (6), 1310-1320.
(159) Myers, A. W.; Jones, W. D.; McClements, S. M., Regiochemical Selectivity in the Carbon-Sulfur Bond Cleavage of 2-Methylbenzothiophene: Synthesis, Characterization, and Mechanistic Study of Reversible Insertion into a C-S Bond. *Journal of the American Chemical Society* **1995,** *117* (47), 11704-11709.
(160) Garcia, J. J.; Mann, B. E.; Adams, H.; Bailey, N. A.; Maitlis, P. M., Equilibria of the Thiametallacycles with Tris(triethylphosphine)platinum(0) and Dibenzothiophene, Benzothiophene, or Thiophene: The Hydrodesulfurization Reaction. *Journal of the American Chemical Society* **1995,** *117* (8), 2179-2186.
(161) Arce, A. J.; Deeming, A. J.; De Sanctis, Y.; Machado, R.; Manzur, J.; Rivas, C., Carbon–hydrogen cleavage versus ring opening in the oxidative addition reactions of furan, thiophene, selenophene and tellurophene with [Os3(CO)10(MeCN)2]. *Journal of the Chemical Society, Chemical Communications* **1990,** (22), 1568-1569.

(162) Herrera, V.; Fuentes, A.; Rosales, M.; Sánchez-Delgado, R. A.; Bianchini, C.; Meli, A.; Vizza, F., Homogeneous Hydrogenation of Benzo[b]thiophene by Use of Rhodium and Iridium Complexes as the Catalyst Precursors: Kinetic and Mechanistic Aspects. *Organometallics* **1997,** *16* (11), 2465-2471.
(163) Bianchini, C.; Herrera, V.; Jimenez, M. V.; Meli, A.; Sanchez-Delgado, R.; Vizza, F., The Catalytic Transformation of Benzo[b]thiophene to 2-Ethylthiophenol by a Soluble Rhodium Complex: The Reaction Mechanism Involves Ring Opening Prior to Hydrogenation. *Journal of the American Chemical Society* **1995,** *117* (33), 8567-8575.
(164) Sigma-Aldrich Thiophene Safety Data Sheet. https://www.sigmaaldrich.com/MSDS/MSDS/DisplayMSDSPage.do?country=US&language=en&productNumber=T31801&brand=ALDRICH&PageToGoToURL=https%3A%2F%2Fwww.sigmaaldrich.com%2Fcatalog%2Fproduct%2Faldrich%2Ft31801%3Flang%3Den (accessed June 13th, 2019).
(165) Figueroa, J. S.; Cummins, C. C., The Niobaziridine−Hydride Functional Group: Synthesis and Divergent Reactivity. *Journal of the American Chemical Society* **2003,** *125* (14), 4020-4021.
(166) Figueroa, J. S.; Cummins, C. C., A niobaziridine hydride system for white phosphorus or dinitrogen activation and N- or P-atom transfer. *Dalton Transactions* **2006,** (18), 2161-2168.
(167) Figueroa, J. S.; Cummins, C. C., Diorganophosphanylphosphinidenes as Complexed Ligands: Synthesis via an Anionic Terminal Phosphide of Niobium. *Angewandte Chemie International Edition* **2004,** *43* (8), 984-988.
(168) Figueroa, J. S.; Cummins, C. C., Phosphaalkynes from Acid Chlorides via P for O(Cl) Metathesis: A Recyclable Niobium Phosphide (P3-) Reagent that Effects C−P Triple-Bond Formation. *Journal of the American Chemical Society* **2004,** *126* (43), 13916-13917.
(169) Piro, N. A.; Figueroa, J. S.; McKellar, J. T.; Cummins, C. C., Triple-Bond Reactivity of Diphosphorus Molecules. *Science* **2006,** *313* (5791), 1276-1279.
(170) Stafford, P. R.; Rauchfuss, T. B.; Verma, A. K.; Wilson, S. R., Titanocene complexes of ring-opened dibenzothiophene and related dimercaptobiaryl ligands. *Journal of Organometallic Chemistry* **1996,** *526* (2), 203-214.
(171) Parks, D. J.; Piers, W. E.; Yap, G. P. A., Synthesis, Properties, and Hydroboration Activity of the Highly Electrophilic Borane Bis(pentafluorophenyl)borane, HB(C6F5)21. *Organometallics* **1998,** *17* (25), 5492-5503.
(172) Parks, D. J.; von H. Spence, R. E.; Piers, W. E., Bis(pentafluorophenyl)borane: Synthesis, Properties, and Hydroboration Chemistry of a Highly Electrophilic Borane Reagent. *Angewandte Chemie International Edition in English* **1995,** *34* (7), 809-811.
(173) Fleige, M.; Möbus, J.; vom Stein, T.; Glorius, F.; Stephan, D. W., Lewis acid catalysis: catalytic hydroboration of alkynes initiated by Piers' borane. *Chemical Communications* **2016,** *52* (72), 10830-10833.
(174) Bushnell, G. W.; Rivett, G. A., The crystal structure of bis(diethylamino)dithiaboretane, a compound with a four-membered alternating boron–sulfur ring. *Canadian Journal of Chemistry* **1977,** *55* (18), 3294-3297.
(175) Conrad, O.; Jansen, C.; Krebs, B., Boron–Sulfur and Boron–Selenium Compounds—From Unique Molecular Structural Principles to Novel Polymeric Materials. *Angewandte Chemie International Edition* **1998,** *37* (23), 3208-3218.
(176) Firth, A. V.; Witt, E.; Stephan, D. W., Thermal Reactions of Titanium Thiolates: Terminal Titanium Sulfides in CS Bond Cleavage Reactions. *Organometallics* **1998,** *17* (17), 3716-3722.

(177) Gelmini, L.; Stephan, D. W., Synthesis, characterization, and chemistry of titanium(IV), titanium(III), zirconium(IV), and hafnium(IV) complexes of phosphine sulfides and selenides. The crystal and molecular structures of Cp2Ti(SPCy2)2, Cp2Ti(S2PCy2), and Cp2Ti(Se2PPh2). *Organometallics* **1987,** *6* (7), 1515-1522.
(178) Aguilar-Calderón, J. R.; Metta-Magaña, A. J.; Noll, B.; Fortier, S., C(sp3)−H Oxidative Addition and Transfer Hydrogenation Chemistry of a Titanium(II) Synthon: Mimicry of Late-Metal Type Reactivity. *Angewandte Chemie International Edition* **2016,** *55* (45), 14101-14105.
(179) Janiak, C., A critical account on π–π stacking in metal complexes with aromatic nitrogen-containing ligands. *Journal of the Chemical Society, Dalton Transactions* **2000,** (21), 3885-3896.
(180) Dance, I., Distance criteria for crystal packing analysis of supramolecular motifs. *New Journal of Chemistry* **2003,** *27* (1), 22-27.
(181) Tokitoh, N.; Ito, M.; Okazaki, R., Formation and reactions of a thioxoborane, a novel boron-sulfur double-bond compound. *Tetrahedron Letters* **1996,** *37* (29), 5145-5148.
(182) Birch, A. J., 117. Reduction by dissolving metals. Part I. *Journal of the Chemical Society (Resumed)* **1944,** (0), 430-436.
(183) Wertjes, W. C.; Southgate, E. H.; Sarlah, D., Recent advances in chemical dearomatization of nonactivated arenes. *Chemical Society Reviews* **2018,** *47* (21), 7996-8017.
(184) P. Rothwell, I., A new generation of homogeneous arene hydrogenation catalysts. *Chemical Communications* **1997,** (15), 1331-1338.
(185) Yu, J. S.; Ankianiec, B. C.; Rothwell, I. P.; Nguyen, M. T., All-cis catalytic hydrogenation of polynuclear aromatic hydrocarbons by Group 5 metal aryl oxide compounds. *Journal of the American Chemical Society* **1992,** *114* (5), 1927-1929.
(186) Fryzuk, M. D.; Kozak, C. M.; Bowdridge, M. R.; Patrick, B. O., Cyclohexadienyl Niobium Complexes and Arene Hydrogenation Catalysis. *Organometallics* **2002,** *21* (23), 5047-5054.
(187) Nikiforov, G. B.; Vidyaratne, I.; Gambarotta, S.; Korobkov, I., Titanium-Promoted Dinitrogen Cleavage, Partial Hydrogenation, and Silylation. *Angewandte Chemie International Edition* **2009,** *48* (40), 7415-7419.
(188) Findlater, M.; Hill, N. J.; Cowley, A. H., Synthesis and structure of two new (guanidinate)boron dichlorides and their attempted conversion to boron(i) derivatives. *Dalton Transactions* **2008,** (33), 4419-4423.

Vita

Rolando Aguilar was born and raised in Chihuahua city, the capital of Chihuahua state where the Mexican revolution of 1910 began. He attended the Autonomous University of Chihuahua to obtain a B. Sc. in Chemistry with a minor in Microbiology. During that time, he joined Dr. Alejandro Camacho's laboratory to work on amino acid synthesis mediated by palladium cross-coupling reactions. Such great experience encouraged him to pursue a Ph. D. in chemistry. In Fall of 2013, he was accepted as a graduate student in the Chemistry program at The University of Texas in El Paso (UTEP). Even though he was looking forward to focusing on an organic synthesis research project, his interests completely changed after a short conversation with Dr. Skye Fortier about the disturbing chemistry of transition metals. After this interaction, joining his lab seemed like a no-brainer. Since then, he has been scrutinizing the chemistry of the untamable low-valent titanium species with emphasis on small molecule activation and catalysis. To further expand the reactivity profile of his compounds, in 2018 he started using high-pressure chemistry at the University of Pennsylvania under the supervision of Dr. Daniel Mindiola. Outside the lab Rolando enjoys synthesizing inorganic sounds with Eurorack and is constantly shaken by the work of Jorge Luis Borges, Fyodor Dostoevsky, Franz Kafka, Mario Vargas-Llosa, Marcel Proust, and Gabriel Garcia Marquez to name a very very few.